
# National Technical University of Athens

School of Mechanical Engineering

## Machine Design Laboratory

Diploma thesis

Nikolaos Kallieros

**Analysis and design of a linear electromagnetic mass accelerator (railgun) using computational methods**

**Supervisor:** Dr. V. Spitas

Associate Professor NTU Athens

Athens, July 2020

# ΕΘΝΙΚΟ ΜΕΤΣΟΒΙΟ ΠΟΛΥΤΕΧΝΕΙΟ


ΣΧΟΛΗ ΜΗΧΑΝΟΛΟΓΩΝ ΜΗΧΑΝΙΚΩΝ

**ΕΡΓΑΣΤΗΡΙΟ ΣΤΟΙΧΕΙΩΝ ΜΗΧΑΝΩΝ**


ΔΙΠΛΩΜΑΤΙΚΗ ΕΡΓΑΣΙΑ


Νικόλαος Καλλιέρος


## Ανάλυση και σχεδιασμός ηλεκτρομαγνητικού γραμμικού επιταχυντή μαζών με χρήση υπολογιστικών μεθόδων


**Επιβλέπων:** Βασίλειος Σπιτάς

Επίκουρος Καθηγητής Ε.Μ.Π.



Αθήνα, Ιούλιος 2020

# Ευχαριστίες

Πρώτα από όλα, θα ήθελα να ευχαριστήσω τον επιβλέποντα καθηγητή κύριο Βασίλειο Σπιτά, για την πολύτιμη βοήθειά του τόσο κατά την εκπόνηση της παρούσας διπλωματικής όσο και για όλη την φοιτητική μου σταδιοδρομία για της πολύτιμες συμβουλές και πολλές γνώσεις που μου έδωσε.

Θα ήθελα ακόμη να ευχαριστήσω την οικογένειά μου για όλη τους την στήριξη τόσο κατά την διάρκεια των σπουδών μου αλλά και για την αγάπη που μου έδωσαν όλα αυτά τα χρόνια. Θα ήθελα να ξεχωρίσω ένα πρόσωπο, τον πατέρα μου που από μικρό μου εμφύσησε την αγάπη για τις φυσικές επιστήμες, και την αναλυτική σκέψη.

Τέλος θα ήθελα να ευχαριστήσω  και τους συμφοιτητές και φίλους Αλέξανδρο Αναστασιάδη, Κωνσταντίνο Αθανασόπουλο και Αριστοτέλη Παπαθεοδώρου τόσο για την καλή παρέα, όσο και για την άριστη συνεργασία στο επίπεδο της σχολής.

# Abstract

In this thesis the design of a novel, efficient high-speed electromagnetic mass accelerator is proposed and analyzed. To do so, a theory is put forth to investigate the way electromagnetic force is produced, as well as the parameters that affect it the most. To investigate its validity, the theory was applied for the analysis of classic electromechanical devices such as the induction and dc motors, as well as for Thompson's jumping ring apparatus. Structural and thermal analyses ensue, to examine all aspects of the device's operation, as well as to envelope its operation and show its all-round behavior. Finally, high power switches were discussed, which make the operation of the device possible and an automatic (passive) switch design was put forth to be used for the device. It was concluded that this device stands as a solid alternative for a conventional railgun or an induction coil-gun solving some of their most important drawbacks. Nevertheless, as for all mechanical devices, the drawbacks of this device were discussed, and methods to mitigate them were proposed.

# Περίληψη

Στην παρούσα διπλωματική εργασία, προτάθηκε και αναλύθηκε ο σχεδιασμός ενός καινοτόμου ηλεκτρομαγνητικού επιταχυντή μαζών, υψηλού βαθμού απόδοσης. Για τον σκοπό αυτό, διατυπώθηκε μια καινούργια μεθοδολογία αντιμετώπισης τεχνικών προβλημάτων που αφορούν εφαρμογές της ηλεκτρομαγνητικής θεωρίας, η οποία και εφαρμόστηκε στην ανάλυση γνωστών ηλεκτρομηχανικών συστημάτων όπως για παράδειγμα ο κινητήρας συνεχούς ρεύματος, οι σύγχρονοι και ασύγχρονοι κινητήρες καθώς και η πειραματική διάταξη του Thompson προκειμένου να ελεγχθεί η εγκυρότητά της. Ακολούθησε η μοντελοποίηση της προτεινόμενης διάταξης μέσω ανάλυσης τάσεων και μετάδοσης θερμότητας ώστε να διαμορφωθούν τα όρια λειτουργίας της διάταξης με τη μεγαλύτερη δυνατή σαφήνεια. Τέλος, μελετήθηκαν και εναλλακτικές λύσης υλοποίησης διακοπτών μεγάλης ισχύος, μέσω των οποίων είναι δυνατή η λειτουργία της διάταξης. Προτάθηκε επίσης και ο σχεδιασμός ενός αυτόματου ηλεκτρομαγνητικού διακόπτη για χρήση στην παρούσα εφαρμογή. Δείχθηκε πως η διάταξη θα μπορούσε να αντικαταστήσει τα συμβατικά railgun και coil-gun, λύνοντας αρκετά από τα προβλήματα που παρουσιάζουν. Επιπλέον εντοπίστηκαν και αναλύθηκαν τα μειονεκτήματα της διάταξης και προτάθηκαν τρόποι αντιμετώπισής τους.

# TABLE OF CONTENTS

# 1 INTRODUCTION

In the introduction, the current state for high velocity launchers will be discussed, as well as the need for a new electromagnetic launcher design. Also, a brief introduction to the synchronous and asynchronous motors ensues since these concepts will be extensively used in the following chapters.

## 1.1 Induction coil gun

The induction coil-gun consists of individual coils, each of whom are connected to a power supply (usually capacitor bank) forming a “primary coil”, and a projectile usually made out of a copper cylinder, which acts as the “secondary” and gets repelled forwards. As the projectile passes each consecutive coil, it triggers the closing of the circuit where the coil belongs (as the figure below shows). Thus, current is generated in the primary coil and the projectile is repelled by means of the action of induced eddy currents. When designing an induction-type coil-gun system, one of the most important facets of the design is the correct timing and shaping of the pulse current. The force is generated by the mutual inductance and current of the coils. The stator coils exert both repulsive force and expansive force, while the armature coil exerts projectile force and contractile force [1].

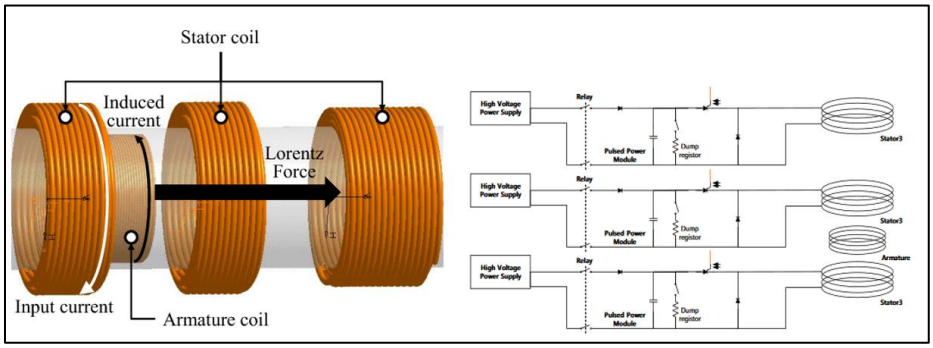


*Figure 1:Operating principle of induction coil-gun*

## 1.2 Railgun

A railgun is a linear motor device, that uses electromagnetic force to launch high velocity projectiles, as the figure below indicates. It consists of two parallel rails, connected to a power supply, and a conductive projectile that bridges the gap between the rails and causes current to flow through the circuit. Both railgun and induction coil-gun will be discussed later in more detail, but it is important to mention the state-of-the-art technology, for electromagnetic launchers, in order to explain why a new launcher is needed and what the requirements of its operation should be.

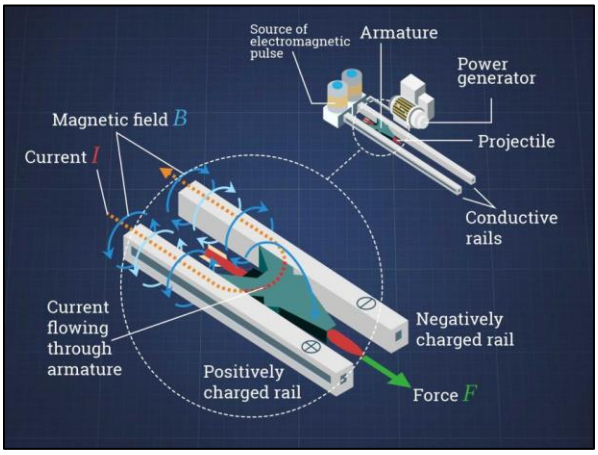


*Figure 2: Operating principle of railgun*

## 1.3 Induction motor overview (asynchronous)

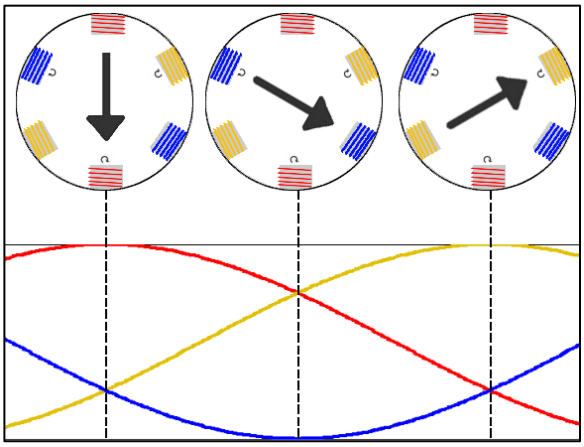

*Figure 3:Rotating magnetic field in synchronous and asynchronous motors*

An induction motor or asynchronous motor is an AC electric motor, where the electric current in the rotor needed to produce torque is obtained by electromagnetic induction from the magnetic field of the stator winding. Thus, an induction motor can be made without electrical connections to the rotor. An induction motor's rotor can be one of two possible configurations. Either wound type or squirrel-cage type. Three-phase squirrel-cage induction motors are widely used industrially, because they are self-starting, reliable and economical. Single-phase induction motors are often used for smaller loads, such as household appliances like fans. In both induction and synchronous motors, the AC power supplied to the motor's stator creates a magnetic field that rotates in synchronism with the AC oscillations. A synchronous motor's rotor turns at the same rate as the stator field, whereas an induction motor's rotor rotates at a somewhat slower speed than the stator field. The induction motor stator's magnetic field is therefore changing or rotating relative to the rotor. This induces an opposing current in the induction motor's rotor, in effect the motor's secondary winding, when the latter is short-circuited or closed through an external impedance. The rotating magnetic flux induces currents in the windings of the rotor, in a manner similar to currents induced in a transformer's secondary winding(s) [2].

## 1.4 Synchronous motor overview

A synchronous electric motor is an AC motor in which, at steady state, the rotation of the shaft is synchronized with the frequency of the supply current; the rotation period is exactly equal to an integral number of AC cycles. Synchronous motors contain multiphase AC electromagnets on the stator of the motor that create a magnetic field which rotates in time with the oscillations of the line current. The rotor with permanent magnets or electromagnets turns in step with the stator field at the same rate and as a result, provides the second synchronized rotating magnet field of any AC motor. A synchronous motor is termed doubly fed if it is supplied with independently excited multiphase AC electromagnets on both the rotor and stator.

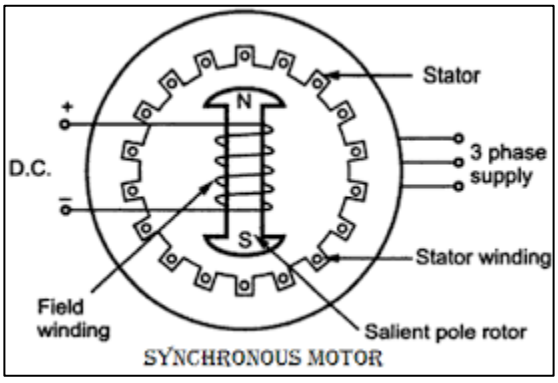


*Figure 4:Simple schematic of synchronous motor*

The synchronous motor and induction motor are the most widely used types of AC motor. The difference between the two types is that the synchronous motor rotates at a rate locked to the line frequency since it does not rely on current induction to produce the rotor's magnetic field. By contrast, the induction motor requires slip: the rotor must rotate slightly slower than the AC alternations in order to induce current in the rotor winding. Small synchronous motors are used in timing applications such as in synchronous clocks, timers in appliances, tape recorders and precision servomechanisms in which the motor must operate at a precise speed; speed accuracy is that of the power line frequency, which is carefully controlled in large interconnected grid systems. Synchronous motors are available in self-excited sub-fractional horsepower sizes to high power industrial sizes. In the fractional horsepower range, most synchronous motors are used where precise constant speed is required. These machines are commonly used in analog electric clocks, timers and other devices where correct time is required. In higher power industrial sizes, the synchronous motor provides two important functions. First, it is a highly efficient means of converting AC energy to work. Second, it can operate at leading or unity power factor and thereby provide power-factor correction [3].

## 1.5 Need for new launcher system

As more detailed analysis present in this thesis will show, both induction coil-guns and rail-guns, due to their operating principle, have fundamental limitations to the final projectile velocity and their efficiency, which for the same reasons are capped by a theoretical maximum. The proposed launcher, sets out to solve these main problems, by introducing a new mechanism for high speed mass propulsion, which will be discussed in great detail in the following chapters. Need for high efficiency and speed mass accelerators exists since they appear as very attractive alternatives to processes that require high amounts of energy and power to be achieved. Some include:

1. Initiation of fusion [4]
2. launch satellites or space shuttles into the upper atmosphere
3. material impact testing
4. high energy physics experiments
5. Research for high pressure physics [5]

- All simulations present in this thesis were done with the COMSOL Multiphysics software.
- All 3D models present in this thesis were created with the SOLIDWORKS software.

# 2 BASICS OF ELECTROMAGNETICS THEORY

## 2.1 Maxwell equations

Maxwell's equations are a set of coupled partial differential equations that, along with the Lorentz force law, form the foundation of classical electromagnetism and electric circuits. The equations formulated in 1865 by James Clerk Maxwell provide a mathematical representation for electrical, optical, radio technologies and more. They are often used in systems containing power generation machines, electric motors, wireless communication, lenses, radar and more. They describe how electric and magnetic fields are generated by charges, currents, and changes of these fields. An important consequence of Maxwell's equations is the derivation of the speed at which fluctuating electric and magnetic fields propagate in a vacuum $(c)$ [6].

*The equations have two major variants:*

***Microscopic equations***

The microscopic Maxwell equations have universal applicability. They describe the electric field $\boldsymbol{E}$ and the magnetic field $\boldsymbol{B}$ in vacuum, along with their sources -charge- and -current-densities-. For this formulation it is assumed that there is no other matter in the system, other than the charges and currents accounted for in the equations.

*Gauss's law:*

$$\boldsymbol{\nabla} \cdot \boldsymbol{B} = 0 \Leftrightarrow \iint_{\substack{closed \\ surface}} \boldsymbol{B} \cdot d\boldsymbol{S} = 0 \tag{1}$$

$\boldsymbol{B}$: magnetic field in vacuum

The differential form can be converted to the integral form through the use of the divergence theorem, by applying it over a volume $V$.

*Faraday's law:*

$$\boldsymbol{\nabla} \times \boldsymbol{E} = -\frac{\partial \boldsymbol{B}}{\partial t} \Leftrightarrow \oint_C \boldsymbol{E} \cdot d\boldsymbol{l} = -\frac{d}{dt} \iint_S \boldsymbol{B} \cdot d\boldsymbol{S} \tag{2}$$

$\boldsymbol{E}$: eclectic field in vacuum

Here the differential form is converted into Faraday's law by integrating left, and right-hand side over a surface $S$ bounded by a contour $C$ and applying Stokes' theorem.

*Gauss's law for electric fields:*

$\rho(r) = charge\ density$ *, charge/unit volume*

$J(r) = electric\ current\ density$ *, electric current/unit area*

$$\boldsymbol{\nabla} \cdot \boldsymbol{E} = \frac{\rho(\boldsymbol{r})}{\varepsilon_0} \Leftrightarrow \iint_{\substack{closed \\ surface}} \boldsymbol{E} \cdot d\boldsymbol{S} = \frac{Q_{total}}{\varepsilon_0} \tag{3}$$

The third Maxwell differential equation is converted to the electrostatic Gauss law by integrating over a volume $V$ and applying the divergence theorem.

Closed surface: surface enveloping $V$

$Q_{tot}$ : total electric charge contained in volume $V$

*Ampere's law:*

$$\boldsymbol{\nabla} \times \boldsymbol{B} = \mu_0 \boldsymbol{J}(\boldsymbol{r}) + \varepsilon_0 \mu_0 \frac{\partial \boldsymbol{E}}{\partial t} \Leftrightarrow \oint_C \boldsymbol{B} \cdot d\boldsymbol{l} = \mu_0 I + \varepsilon_0 \mu_0 \frac{d}{dt} \iint_S \boldsymbol{B} \cdot d\boldsymbol{S} \quad (4)$$

The fourth Maxwell equation is converted into Ampère's law by integrating left- and right-hand side over a surface $S$ bounded by a contour $C$ and applying Stokes' theorem

***Macroscopic equations***

The macroscopic equations relate the electric and magnetic fields to total charge and total current, including the complicated charges and currents in materials at the atomic scale. Here it is assumed that, instead of a vacuum, there is a continuous medium present, like air for example, that is polarizable and magnetizable. Thus, two additional vectors, $\boldsymbol{P}$ (the polarization vector of the medium) and $\boldsymbol{M}$ (the magnetization vector of the medium) have to be taken into consideration. These new auxiliary fields describe the large-scale behavior of matter without having to consider atomic scale charges (like the microscopic formulation does) and quantum phenomena like spins. It is convenient however to replace these two vectors by two supplementary vectors, the electric displacement $\boldsymbol{D}$ and the magnetic field $\boldsymbol{H}$.

$$\boldsymbol{D} \equiv \varepsilon_0 \boldsymbol{E} + \boldsymbol{P} = \varepsilon \boldsymbol{E} \quad (5)$$

$\mathbf{P}$: polarization of the medium

$\varepsilon$: relative permittivity (dielectric constant)

$$\boldsymbol{H} \equiv \frac{1}{\mu_0} \boldsymbol{B} - \boldsymbol{M} = \frac{1}{\mu} \boldsymbol{B} \quad (6)$$

$\mathbf{M}$: magnetization of the medium

$\mu$: magnetic susceptibility

*Difference between magnetic permeability and magnetic susceptibility:*

Magnetic permeability of a material is the ability of a material to support the formation of a magnetic field inside itself.

Magnetic susceptibility is the measure of magnetic properties of a material which indicates the degree of magnetization of a material in response to an applied magnetic field.

***Units of Measurement:***

*Magnetic permeability*: in the $SI$ unit ($H/m$ or $H \cdot m^{-1}$)

*Magnetic susceptibility* is a dimensionless property.

***Value for Diamagnetic Materials:***

The value of magnetic permeability for diamagnetic materials is less than $1$.

The value of magnetic susceptibility for diamagnetic materials is less than zero.

***Value for Paramagnetic Materials:***

The value of magnetic permeability for paramagnetic materials is greater than $1$.

The value of magnetic susceptibility for paramagnetic materials is greater than zero

*Set of differential equations expressed in macroscopic formulation:*

$$\boldsymbol{\nabla} \cdot \boldsymbol{B} = 0 \tag{7}$$

$$\boldsymbol{\nabla} \times \boldsymbol{E} = -\frac{\partial \boldsymbol{B}}{\partial t} \tag{8}$$

$$\boldsymbol{\nabla} \cdot \boldsymbol{D} = \rho(\boldsymbol{r}) \tag{9}$$

$$\boldsymbol{\nabla} \times \boldsymbol{B} = \boldsymbol{J}(\boldsymbol{r}) + \frac{\partial \boldsymbol{D}}{\partial t} \tag{10}$$

***Connection between microscopic and macroscopic formulation***

The Dutch physicist Lorentz in the 1890s showed that the macroscopic equations can be attained from the microscopic equations by an averaging of electric and magnetic dipoles over the medium. It is therefore evident that in that sense the microscopic equations are the most basic.

*Description of Gauss's law for magnetism:*

Gauss's law for magnetism states essentially that no magnetic monopoles exist (in contrast to electric charges). this means that magnetic field lines, always form closed loops. Or in other words, the integral of the magnetic lines cutting through a closed surface in space will always be zero, even if a "magnetic charge" exists in the volume defined by this surface.

*Description of Gauss's law for electric charges:*

Gauss's law describes the relationship between an electric charge, and the static electric field that it creates. The field created by a negative charge points towards it, and away from a positive charge. It is clear from the integral form of the equation, that the electric field, is directly proportional to the charge enveloped by the closed surface over which the integration occurs.

## 2.2 Faraday's law

Faraday's law essentially predicts how a magnetic field will interact with an electric circuit to produce an electromotive force (EMF). This phenomenon is also known as electromagnetic induction. It is the fundamental principle that governs the operation of electromagnetic transformers, induction motors, solenoids etc. The differential equation associated with this law describes the fact that a time varying magnetic field produces an associated electric field.

In a simplified example for a loop of wire, we can define the magnetic flux cutting the surface defined by the perimeter of the loop, as:

$$\Phi_B = \iint_{S(t)} \boldsymbol{B}(t) \cdot d\boldsymbol{A} \tag{11}$$

Where, $S(t)$ the surface defined by the loop, which can also change in time, if for example the loop is stretched, rotated, moved etc.

Faraday's law states that the EMF is also given by the rate of change of the magnetic flux:

$$E = -\frac{d\Phi_B}{dt} \tag{12}$$

$E$: electromotive force (EMF)

The scenario can be imagined for instance, where a magnet producing a stationary magnetic field, and a loop of wire moving vertically above it. This is equivalent to a stationary loop of wire, and a moving magnetic field, produced by the movement of the magnet, since motion between the two is relative. Although the field produced by the magnet in and of itself is stationary in time, because of the motion of the magnet at every time instance, a specific point in space will have a varying value for the magnetic field. Thus, a **time** varying magnetic field is produced.

$$\left.\begin{array}{l} B_{magnet} = B(x, y, z) \\ \\ (x, y, z) = (x(t), y(t), z(t)) \end{array}\right\} \quad B_{magnet} = B(x(t), y(t), z(t)) \tag{13}$$

And as a consequence of the law of induction, a voltage (EMF) will be produced in the loop, which will create a current.

The minus sign in the above equation is due to the Lenz's law.

## 2.3 Lenz law

Lenz's law, named after physicist Emil Lenz who formulated it in 1834, states that the direction of the electric current produced by the EMF which is induced in a conductor due to Faraday's law, is such that the magnetic field created by the induced current opposes the initial changing magnetic field. It is a qualitative law that specifies the sign of the induced voltage, and tells us nothing about its magnitude.

To be more exact, Lenz's law does not directly predict the direction of current in the conductor. Instead it correlates the sign of the voltage induced in it, with the changing magnetic field which created it. The current produced, depends not only on the voltage, but also the circuit in which the conductor exists. Therefore, one cannot talk about the current induced in a circuit, without also analyzing the circuit itself.

Lenz's law can be thought of in many ways as an implication of conservation of momentum. If charge q1 is pushed in one direction, then charge q2 is pushed in the opposite direction by the same force at the same time. If it's taken into consideration what is stated in the paragraph above, and in this one, it can be seen, that the primary magnetic field (that induces a current in the loop) creates a voltage in the loop with an opposing sign to the original magnetic field, whose associated current creates a magnetic field that interacts with the primary circuit in such a way as to obey the conservation of momentum. Thus, a coupling between the two systems is created, which is the basic operating principle of transformers.

## 2.4 Inductance

**inductance** is the tendency of an electrical conductor to oppose a change in the electric current flowing through it. The flow of electric current creates a magnetic field around the conductor, which in turn interacts with the current in the conductor (as Faraday's law states) and an opposing current (due to Lenz's law) is created. The summation of the two currents is the total current through the inductor.

$v(t) = -\frac{d}{dt}\Phi(t)$

Definition of inductance:

$L = \frac{\Phi(i)}{i}$

$$v(t) = -\frac{d}{dt}(L \cdot i), \quad (14)$$

characteristic equation for inductor

$L = \frac{\iint_{S1} \boldsymbol{B}\cdot\boldsymbol{n}dS}{I}$, n: vector normal to surface, over which integration occurs.

Energy stored in inductor: $E_L = \frac{1}{2}Li_L^2$, this produces a very handy derivation for the calculation of inductance

**Magnetic energy***:* energy stored in magnetic field produced by a magnetic or an electromagnet due to its inductance.

## 2.5 Model of non-ideal transformer

Primary coil: is the coil directly connected to the power supply

Secondary coil: coil connected to the load

$L1, L2$: inductances of primary and secondary coils

$\mathrm{T} = \sqrt{\frac{L1}{l2}}$ *: turn ratio*

$\mathrm{M} = \mathrm{k}\,\mathrm{L1}, \mathrm{k} = \text{coupling factor}$ *: mutual inductance*

$L_{1_{new}} = L1 - M = L1(1-k)$ *: primary inductance of transformer*

$L_{2_{new}} = L2 - \frac{M}{T^2} = L2(1-k)$ *: secondary inductance of transformer*

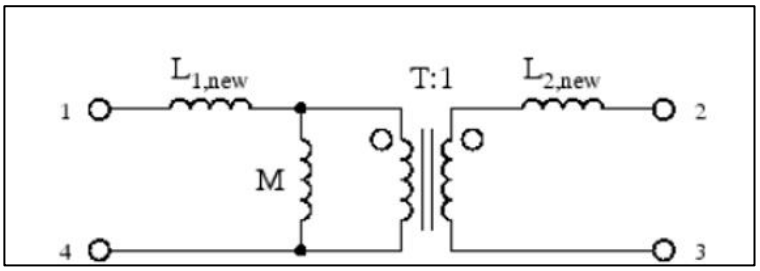


*Figure 5: Equivalent lumped parameter model for non- ideal transformer [7]*

## 2.6 Skin effect

Skin effect is the tendency of an alternating electric current (AC) to become distributed within a conductor such that the current density is largest near the surface of the conductor, and decreases with greater depths in the conductor. It is the phenomenon that leads to a non-homogeneous distribution of current density in a solid conductor. The cause of the skin effect is the varying magnetic field produced by the time varying current, which produces a secondary current inside the inductor, whose superposition with the primary leads to a non-uniform current density.

# 3 ELECTROMAGNETIC OPERATION

In this chapter the operating principle of the launcher will be considered, and thus the way the electromagnetic force is produced needs to be discussed. The force propelling the projectile forward is known as the Lorentz force, which is calculated by the formula below.

$$F_{lorentz} = I \int \boldsymbol{B} \times d\boldsymbol{l} \tag{15}$$

It can be seen, that to derive the force, a path integral needs to be calculated, which although not computationally intensive, does not provide an intuitive way of calculating force. It would be more useful, if it could be derived from an energy perspective, since doing so would produce a physical explanation behind the force. This is possible, since the magnetic field creating the Lorentz force is a conservative one.

$$E_{magnetic} = \frac{1}{2} L i^2 \tag{16}$$

It is also known that for movement in only one axis:

$$F = -\frac{dE}{dx} \tag{17}$$

$$F_{energy} = \frac{1}{2} \frac{dL}{dx} I^2 \tag{18}$$

It is evident from the equation above, that an electromagnetic force corresponds with a change in the total inductance of the system. Or in other words, in order for a force to exist, for an infinitesimal displacement a nonzero change in inductance needs to occur.

It would be easier to visualize this point with a simple example. Let's examine the simple scenario where two coils with opposite but equal in magnitude currents face each other. The magnetic field produced is the superposition of both of the individual magnetic fields created by the coils. Or in other words, the magnetic field at each point in space, and for all three directions, is equal to the algebraic summation of the individual fields.

$$B_1 = B_1(x, y, z)$$

$$B_2 = B_2(x, y, z)$$

$$B_{total} = B_1(x, y, z) + B_2(x, y, z)$$

Assuming that one coil remains stationary and the other is moved relative to it, while the field created by the stationary coil remains the same in every point in space, the magnetic field by the moving coil in respect to the stationary has moved. Therefore, since the total magnetic field is the summation of both fields in each point in space, it has changed with a change in displacement. Furthermore, inductance is a property correlated with energy divided by current squared. Assuming, constant current before and after the movement of the coil, and since the energy stored in the system after the movement is larger, this means that inductance will also be larger, hence a force will be produced. The theory presented above, is the basic theory behind the operation of the railgun. A generalization of this theory will ensue, where the railgun's operating principle is generalized for all electromagnetic motors, thus simplifying greatly their analysis.

## 3.1 Derivation of equivalent inductance

Two methods exist to calculate the equivalent inductance of a system. The one is force based, and makes use of what was stated earlier. The other, and perhaps easier to implement, is based on an energy method.

*Force method:*

Here the reverse process than the one described above is implemented. Knowing that force, is given by the formula:

$$F = \frac{1}{2}\frac{dL_{equivalent}}{dx} I^2_{equivalent} \tag{19}$$

If force is known, from a simulation for example, the inductance gradient can be calculated. By integrating, the equivalent inductance of the system can be found. A similar expression stands true for the calculation of torque.

*Energy method:*

$$E_{magnetic,total} = \frac{1}{2} L_{equivalent} I^2_{equivalent} \tag{20}$$

The problem thus gets reduced to finding the equivalent current of the circuit. By using the equivalent graph of a non-ideal transformer, the current can be derived for each brunch of the equivalent circuit, and by adding all inductors together in a single branch, the equivalent current results. In many applications however like the one presented here, the current can be thought of as the same in the primary as well as the secondary [Paragraph 2.4], thus simplifying the problem greatly. Of course, inductance can also be calculated analytically with the use of the mutual Inductance formula.

To sum up, like the theory above shows, a change in inductance is needed to create a force. This is true for a railgun, as well as for the design presented here. Therefore, the problem of force generation is converted, to the equivalent problem of finding a mechanism, operation, that leads to an inductance gradient. To make this clearer, a brief look at how a rail gun operates will be taken [Paragraph 3.4].

## 3.2 Difference between energy and force method (definition of inductance jump)

Both methods presented earlier are valid for calculating the equivalent inductance of the ciruit. However, they present some differences when indutance changes in a non smooth, irreversible, way (inductance jump).

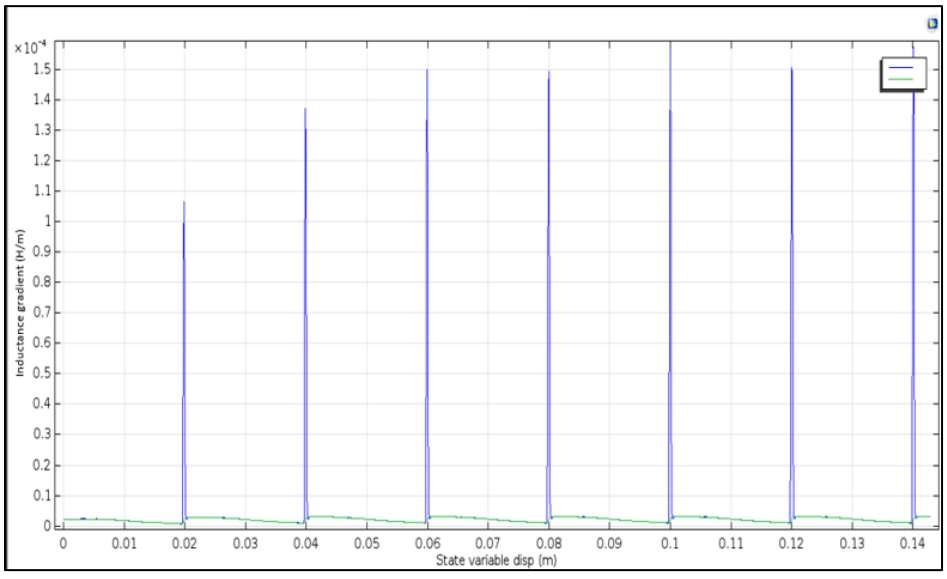


*Figure 6: Inductance gradient as a function of projectile's displacement, as calculated via the energy and force methods*

Inductance gradient for energy and force method (blue: energy, green: force) are graphed in the figure above. It is observed that at regions where change is reversible (smooth) both methods output the same result. In regions however where inductance changes in a non-reversible manner (inductance jump), the energy method outputs big gradient spikes, indicating that a huge force is produced. This however is not the case, which can be seen from the force method, which does not produce a huge force. On the other hand, if the force method is trusted, no loss due to inductance jump will be produced, which once again is not the case. Thus, Inductance jump can be defined in the regions where two methods have non converging results (like above), and its magnitude is equal to the energy inductance jump.

## 3.3 Inductance jump

So far inductance change has been very closely correlated with the generation of a force, which converts the energy stored in the magnetic field to kinetic energy. In many cases however, an inductance change does not create a force. This is true in scenarios where no smooth transition between initial and final inductance exists, or in other words for non-reversible operations.

Such a scenario is presented here, where $inductor\ 2$ is added to the circuit, with the use of a switch as the diagram below shows. Here, it is obvious that inductance changes suddenly and irreversibly.

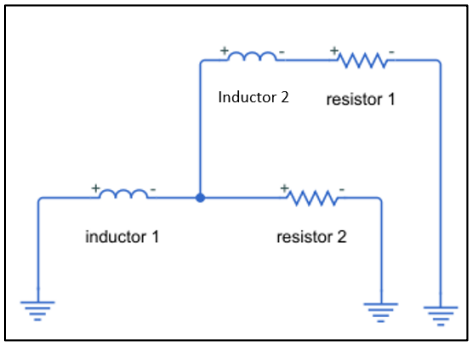


*Figure 7: equivalent diagram to simulate inductance jump*

*Initial conditions:*

$$I_{L1} = 10[A]$$

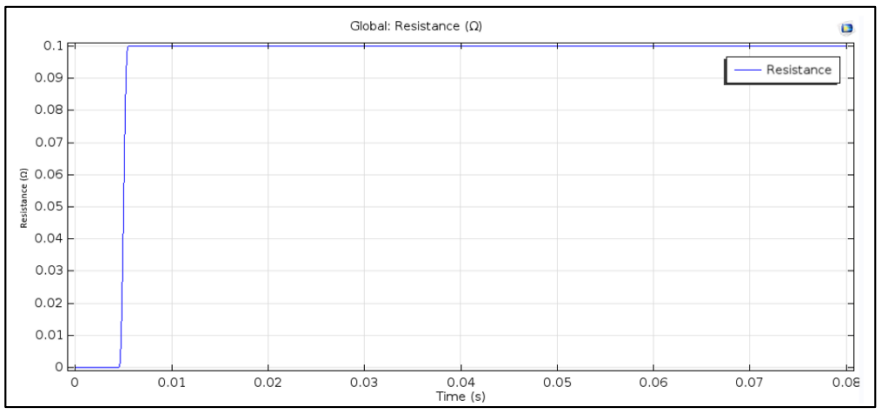


*Figure 8: Resistance 2 triggering inductance jump*

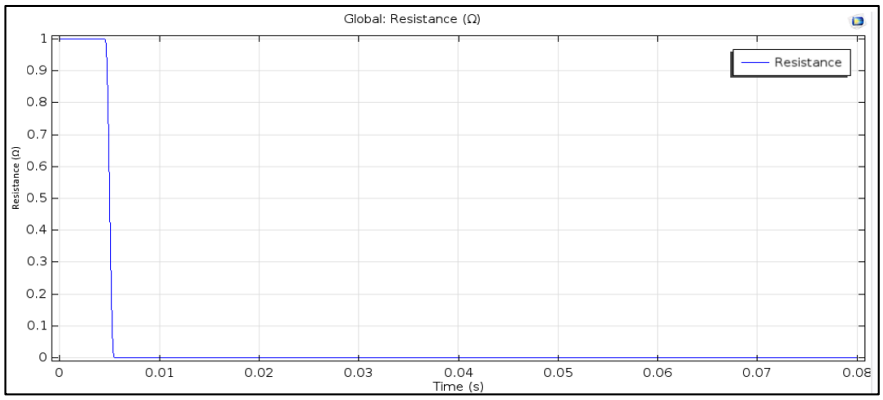


*Figure 9: Resistance 1 triggering inductance jump*

*Hypothesis:* Energy lost is equal to the mechanical energy that would have been transferred to the mechanical system, if change would have happened in a smooth way. Here for example, initial inductance is $L_{initial} = 1[mH]$ (since inductor 2 is isolated from the system due to resistors 1,2). Final inductance is equal to $L_{final} = 2[mH]$. Since inductance doubles, it is expected that energy still stored in the system (magnetic energy) will be the half of the initial magnetic energy: $E_{final} = \frac{E_{initial}}{2}$, since the other half would have been transformed to mechanical energy.

*Results:*

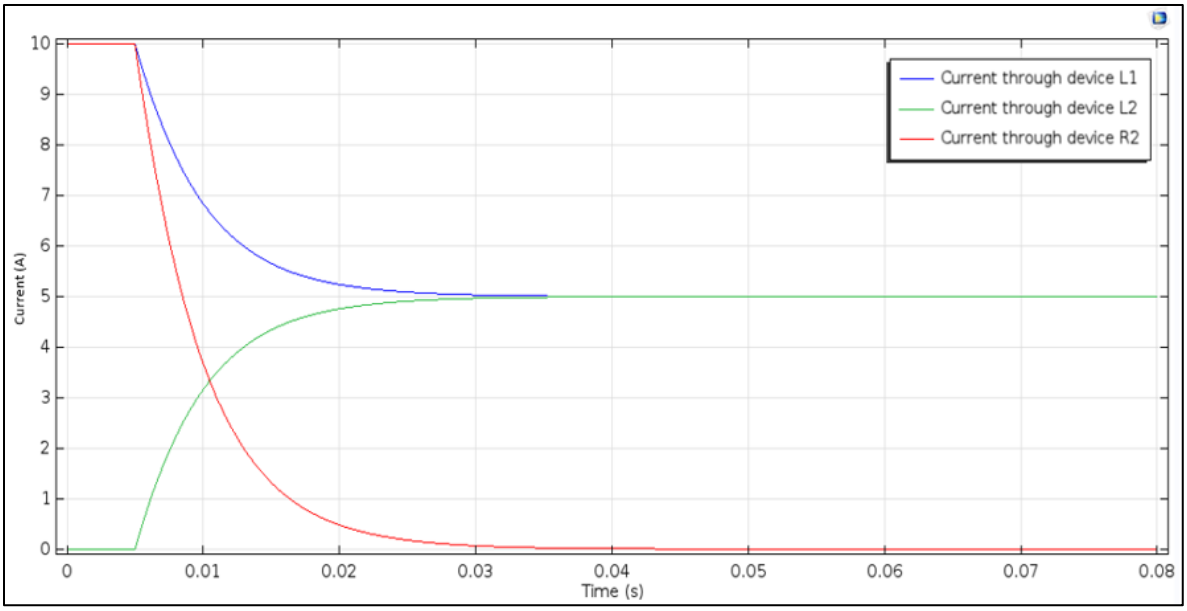


*Figure 10: current before and after inductance jump*

Even though resistance change is implemented in a very quick and sharp manner, current due to the system's inductance follows a less steep path towards equilibrium. Since inductance jump in the operation of the device is relatively small however, and so is the current change, time this transient phenomenon takes can be neglected.

*Energy:*

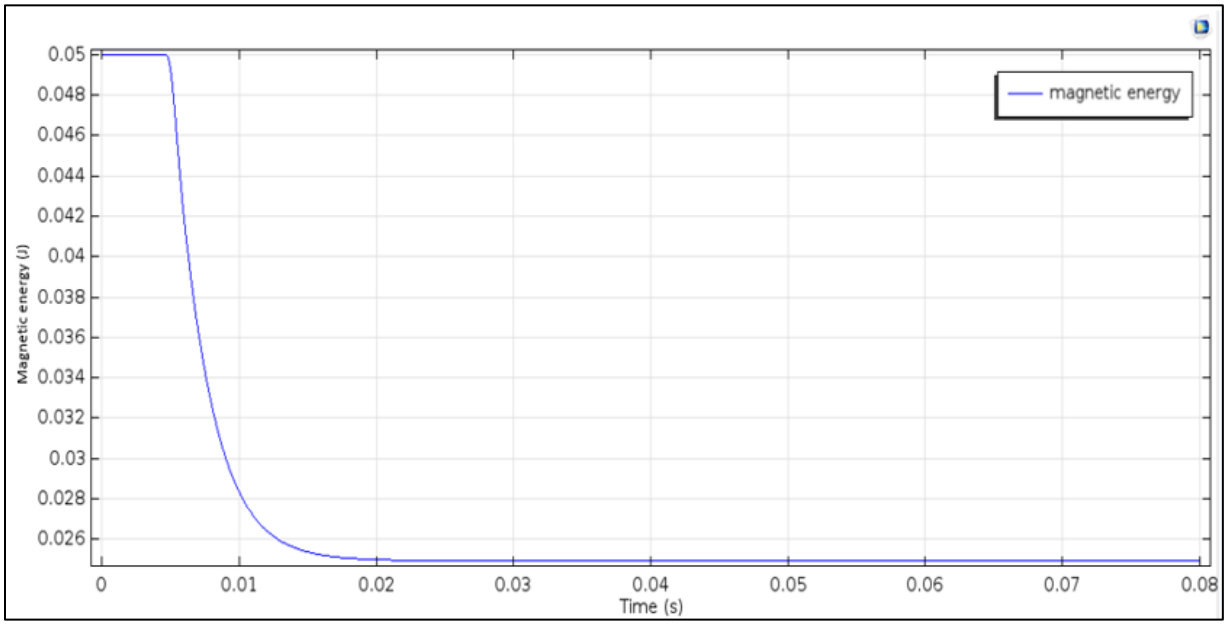


*Figure 11: Energy change during inductance jump*

Final equilibrium state does not depend on the way that the change occurs (as long as change does not happen in a very slow rate). If for example step function does not change as abruptly, but in a smoother fashion, still the final current through the circuit will remain the same, regardless of the shape of the resistance function.

*Smoother resistance step functions:*

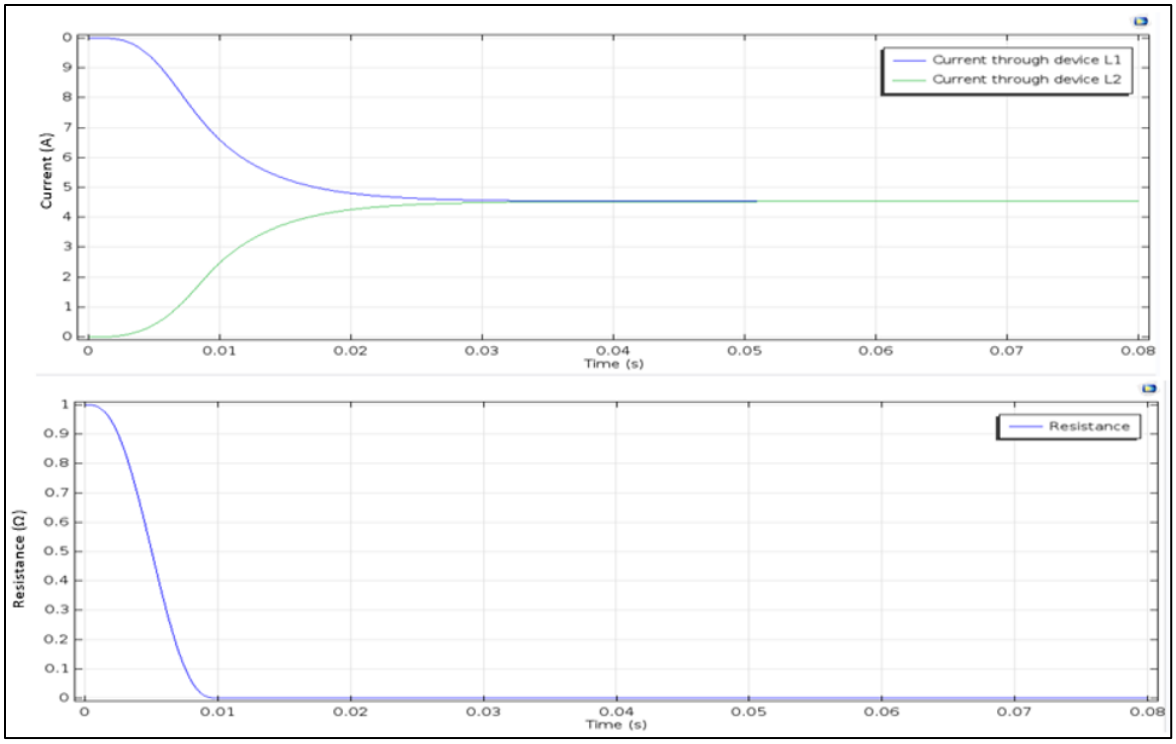


*Figure 12: current during inductance jump simulation(up), resistance change(down) for slow resistance changes*

It can be seen that for a smoother resistance change, the steady state current is almost half of the initial current, as is for the more sudden change.

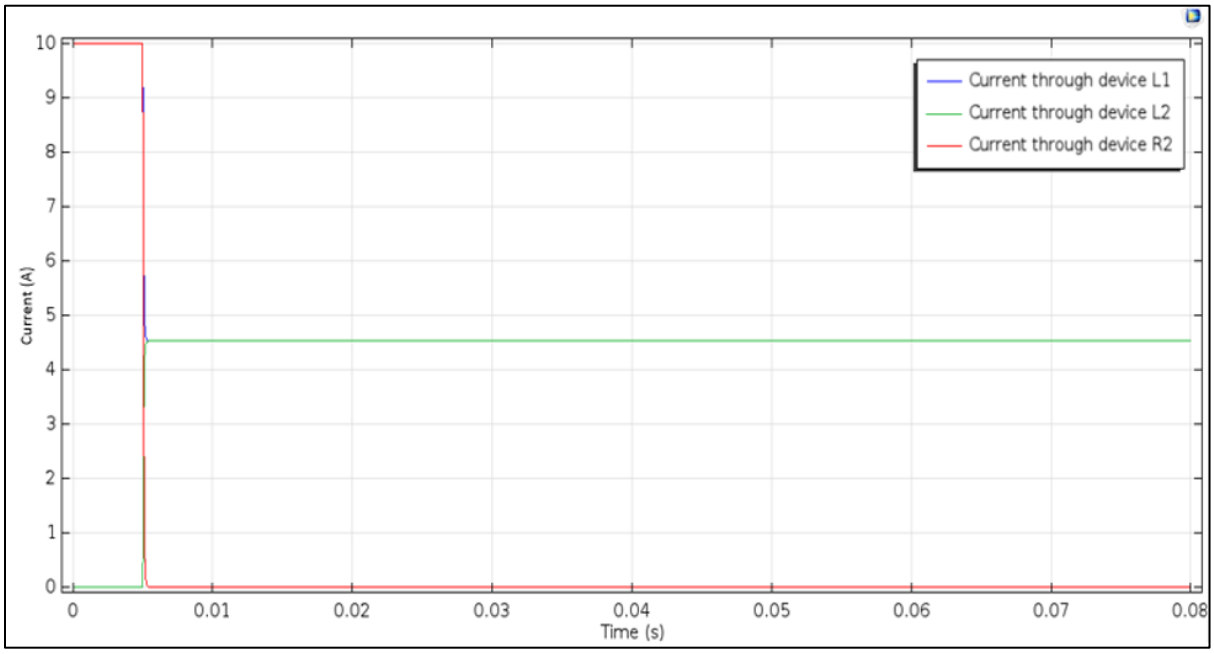


*Figure 13: Current change, with very steep resistance change*

*<u>For higner final resistance:</u>*

Change occurs almost immediately, but ohmic losses are slightly higher. The speed at which the change occurs however, offsets the negative of higher energy losses. Thiscan be delt with by adjusting the resistance of the switch when its open and close. A more correct simulation can be seen later on, where the whole system is simulated in the circuit level.

*Analysis in 2D axisymmetric model to verify results above:*

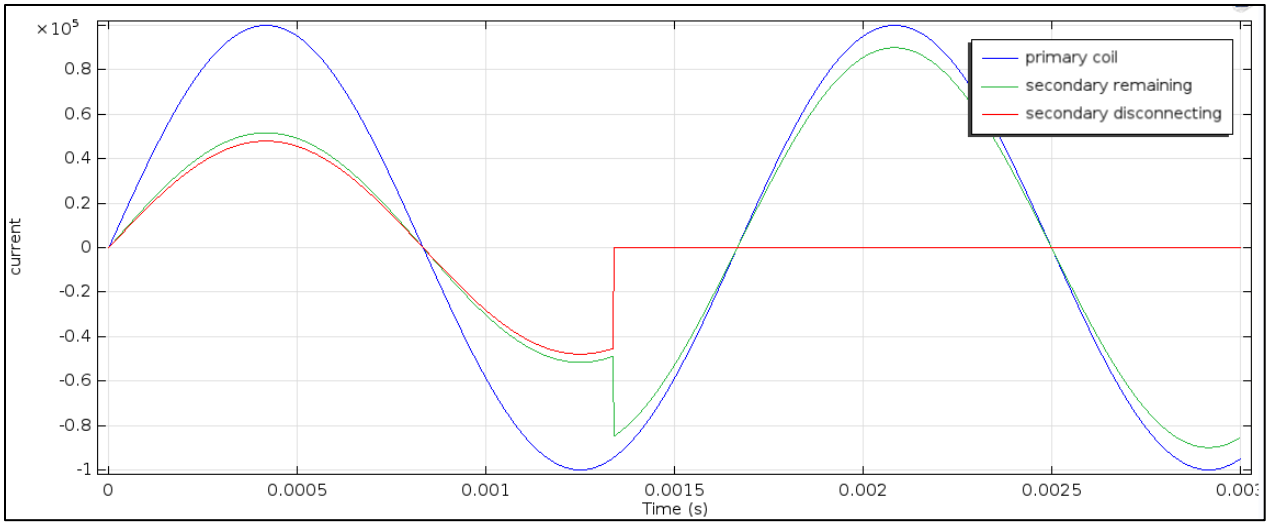


*Figure 14: Primary, and secondary currents for disconnection of secondary coil (time dependent analysis)*

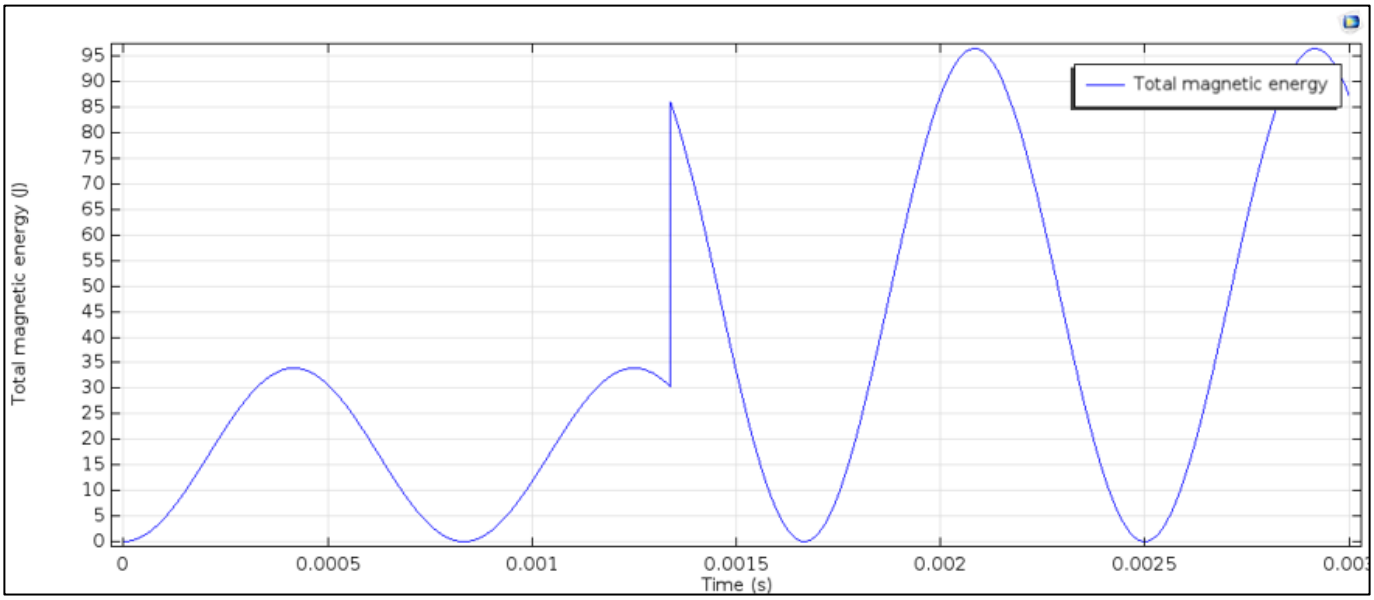


*Figure 15: Energy stored in system, before and after sudden change, as a function of time*

Ratio of energies before and after change occurs is $2.85$, exactly the same as calculated from the frequency analysis performed later (Paragaph 5.3.5).

## 3.4 Case study: Investigation of synchronous frequency in an asynchronous motor

In an inductance motor, the synchronous speed denotes the speed at which the primary field is rotating. If the rotor rotates at a lower speed, then the device acts as a motor, else, as a generator. In other words, the synchronous speed can be defined as the speed at which the motor stops acting as a motor, and begins acting as a generator. According to the theory stated above, which applies essentially whenever an electromagnetic force is produced, during the motor operation (motoring) the inductance gradient is such that produces a positive torque (positive meaning useful) whereas during the generator mode, a negative torque (given to the system) is produced

Correlating the sign of the torque (force) with the theory above, it is shown that:

$$F_{MAGNETIC} > 0 \leftrightarrow \frac{dL}{dx} > 0, I \neq 0 \tag{21}$$

$$F_{MAGNETIC} < 0 \leftrightarrow \frac{dL}{dx} < 0, I \neq 0 \tag{22}$$

Therefore, the synchronous speed can now be associated with the gradient of the inductance.

$$\frac{dL}{dx} > 0 \leftrightarrow f, \omega < f, \omega_{\text{synchronous}} \tag{23}$$

$$\frac{dL}{dx} < 0 \leftrightarrow f, \omega > f, \omega_{\text{synchronous}} \tag{24}$$

At synchronous speed:

$$f = f_{synchronous} \leftrightarrow I_{secondary} = 0 \tag{25}$$

*Result:*

Synchronous speed in inductance motor exists, in the sense that the rotor's speed cannot overpass it, because inductance gradient does not vary monotonously, as the figures below show. This can be seen more clearly in the case of a simple DC motor. in this example, the primary magnetic field is stationary, and an initial phase shift exists between the primary magnetic field and the field of the rotor. This has as a result, the rotor aligning itself with the magnetic lines of the field in equilibrium condition. This is in other words a local maximum of the system's inductance. To better understand the meaning of synchronous speed, and investigate its applicability in the launcher presented here, a brief analysis of the synchronous and asynchronous motors will ensue.

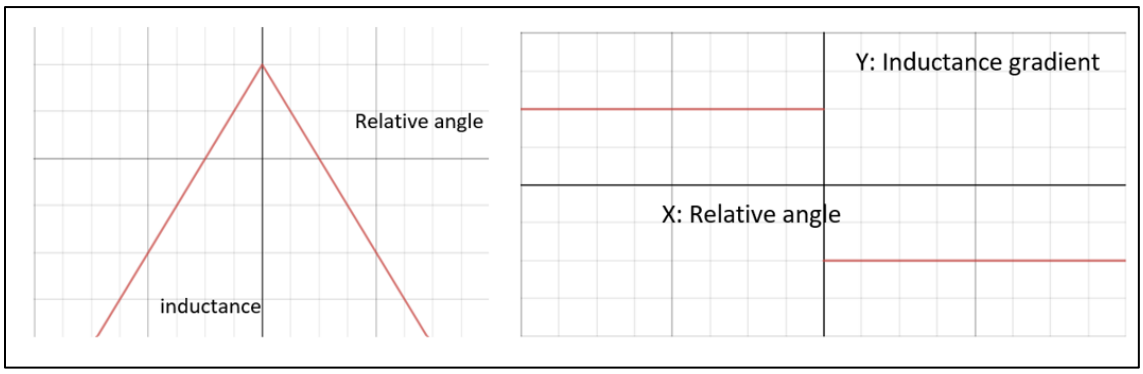


*Figure 16: inductance as a function of relative angle between rotor and rotating magnetic field (left), inductance gradient with relative angle (right)*

*All lumped parameter diagrams that follow were based on the theory discussed above, and differ in a significant way from the ones that are usually being taught.*

## 3.5 Application for railgun

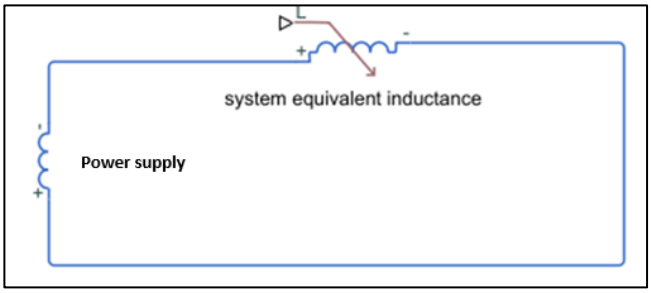


The operation of the railgun can be excellently described by the theory stated previously. It is much simpler to implement and simulate, since there is no secondary connected to the primary through a transformer [as in Thompson's apparatus Paragraph 3.6], yet remains under the same guiding principles. It is the simplest possible configuration an electric motor can have, and thus will be examined first.

*Figure 17: Equivalent diagram for railgun*

1. Force depends on the inductance gradient exclusively
   a. Inductance gradient describes the way energy stored in the system, in the form of magnetic energy changes to kinetic, as the system's geometry changes, due to motion of the projectile.
   b. Inductance gradient is always positive; thus, force always accelerates the projectile forward.
   c. $$\frac{dL}{dx} = \mu_0 \pi \ln\left[\left(\frac{2s+w}{w}\right)^2\right], where\ s = projectile's\ width, w = conductor's\ width \quad (26)$$

## 3.6 Application for Dc motor

Like in a railgun, in all rotating motors, equivalent inductance changes as a function of the rotor's rotation, relative to the primary magnetic field (which in the case of the DC motor is produced by stationary magnets). When total inductance becomes maximum and starts changing sign (this happens when primary and secondary magnetic fields are parallel to each other, with the same direction), the current in the rotor changes direction (due to brushes), effectively lowering the total system inductance (phase shift added between the two fields), and thus producing a torque. One would think that since no geometry change occurred that the total inductance of the system would not change. Equivalent inductance of the system however, based on energy method, depends on an equivalent circuit current, which in this case does change. In other words, for different current polarities, state with least magnetic energy (max inductance, zero inductance gradient) is different, as if rotor had rotated 180 degrees relative to the stator. The diagram for a dc motor based on the theory above, and for one rotor coil winding is as follows:

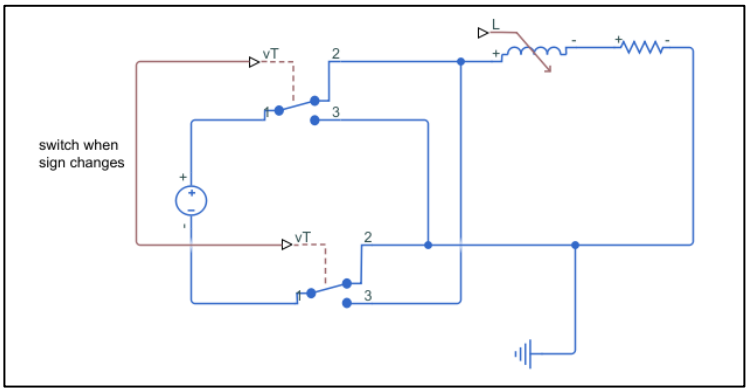


*Figure 18: Equivalent diagram for dc motor, based on theory presented above*

Switches are used to simulate the action of the brushes, which effectively switch the sign of the current, and thus rotate the secondary magnetic field by 180 degrees, increasing the angle between the two magnetic fields. This forms a feedback loop with the variable inductance, adding a phase shift between the magnetic fields, and thus continue to produce torque. In this example no synchronous speed exists due to this aforementioned feedback loop. As it's known from classic DC motor theory, torque is proportional to current, and not current squared as the model above would imply. Indeed, in the model above, a current is assigned to the primary magnetic field produced by the stationary magnets and a transformer is inserted connecting the primary with the rotating magnetic field of the rotor (as done in the analysis of the synchronous motor), it can be seen that torque will depend on both primary and secondary currents, or in other words from the stationary and rotating magnetic fields. The primary current affects the torque constant of the rotor, and thus indeed torque produced will depend only linearly with the current of the rotor (as expected).

## 3.7 Application for Thompson jumping ring apparatus

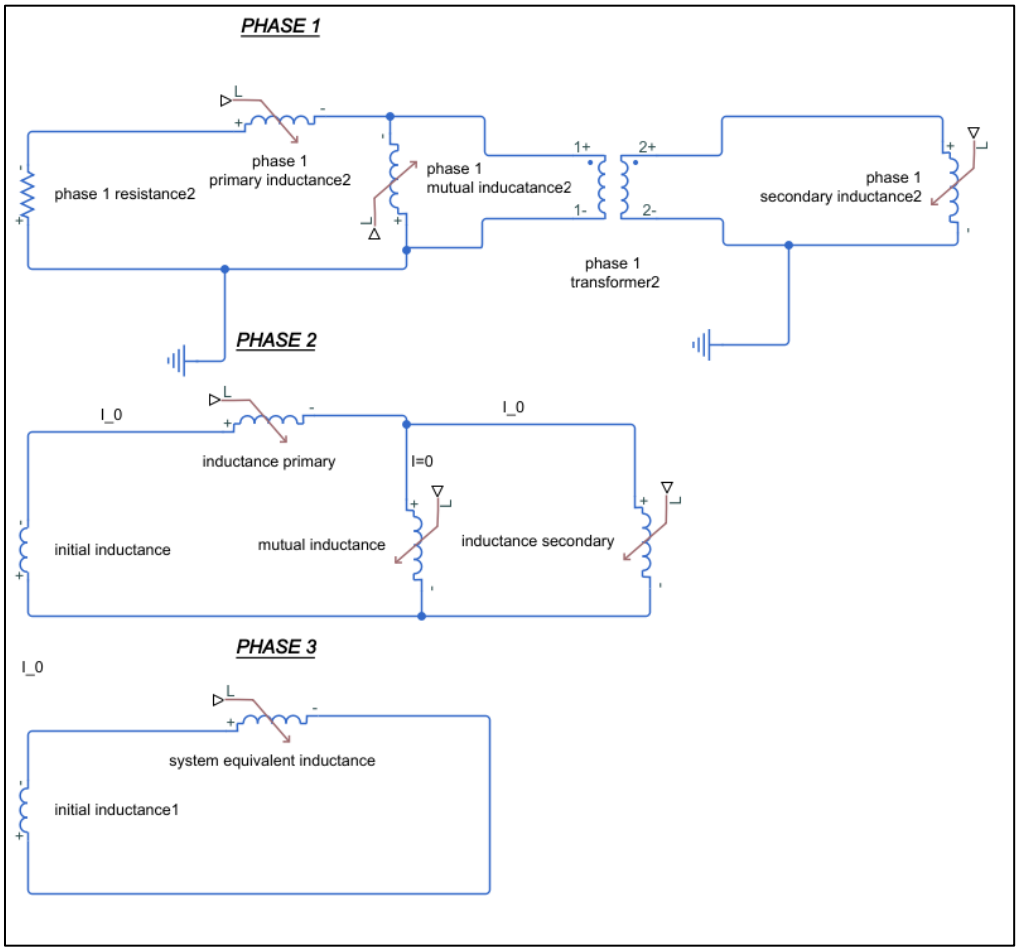


*Figure 19: Equivalent diagram for Thompson's jumping ring experiment, and simplified stage*

Above is presented the lumped parameter model for the Thompson jumping ring apparatus, in its full model as well as with its simplified diagram. Same as before, inductance gradient can either be calculated analytically or from a frequency analysis done to the 3D model. As the phenomenon evolves the following can be noticed:

1. Coil current will be the same for both coils, if power supply voltage is zero, and both coils had the same initial current
2. Force repels the coils, since inductance gradient is greater than zero ($L_g > 0$)
3. If primary coil is connected to a power source:
    a. Coils can be modelled with the use of a transformer, with variable coupling factor, since the distance between them changes
    b. From transformer theory, a change in primary due to coupling causes change in secondary
    c. If for instance the coupling factor is 100%, then the same change occurs in the primary and the secondary
    d. If the coupling factor is 50%, current in the primary will quadrupled, whereas in the secondary only double.
    e. From a parametric analysis the following can be defined:
        i. Total equivalent inductance of system. The electromagnetic force is attributed to change of this magnitude
        ii. Mutual inductance between relatively moving parts, denoting the coupling between the primary and the secondary, and how a change in one coil affects the other.
        iii. Synchronous speed is the speed at which the net voltage at the secondary sums to zero. Or in other words, voltage drop due to position change, associated with inductance gradient equals voltage

induced from the power supply. The main difference with induction motors is the fact that inductance gradient in this apparatus never changes sign, and thus force always accelerates the projectile, even when "synchronous speed" is reached and even overpassed.

*Equivalent synchronous speed for linear motion, where secondary is connected to power supply.*

In the aforementioned scenario, where two coils are facing each other, the equivalent synchronous speed can be derived as follows. Primary coil has an initial current $I_P \neq 0$. If the primary coil is physically moved towards the secondary (reducing their distance), then is speed, is the equivalent synchronous speed for the linear system.
*Simulation setup:*

1. Same initial current in primary and secondary: $I_p = I_s = 1000[A]$
2. Voltage source: $V_s = 0$

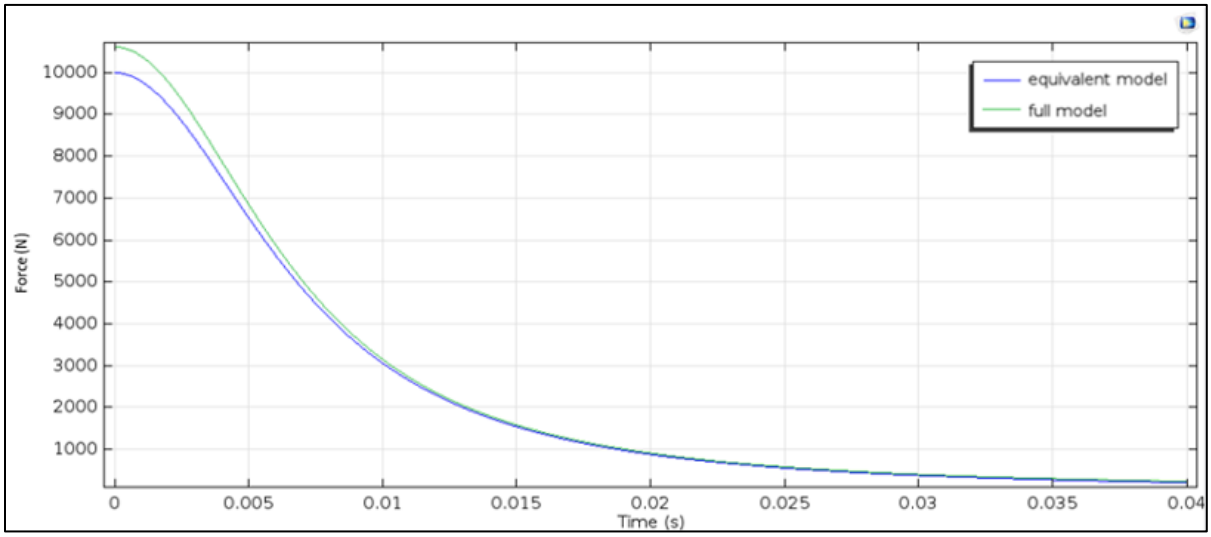


*Figure 20: Force comparison between simplified model (phase 3) and full model (phase 1) for Thompson's jumping ring*

$$equivalent\ model \equiv phase\ 3\ of\ Fig.20, \quad full\ model \equiv phase\ 1\ of\ Fig\ 20$$

Excellent matching between two different simulations is observed, apart from a small difference which can be associated with improper initial conditions of the simulation setup.

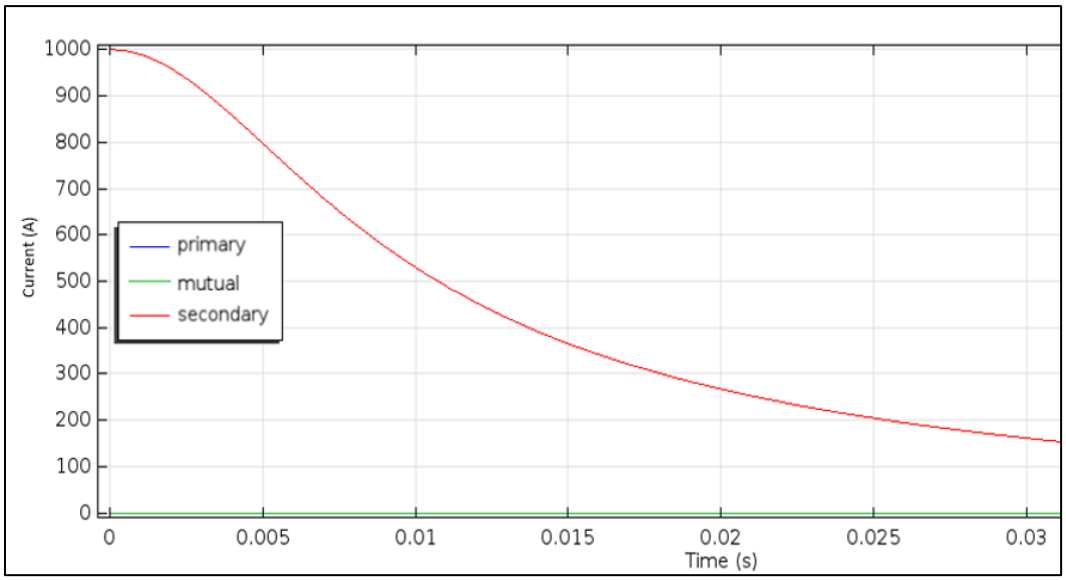


*Figure 21: Graph of current at primary and secondary coils for Thompson jumping ring apparatus as well as current through the intermediate mutual inductance branch.*

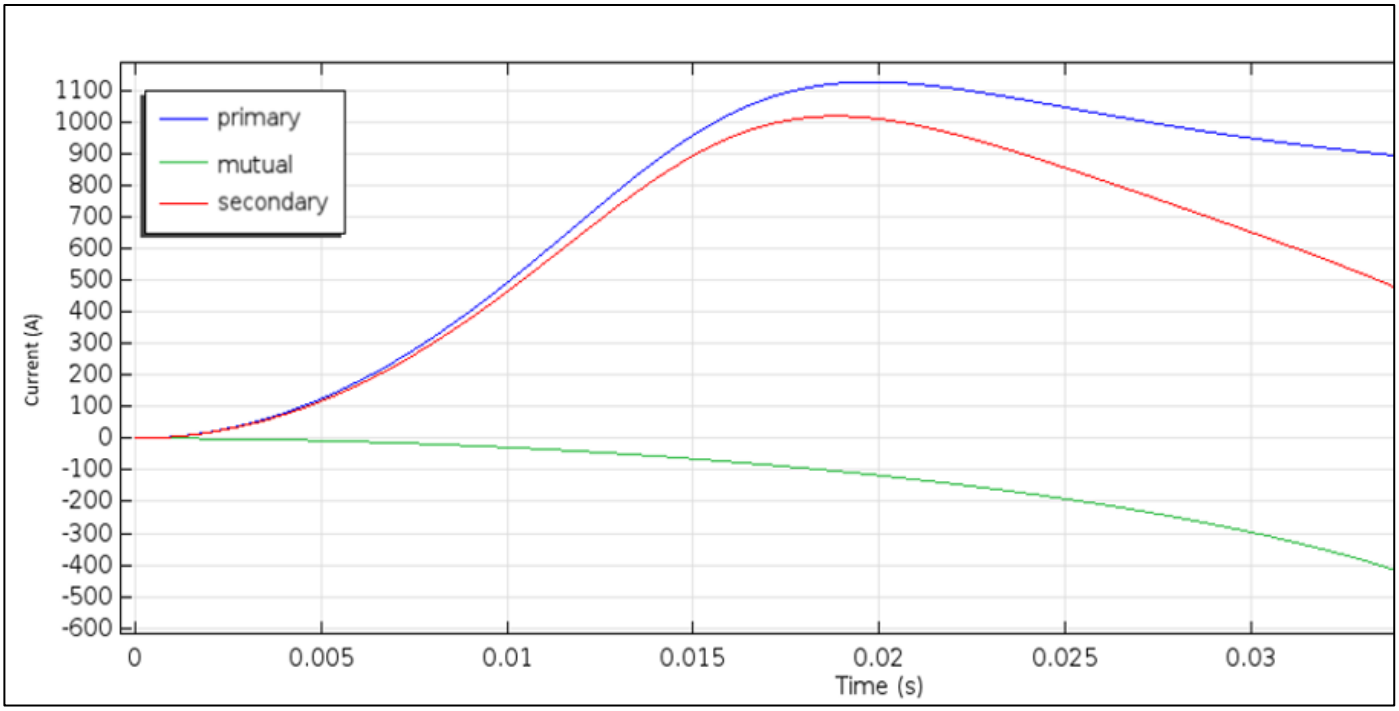


*Figure 22: Current for Thompson jumping ring (phase 1) for 0 initial current and nonzero voltage*

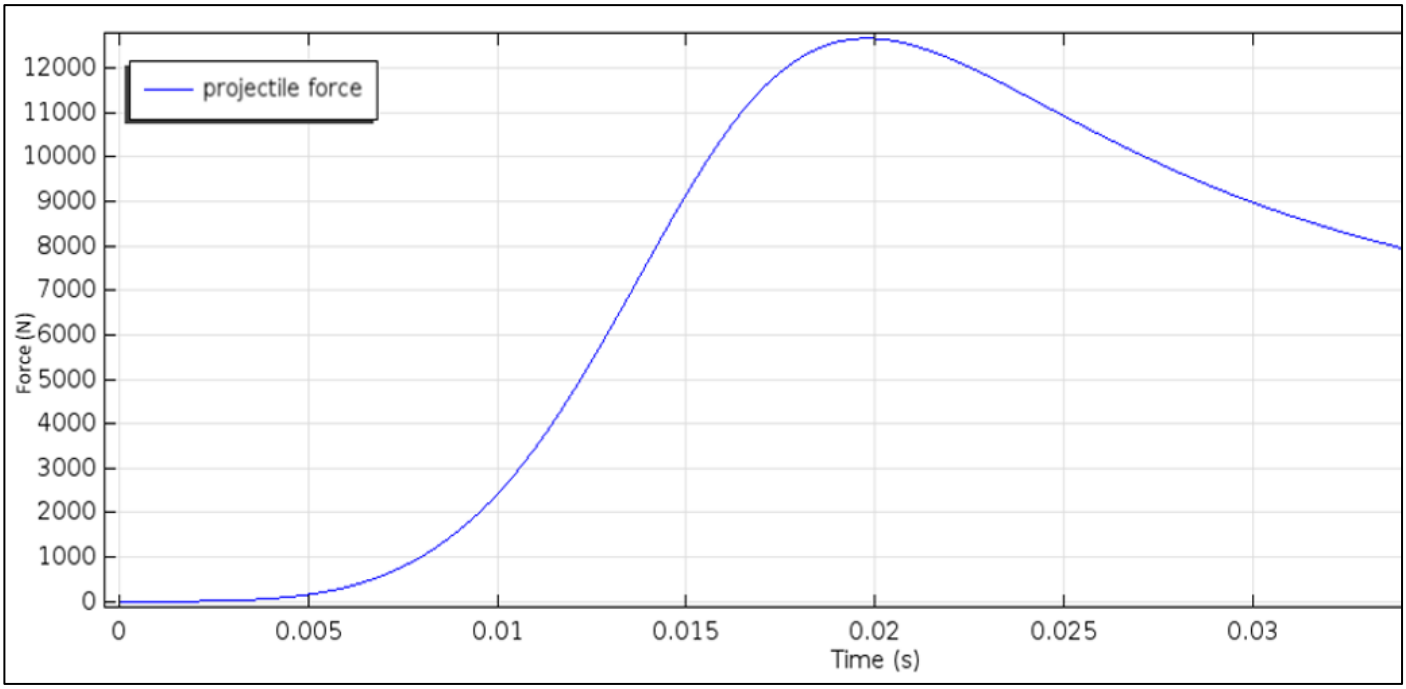


*Figure 23: Force created, propelling secondary forward, Voltage: $V_p = 100000 \cdot t\ [V]$*

In the figures above the operation of the Thompon jumping ring apparatus can be seen for zero initial currents, and for a voltage source whose output voltage changes linearly with time. Maximum force is reached when primary and secondary currents are at their maximum. From then on, force diminishes since currents and the gradient of the inductance as a function of displacement diminish as well.

## 3.8 True inductance gradient voltage vs total voltage at secondary

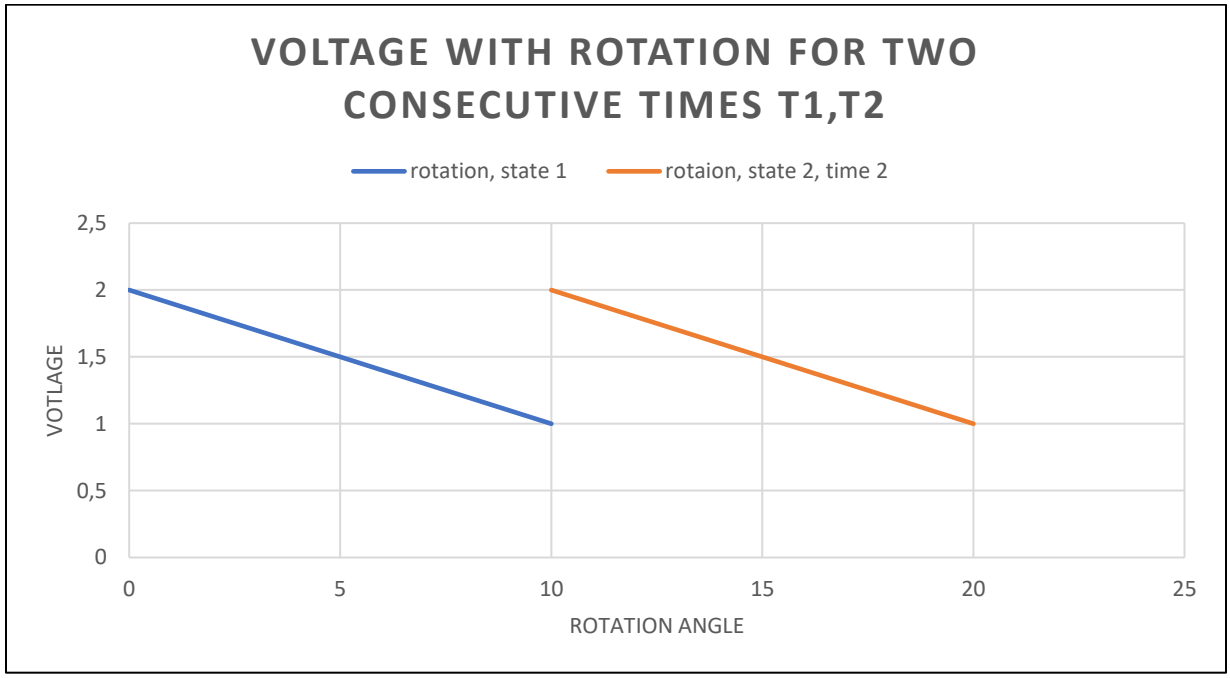


*Figure 24: Voltage due to inductance gradient, versus voltage from power supply, for two different times (dt)*

The difference between total voltage versus induced voltage at the secondary will now be discussed. In order to calculate the voltage produced due to inductance gradient (movement) comparison between the same time should be made, or in other words compare first blue point with second blue point in the diagram above, and the same for the orange graph. Comparison between first point of blue line and first of the orange line is equivalent to the total voltage change in the secondary, due to the power source and the movement of the rotor. Or in other words, it is the superposition of voltage produced due to inductance gradient, and an equal voltage of opposite sign induced to the secondary by the primary. in this case, the total voltage is zero. This state characterizes what happens at synchronous speed for an asynchronous motor.

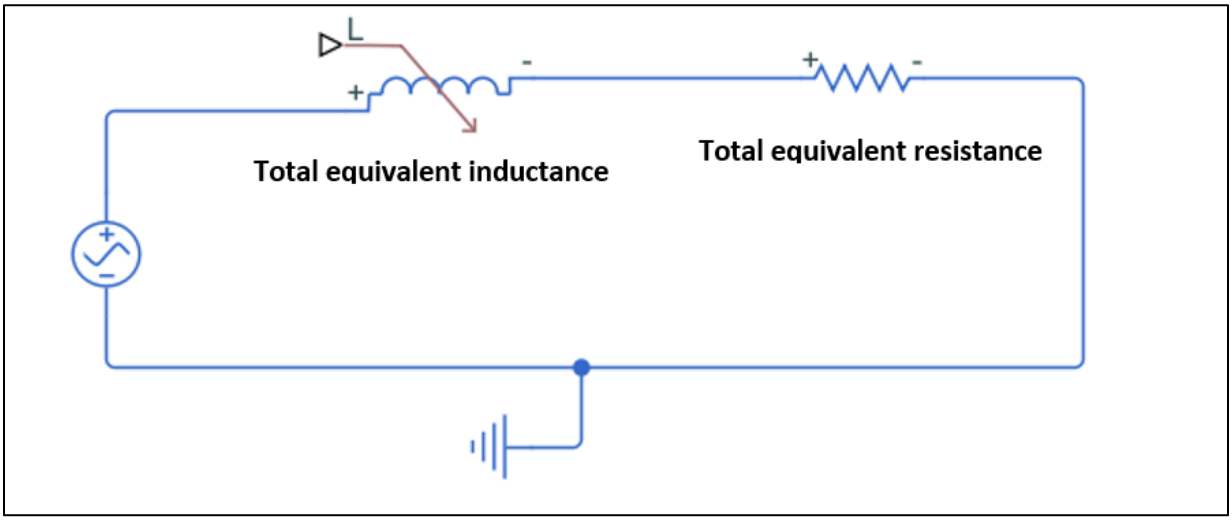


*Figure 25: Simplified diagram for asynchronous motor as presented above*

## 3.9 Application for synchronous motor

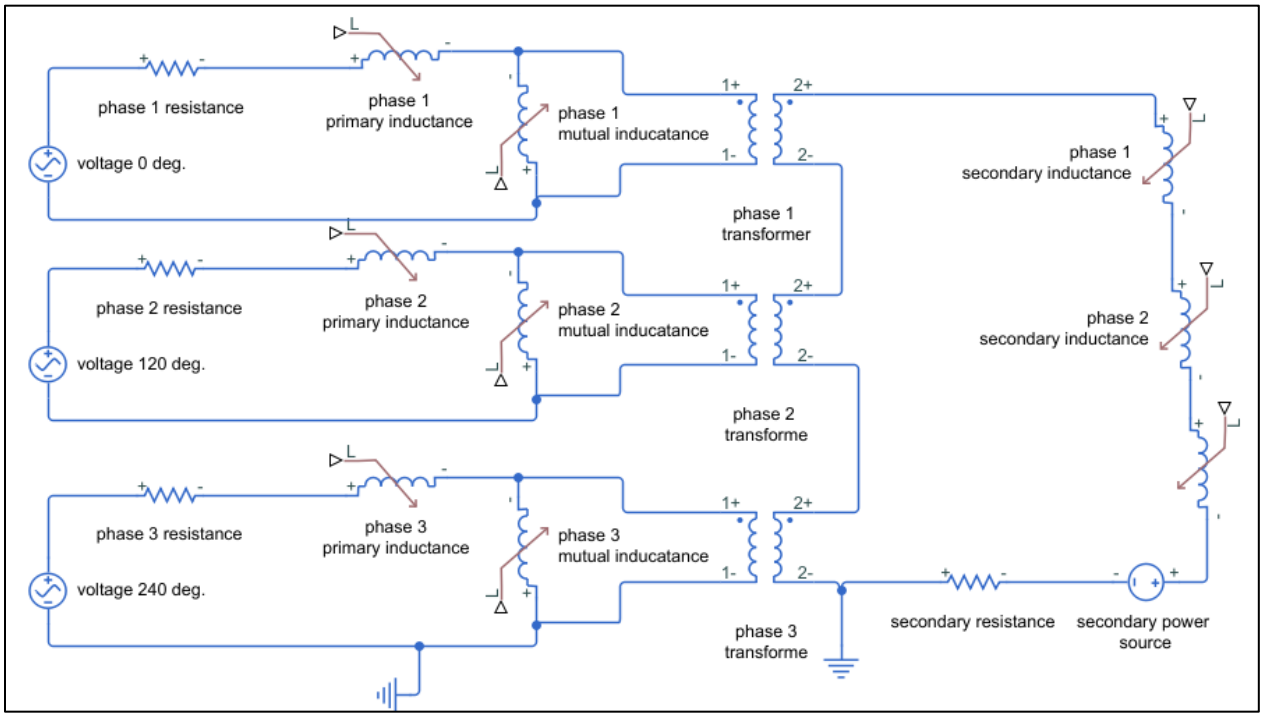


*Figure 26: Full diagram for synchronous motor*

In a synchronous motor, three primary coils exist, each with a phase difference to the others, and one secondary (the rotor), which is connected to a DC power source. All of these can be seen in the equivalent circuit presented above.

*Voltage sources:*

Synchronous motor operates due to the formation of a rotating magnetic field. In reality this field is produced by three coils, with 120 degrees phase shift, whose fluctuating magnetic field as a superposition creates a rotating magnetic field. This exact configuration is presented above. The diagram does not however in an intuitive way explain why a rotating magnetic field is produced by this coil arrangement.

*Transformers:*

Each primary coil, is connected with the secondary through transformer action. The coupling factor of each transformer depends on the rotation of the secondary coil relative to the angle of the primary magnetic field. The phase difference between the primary and the secondary magnetic fields, can be derived from the model above, from the current phase shift between the primary and secondary coils. No synchronous speed needs to be calculated beforehand to correctly simulate the model, since relative angle between primary and secondary fields is calculated from the currents. This model can also be directly connected to a mechanical system (containing friction, inertia etc.) and be simulated as a whole [more details in Paragraph 3.9].

*Secondary source:*

In synchronous motors secondary is also connected to a dc power supply.

*Simple model:*

When the physical phenomena in action during the operation of the synchronous motor are well known, the simulation can be greatly simplified with the use of one equivalent inductance, and a power supply that would emulate the rotating magnetic field (a constant dc power supply for example). This is done in the example of the Thompson jumping ring experiment.

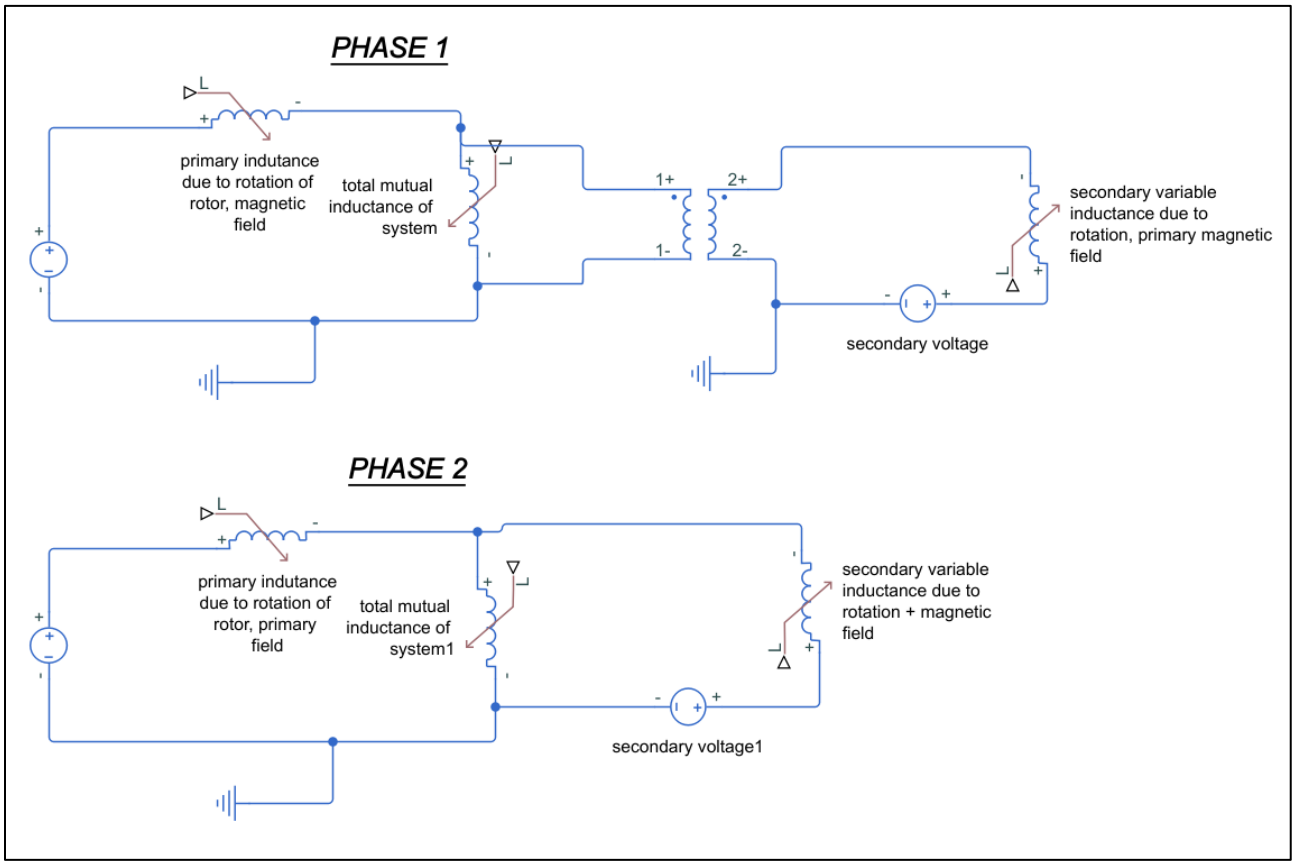


*Figure 27:Steps to simplify complex diagram seen in figure 25*

## 3.10 Application for asynchronous motor

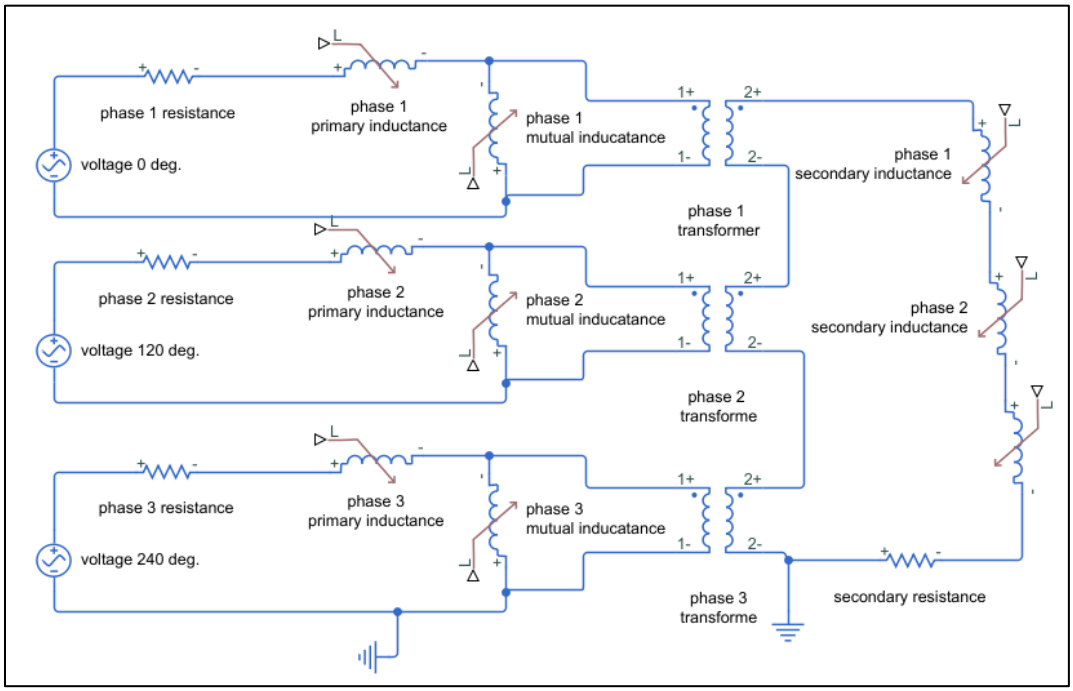


*Figure 28:Equivalent full model describing the operation of an asynchronous motor*

In the model presented above the equivalent diagram of an asynchronous motor can be seen. Same as for the synchronous motor, the synchronous speed does not really have any kind of physical meaning, in the sense that it needs to be entered in the model beforehand. It is instead calculated by the model. Also, power supply is $120\ degrees$ phase shifted for each branch of the primary circuit.

*Synchronous speed is derived from*

1. Power supply frequency
2. Number of phases
   a. Rotating secondary does not have its own current in contrast with synchronous motor, and thus its operation is termed as asynchronous, since if speed was equal to the synchronous, current induced to secondary would be zero as extensively explained in Paragraph 3.7.
   b. This can be understood from the three transformers, whose total voltage plus the voltage due to the rotor's movement at the secondary will add up to zero, for synchronous speed.

Variable inductance in the model above is a function of the absolute mechanical angle of the rotor, relative to the assigned zero, and not of the relative angle between the primary and secondary magnetic fields. Each inductance assigned to a different phase, also has a phase shift of $120\ degrees$ .

*Equivalent diagram with 1 phase (simplified)*

First of all, a good way to represent the rotating magnetic field needs to be found. One possible way is to have a dc power supply, and a variable inductance, whose inductance gradient represents the "movement", rotation, of the primary field according to the electrical speed (synchronous speed). It is easier to group these added inductances with the already existing variable inductances of the system (that depend on the geometry of the system), which depend on the rotational speed of the rotor. This can be seen in the figure below.

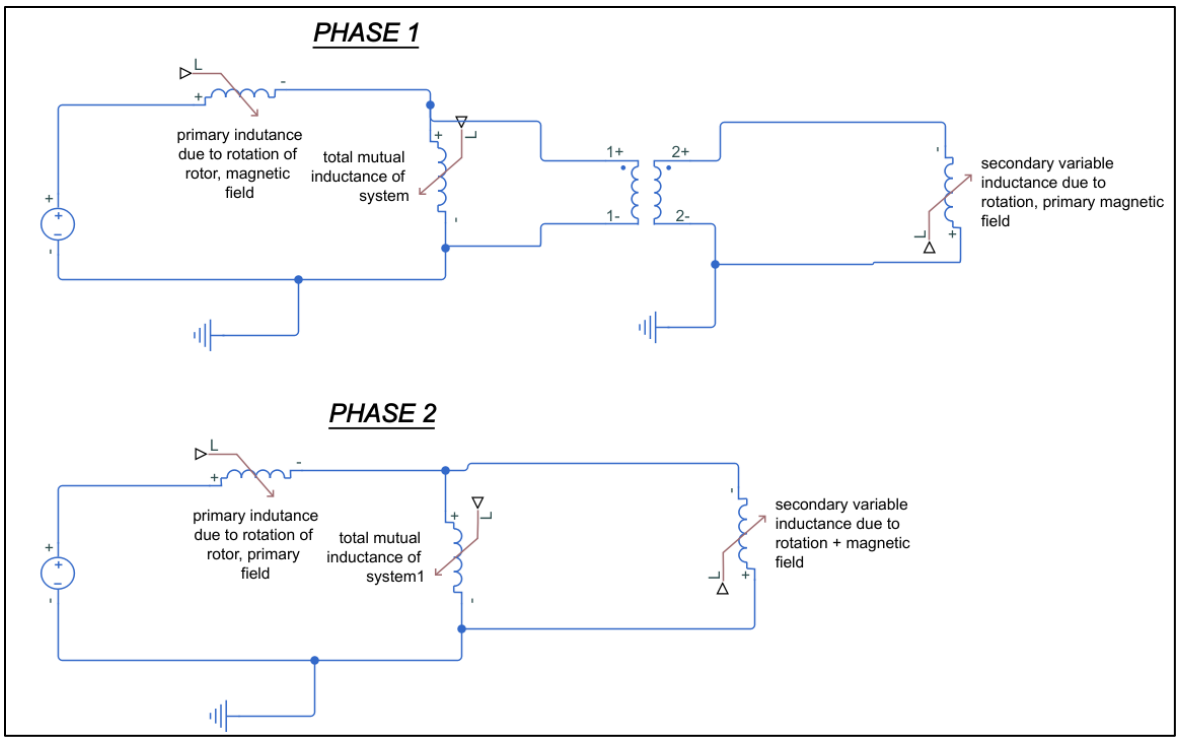


*Figure 29: Simplified model for asynchronous motor operation*

Torque depends on $\frac{dL}{dx}$, whereas in the circuit variable inductance depends on time ($\frac{dL}{dt}$). The two are connected through the velocity. An inductance gradient can still exist even if inductance remains stationary with time, as seen here.

$$\frac{dL}{dt} = \frac{dL}{dx_{relative}} \frac{dx_{relative}}{dt} = \frac{dL}{dx_{relative}} \frac{d(x_{electric} - x_{rotor})}{dt} \tag{27}$$

$$P_{electric} = \sum \frac{dL}{dx} \frac{dx_{electric}}{dt} I^2 \tag{28}$$

$$P_{rotor} = \sum \frac{dL}{dx} \frac{dx_{rotor}}{dt} I^2 \tag{29}$$

$$\frac{dL_{primary}}{dt} = \frac{dL_{primary}}{dx_{relative}} (\omega_{el} - \omega_{rot}) \tag{30}$$

$$\frac{dL_{rotor}}{dt} = \frac{dL_{rotor}}{dx_{relative}} (\omega_{el} - \omega_{rot}) \tag{31}$$

$$Torque = \frac{1}{2} \frac{dL_{primary}}{dx} I_{primary}^2 + \frac{1}{2} \frac{dL_{mutual}}{dx} I_{mutual}^2 + \frac{1}{2} \frac{dL_{secondary}}{dx} I_{secondary}^2 \tag{32}$$

When $\omega_{el} = \omega_{rot}$ :

1. $\omega_{el} - \omega_{rot} = 0 \leftrightarrow \frac{dL}{dt} = 0$

Current flows from path of least resistance which in this case is the branch of the mutual inductance (since other brunches have resistive elements as well (which are not depicted here)

$$I_{secondary} = 0$$

2. $Torque = 0$

$$Torque = Torque_1 + Torque_2 + Torque_3 \tag{33}$$

$$Torque_3 = 0, since\ I_{secondary} = 0 \tag{34}$$

$$Torque_1 = -Torque_2, since\ I_{primary} = I_{mutual}\ and \frac{dL_{primary}}{dx} = -\frac{dL_{mutual}}{dx} \tag{35}$$

3. $P_{electric} = P_{rotor} = 0, I_2 = 0, \frac{dL_{mutual}}{dx} = -\frac{dL_{primary}}{dx}$
4. Even though $\frac{dL}{dt} = 0, \frac{dL}{dx} \neq 0\ (depends\ on\ geometry\ only)$
5. Difference with synchronous motor, where same diagram applies but branch with secondary has an added voltage source.
    a. As a consequence, at synchronous speed, power won't be zero, unless of course when $\frac{dL}{dx} = 0$ .
    b. Investigation of torque as a function of relative angle between the fields
        i. This depends on inductance gradient, if its assumed that everything else is constant (current etc.), then as phase shift increases inductance gradient should increase as well. Limits of torque angle: $0 \leq \delta \leq \frac{360}{\frac{N}{2}}$, since for an angle greater than this model is axisymmetric, where $N$ =Number of poles of the rotor

*Possible design space, inductance change rules:*

To sum up, force gets produced due to an inductance gradient; the total system inductance can change in one of the three ways presented below:

1. Mutual inductance change as, as a function of geometry (displacement, rotation etc.), when stationary and moving components consist of different inductors, in device's equivalent circuit.
2. Inductance change, as a function of geometry, when moving and stationary components form a single inductor (like in railgun for example) as seen from the device's equivalent circuit.
3. Inductance change due to current change, when system's equivalent current and total magnetic energy change in a non-linear way to each other (this is related to magnitude of inductance jump):
    a. Total magnetic energy
        i. Depends on all individual magnetic fields produced by all stationary and moving components, which depend on magnitude and direction of current flow through every inductive element in the equivalent circuit.
        ii. For energy a sense of directionality exists, in the sense that opposite magnetic fields cancel each other out, and thus system's total magnetic energy will be less.
            a. Directionality (field in every point in space) in a magnetic field can change with physical movement (move magnet in space), or virtual (change current polarity in magnet, like in DC motor and rotating magnetic field in induction motor). Although this rule has merit, I could not express it in a more formal way.
        iii. Max current in equivalent circuit remains constant. If other currents change relative to it then system's inductance changes as well. This can be thought of as changing the number of turns of the coil whose current changes, in a way that its individual magnetic energy changes in the same way, while keeping its current constant. It is obvious that inductance in this case does change (this is not entirely accurate).
            1. Current change can occur due to:
                a. Resistance change, where energy difference is dissipated as heat
                b. Capacitance change, resonant $LC$ circuit gets formed
                c. External power supply

From the Lorentz force, and formula for force through inductance gradient, a correlation can be made between their constituent parameters.

$$F_Z = B_R(I)Il = \frac{1}{2} L_g I^2 \tag{36}$$

$$B_R l = \frac{1}{2} L_g I, I = I \tag{37}$$

A correlation between the magnetic field perpendicular to the axis of motion with inductance gradient can be established. It is obvious that for force to exist, the moving component has to have a current passing through it. For the two categories mentioned above, common and different inductors, current can be produced by :

1. Single (common inductor between stationary and moving components) (planar problem)
    a. Moving electrical contact (like railgun), can be made through one-dimensional change in geometry of device (stretching in one axis)
    b. Deformation of structure in 2 dimensions (total length of current currying wire remains the same). An example is a loop of wire whose boundary expands when current passes through it, in order for area enclosed between its boundaries to grow.
2. Different inductors (general 3D problem):
    a. Current in moving inductor(s) exists purely due to electromagnetic induction (induction motors)
    b. From power supply, with moving contacts (DC motor)

# 4 ALTERNATIVES-PAST DESIGNS

In this chapter the models designed leading to the final concept will be discussed. Many alternatives where considered, before a more rigorous analysis was done to correctly identify the parameters creating the force to accelerate the projectile [Paragraph 3]. Here not all of the models studied will be presented, since many of them where at an entirely different philosophy than the final design. The operating principle of each device will be briefly examined as well as the reasons that led to its abandonment. Although the theory presented earlier is still valid for all of these electromagnetic devices, no simulation was done, since the designs were discarded. Step by step however, they led to the final design presented in depth in this thesis.

A list of requirements needs to exist, in order to abandon a design. This will be presented below:

*Requirements, design goals:*

1. Electrical isolation between primary and secondary
2. Simple construction
3. Device should be as easy to repair as possible, since large forces will be acting on it and something might fail
    a. Thus, components serving different roles should be placed in different subassemblies, because in this way construction, repair and problem diagnosis is simpler.
4. If possible, allow for cooling circuit to be implemented
5. Skin effect does not cause problems to the movement of the projectile
6. Fore as high as possible (in order to achieve high velocities)
7. Low mechanical interaction between stationary and moving parts
8. Efficient, low mechanical and resistive losses

For a better understanding of the desired requirements, they will be applied to the railgun design, the most prevailing device for high velocity projectile accelerators.

| ***ADVANTAGES*** | ***DISADVANTAGES*** |
|---|---|
| Simple construction | Electrical isolation |
| Easy repair | Skin effect causes problems to the movement of projectile |
| Cooling circuit implemented | High mechanical interaction between stationary and moving parts (high contact pressure for low contact resistance) |
| High force | Low efficiency |

*Table 1: requirements satisfaction for railgun design*

*All designs studied, as well as the final solution, have the following in common.*

1. The implementation of some type of switch as part of the design
2. Formation of a coil behind the projectile

## 4.1 Past design 1

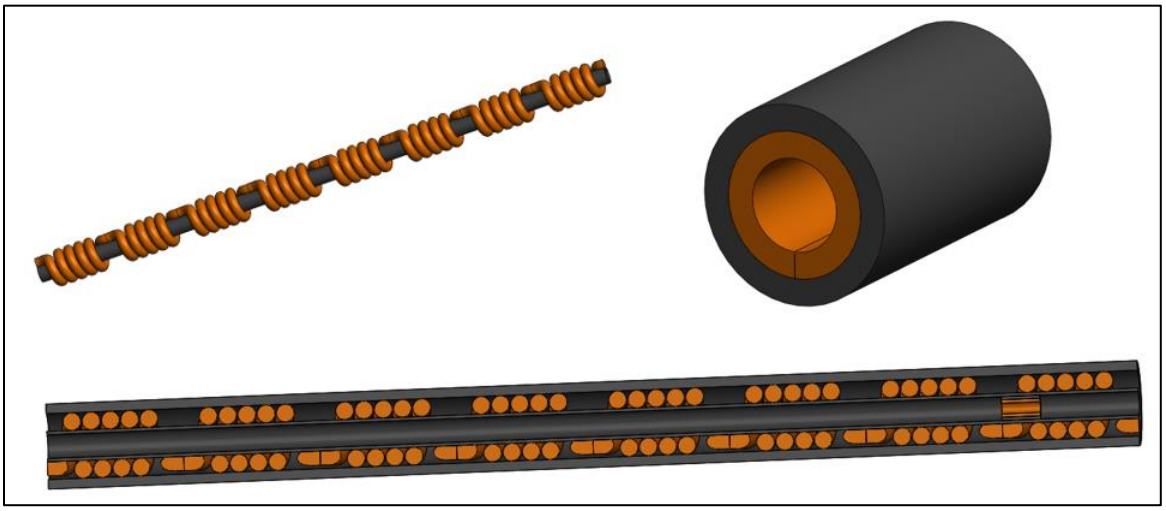

*Figure 30: Assembly of first past design*

This device consists of:

1. The primary (barrel)
2. Secondary (projectile)
3. Outer conductive sleeve to restrict the magnetic field

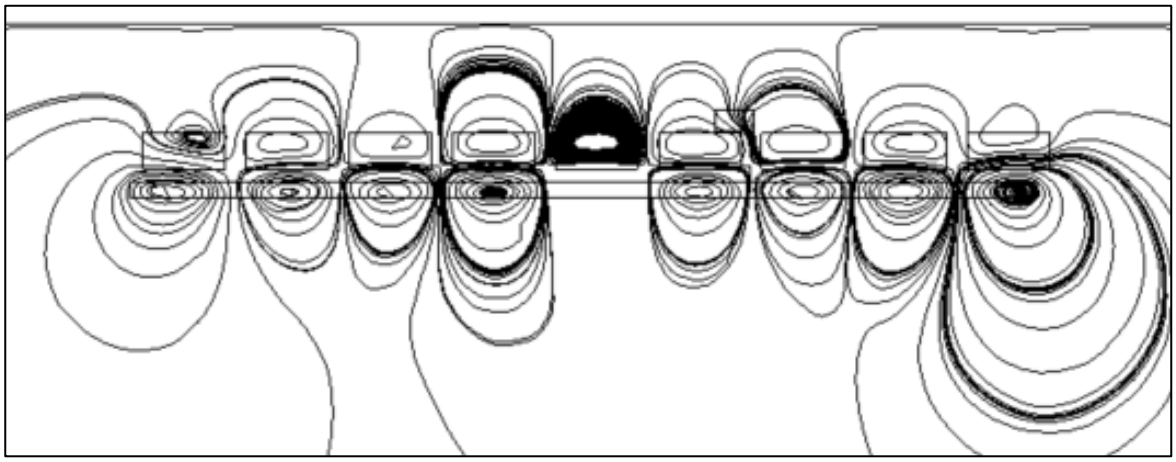

*Figure 31: Magnetic field created by primary coil*

Each consecutive smaller coil forming the primary coil, has a change in the direction of rotation of its windings. This way the field presented above is produced, which is equivalent to that produced by an array of magnets positioned in such a way that similar poles are facing. Projectile is a simple wire coil, whose leads touch in such a way, where they contact only when force acting on the projectile propels it forward. In many ways this design is a combination of an induction motor and a dc motor, but in a linear arrangement. If the primary magnetic field was stationary, and the secondary coil was connected to a power supply with brushes alternating its current, this would form the equivalent of a rotating dc motor. Since however current is induced to the secondary, the device has similarities with the induction motor as well.

### 4.1.1 operating principle

It is obvious from the theory presented earlier that as the projectile moves along the barrel, the equivalent inductance of the system does not vary in a monotonous manner. This produces a force that periodically attracts and repels the projectile as it moves along the barrel, and effectively traps the projectile in a place where a local maximum of the equivalent inductance exists. To avoid this, the force on the projectile should act only when it is

positive. This can be done by opening the secondary circuit when force is negative, and closing it again as soon as force becomes positive. This can be accomplished with a variable contact resistance, whose contact pressure (and thus resistance) depends on the magnitude and direction of the axial force. In this design, skin effect, being the major disadvantage of the railgun is eliminated. The construction of the device is fairly simple, excluding the projectile design that is more complex. It however presents a major disadvantage. When the secondary coil switching occurs, current through the secondary reaches very small values. Afterwards when it becomes connected once again the current starts rising from zero once again. This has as an effect a much smaller axial force, thus limiting the maximum speed of the projectile. What is more, once the projectile starts building up speed, the time the current has to also build up gets even smaller, and the force as a consequence gets smaller too. This can be seen in the graph below for the current (similar drawback with induction coil-gun as mentioned in Paragraph 7.7].

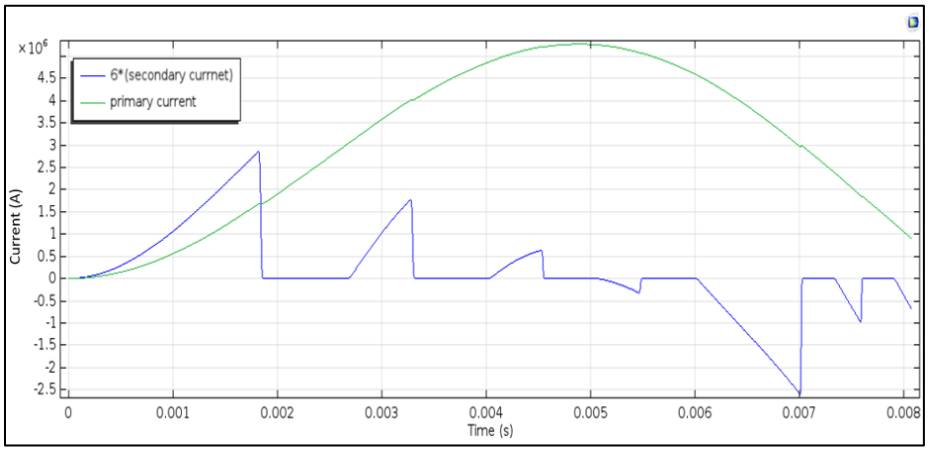


*Figure 32: Primary and projectile currents*

Current if disconnection occurs at standard projectile displacement, as seen above. It is obvious that this is not the desired result, since force is also negative. In this design disconnection occurs only when force is about to go negative, and not at a fixed displacement.

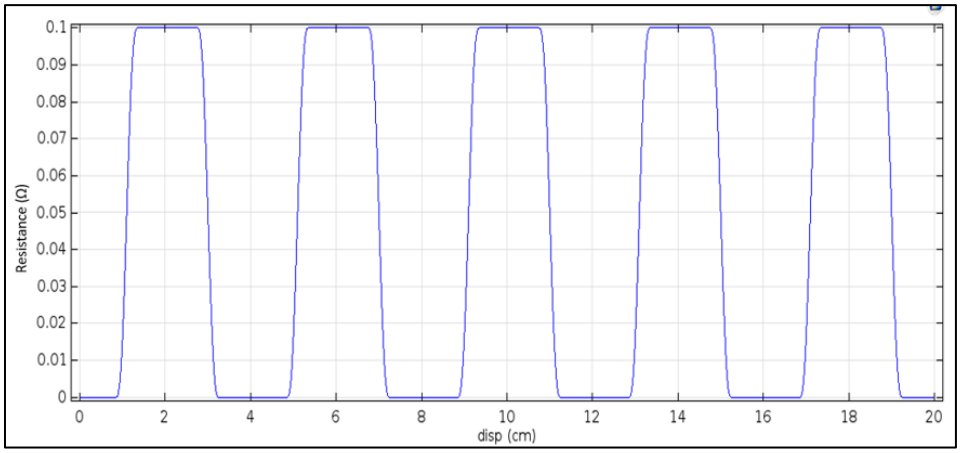


*Figure 33: Variable resistance triggering switching of the projectile*

| ***ADVANTAGES*** | ***DISADVANTAGES*** |
|---|---|
| Simple construction | Low force |
| Easy repair | Low efficiency |
| Cooling circuit implemented | |
| Electrical isolation | |
| Skin effect causes problems to the movement of projectile | |
| low mechanical interaction between stationary and moving | |

*Table 2: Requirement satisfaction for past design 1*

## 4.2 Past design 2

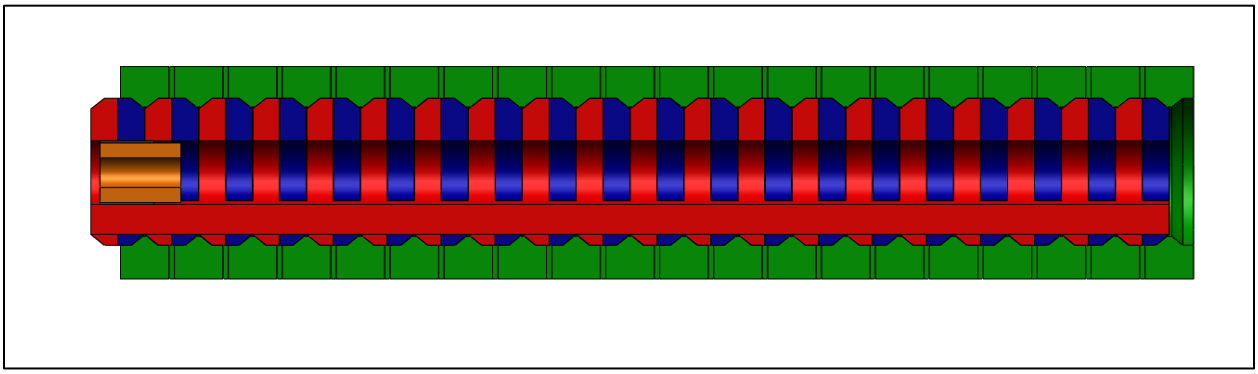

*Figure 34: Simple schematic representation of second alternative (past design)*

In this model, the blue coil is connected to one lead of the power supply, and the red to the other. Current flows in the peripheral direction, only when the two coils touch axially since only then does the circuit close. In this way, the surface area over which the current flows is larger, and thus current density is small. In essence, the basic operating principle is the same as in the design chosen, but the implementation differs. The green part acts as a die, that forces the coils to make contact when a radial force is applied to them. Here the disadvantages are obvious. Much more complicated design, and many places where contact occurs that need extra attention. Also, negative effects of skin effect (moving electrical contact etc. are not resolved). This however led to the next design presented here, which attempts to solve some of the problems present here.

Essentially, current flows only where the projectile exerts a radial force to the primary coil, which forces it to close circuit. In this way a coil is formed, that always follows the motion of the projectile as it moves, and is in all cases behind the projectile (secondary coil).

| ***ADVANTAGES*** | ***DISADVANTAGES*** |
|---|---|
| Electrical isolation | High mechanical interaction between stationary and moving |
| High force (further analysis needed to establish this) | Skin effect causes problems to the movement of projectile |
| | Low efficiency |
| | Complex construction |
| | Difficult repair |
| | Cooling circuit not implemented |

*Table 3: Requirement satisfaction for past design 2*

## 4.3 Past design 3

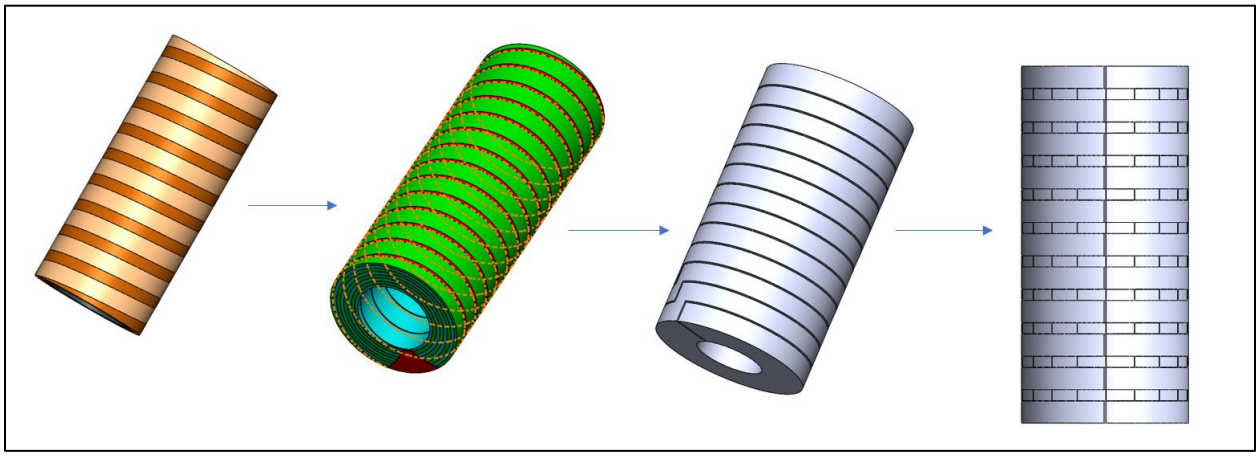

*Figure 35: Different phases of evolution of third and last past design*

The new idea and insight implemented here is that current in the primary coil (barrel) can flow either axially or in the phi direction (forming a coil), depending on the position of the projectile as before. In this way an inductance gradient is formed, which propels the projectile forward.

As the figure above shows, the primary coil consists of a coil where current can either flow peripherally (forming a coil) or axially, essentially forming a hollow wire. The operation of this as well as the previous models, depend on the force that the projectile exerts on the primary. In the places where force is not exerted, current flows in the axial direction since two neighboring loops are in electrical contact. When the projectile passes, the electrical contact is broken, and current is forced to flow in the peripheral direction. The idea presented here is simple, but the crucial part of this design is how electrical contact becomes broken, and restored once again as soon as the projectile's displacement changes. This is accomplished through the current diverter whose design will be discussed later.

*Advantages:*
advantages of this design include:

1. Electrical isolation between secondary (projectile) and primary (barrel), since no current flows from the secondary to the primary or vice versa.
    a. No moving electrical contact, low frictional forces (since no contact has to exist between primary and secondary, as in the railgun for example)
2. Simple construction, of two subassemblies which are linearly patterned to form a longer coil.
    a. Design consists of two subassemblies
        i. The main coil, where current flows
        ii. The main coil is a copper tube, with a through all axial cut
        iii. The current diverter, which essentially defines from where current will flow (axially or not), according to the position of the projectile. The current diverter is the most essential part of this design, and will be analyzed in more detail later.
3. Although skin effect still exists, since coils are electrically isolated, does not pose the same problems as in the railgun, where it impedes the displacement of the projectile.

*Disadvantages:*

1. Current diverter poses some design problems, because it is composed of moving parts, and at the speeds at which the accelerator will be operating cause many dynamic and structural problems.
2. Even though coils are electrically isolated, they are not isolated mechanically, in the sense that the projectile triggers the primary to change operation at different axial displacements, through a force. This could cause instability problems to the projectile (of course depending on its speed), as well as to the primary. In a perfect

design, as little interaction between the primary and the secondary would exist. here however this is not the case.

3. Design does not allow for parts to be easily replaced
4. As in the design chosen, sudden inductance jumps exist here as well. Minimizing them however is a much more difficult process, since:
   a. A theoretical analysis of this model is more strenuous and difficult
   b. Few design parameters exist, apart from the inner diameter and the width of the primary coil that can be changed, to mitigate this issue.
5. In the design diverter proper cooling should exist, because where sudden inductance changes exist so do accompanying resistive losses. Since however all parts are so closely crammed to each other, cooling would become complicated and not effective if not close enough to the diverter.

| ***ADVANTAGES*** | ***DISADVANTAGES*** |
|---|---|
| Electrical isolation | High mechanical interaction between stationary and moving |
| Easy repair | Skin effect causes problems to the movement of projectile |
| High force | Low efficiency |
| | Complex construction |
| | Cooling circuit not implemented |

*Table 4: Requirements satisfaction for past design 3*

### 4.3.1 Break of electrical contact alternatives (current diverter)

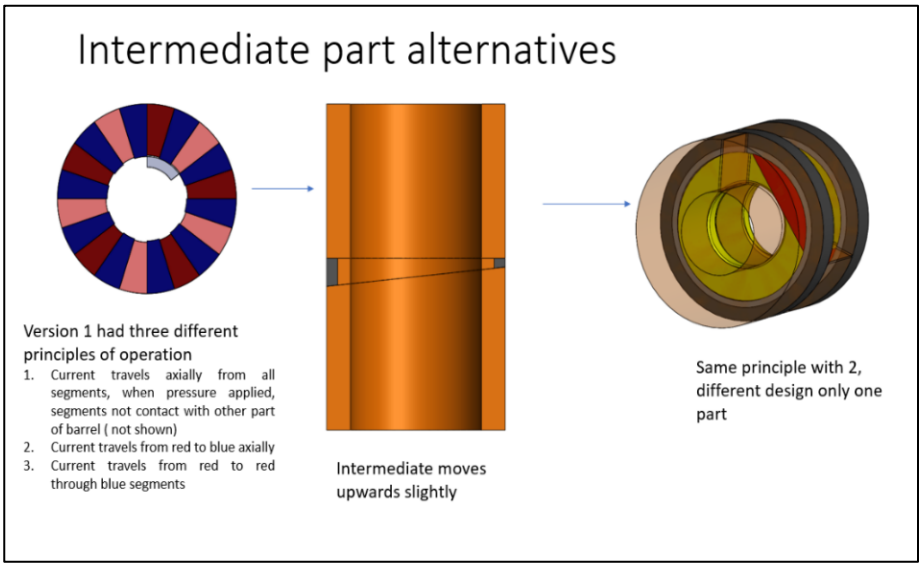


*Figure 36: Possible designs for current diverter*

Three different designs were thought for the implementation of the current diverter, all of which are based on the same physical principle, that contact resistance depends on contact pressure, and thus by changing the contact pressure between diverter and rest of the coil assembly, which is situated before and after each diverter, current will flow in different directions (axially or peripherally).

*Alternative 1 (see figure above):*

Diverter consists of copper pieces, which fit together as version 1 in the figure above shows. It is made from one solid piece of copper, which is later cut, thus forming $N$ smaller pieces which fit well with each other. This design itself has three different configurations which will be discussed below.

*Configuration 1:*

In this configuration, electrical contact exists between all of the pieces of the diverter (red and blue) and the main coil. When current flows axially, it moves from main coil subassembly to all red and blue pieces of the diverter, and then to the adjacent main coil. When radial force is applied however, red pieces of diverter move radially, and due to a wedge shape do not contact the two adjacent coils. Therefore, current is forced to travel peripherally from previous main coil and from a stationary piece of the diverter through the other coil.

*Configuration 2:*

Alternating red and blue pieces make electrical contact with either coils adjacent to the diverter but not both. In this way, when current flows axially it moves from previous coil to blue piece of diverter, then from the blue to the red piece, and finally to the other main coil. When radial pressure is applied, blue pieces move radially outwards, thus breaking contact between two adjacent main coils. Therefore, current travels peripherally from main coils.

*Configuration 3:*

In this configuration, alternating red pieces make electrical contact with either main coil but not both. In this way, when current travels axially it goes from one red piece, through the blue to the other red piece, and finally to the other coil. When pressure is applied, blue pieces move radially, breaking the axial contact between the two main coils, forcing the current once again to travel peripherally. It is obvious from the way this design for the diverter works, that radial force needed to move the pieces of the diverter is very important, because if this force is high, it impedes with the movement of the projectile. The configurations above aim at minimizing this radial force, with the force being higher at the first configuration and smaller at the last.

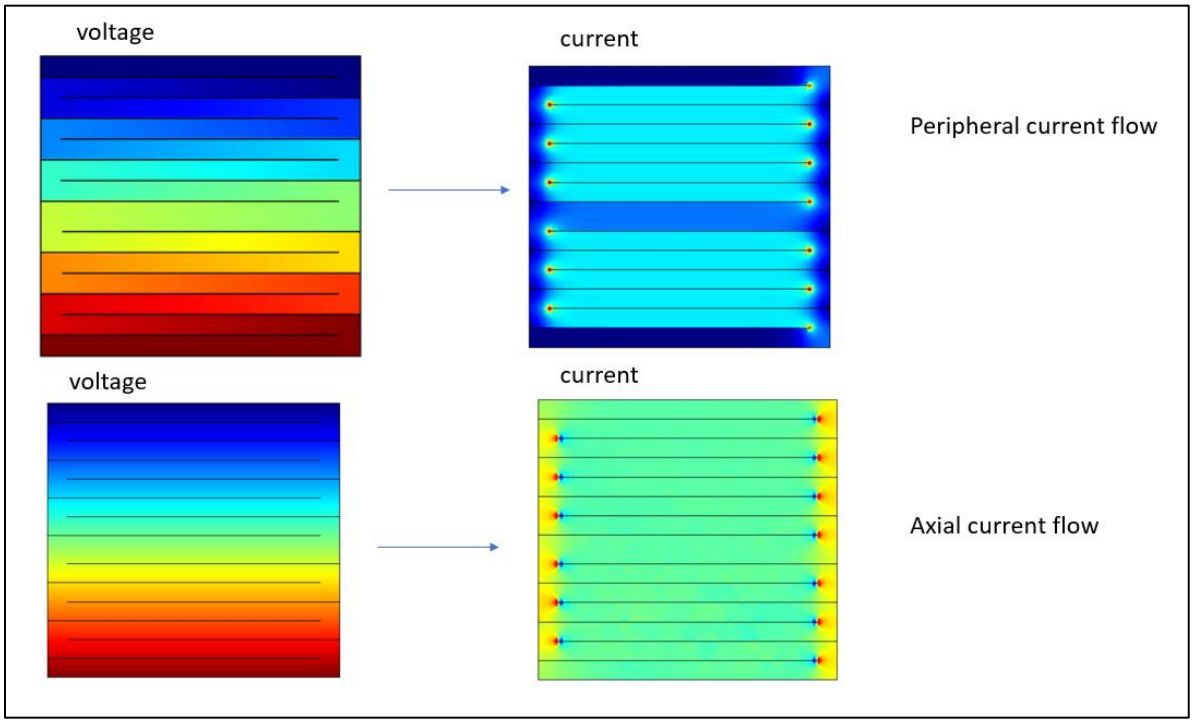


*Figure 37: Two possible current states, in equivalent 2D scenario*

*Current as a function of contact pressure*

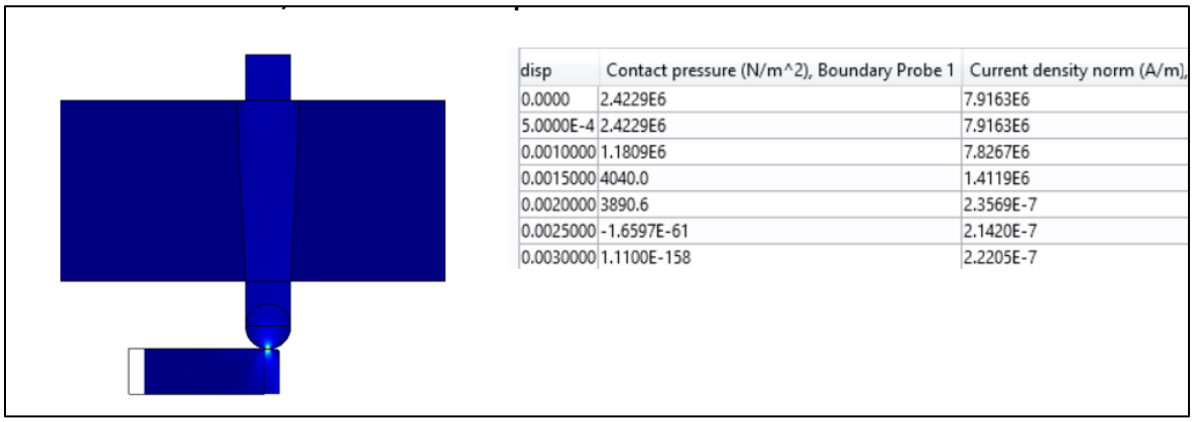

| disp | Contact pressure (N/m^2), Boundary Probe 1 | Current density norm (A/m), |
|---|---|---|
| 0.0000 | 2.4229E6 | 7.9163E6 |
| 5.0000E-4 | 2.4229E6 | 7.9163E6 |
| 0.0010000 | 1.1809E6 | 7.8267E6 |
| 0.0015000 | 4040.0 | 1.4119E6 |
| 0.0020000 | 3890.6 | 2.3569E-7 |
| 0.0025000 | -1.6597E-61 | 2.1420E-7 |
| 0.0030000 | 1.1100E-158 | 2.2205E-7 |

*Figure 38: Contact pressure as a function of projectile displacement*

*Alternative 2:*

In this design, the current diverter is not implemented in an axisymmetric design, but rather in a 2D approximation, where contact is established and lost due to upwards motion of the whole current diverter subassembly, as triggered by the motion of the projectile. More specifically at normal operation (without the presence of the projectile) current flows due to the current diverter axially from one main coil to the next. When the projectile pushes the current diverter slightly upwards, contact is lost between two coils and the diverter, and thus current flows peripherally from one coil to the other.

*Alternative 3:*

This alternative is the same as the one presented above. Here however, the implementation of the diverter is slightly different, as it is constructed only with one moving part (in contrast with the design above, which consists of two parts, one which moves upwards, and one which remains stationary. The geometry of the diverter here is such that even if the whole part is moved slightly upwards contact is lost in one part of the design (as to prevent current from circumventing the coil), but the other still makes contact with the two coils (as to allow for current to flow from one col to the other). This is accomplished through the use of different angles of contact between the three parts. Above, a simple contact analysis is done, where the projectile moves axially pushing the “current diverter” upwards. It can be clearly seen that as contact pressure diminishes, so does the current (since resistance gets larger)

# 5 PROPOSED DESIGN OF ELECTROMAGNETIC LAUNCHER

## 5.1 Construction

The final design consists of :

1. A primary coil, to which the power supply is connected. It spans all the length of the device, and is made out of one solid coil, or multiple connected coil subassemblies.
2. Stationary secondary coils. The stationary secondary coil consists of many individual,unconnected to each other coils, with length $L_{secondary}$. All coils operate independently from each other and occupy two possible states. State 1, where they conduct curren, and state 2 in which they do not.
3. Moving secondary, or else projectile. Its construction is as simple as that of a copper tube, of legth $L_{secondary_{moving}}$.

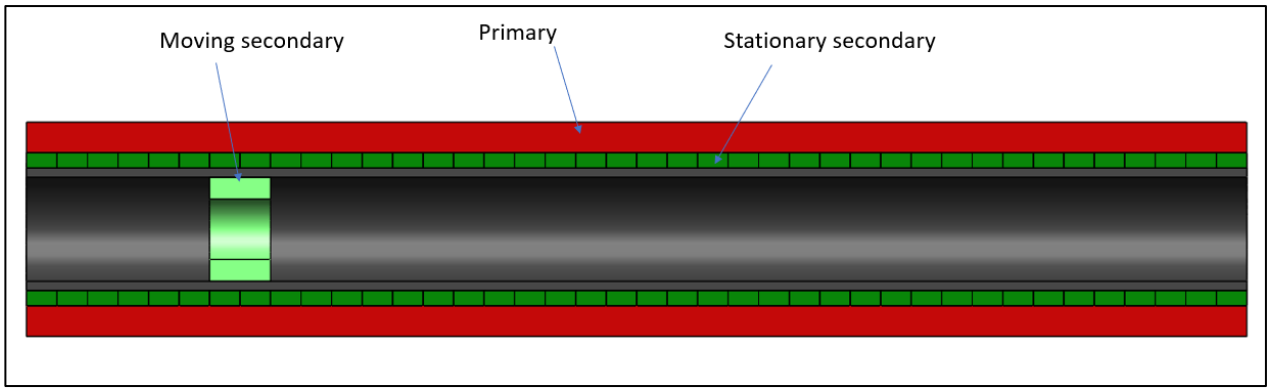


*Figure 39:Simplified construction for original design of proposed launcher*

## 5.2 Operation

The goal of this design, is to create an almost constant inductance gradient, propelling the projectile forwards. This is done by changing the mutual inductance of the system, by transitioning the stationary secondary coils from a conducting state to a non-conducting. This is achieved by disconnecting the stationary secondary coils as the projectile passes them. Effectively, before the projectile, towards the left, magnetic field exists due to the primary coil, whereas after the projectile, since secondary coils are connected, their magnetic field cancels out the one created by the primary coil. This magnetic field gradient, causes an inductance gradient which produces an accelerating force. This can be seen in the figure below, where the current density is also plotted.

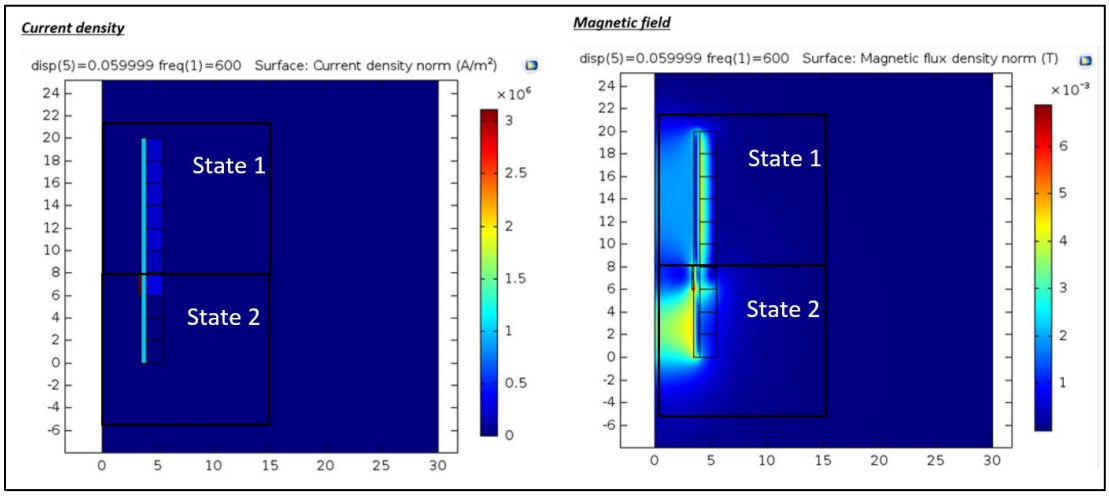


*Figure 40:Current density to the left, magnetic field plot to the right, showing two different operational states of the device*

*Simulations required to show the operation of the electromagnetic launcher:*

1. Simulation in order to find the properties of the launcher, which only depend on its geometry, materials and the displacement of the projectile. This study is done in the frequency domain, for a frequency which corresponds with the high frequency phenomena present during the operation of the device (the natural frequency of the device as discussed later) $(study_1)$
    a. Inputs of the simulation include:
        i. Structure material
        ii. Operating frequency
        iii. Geometric characteristics:
            1. Inner diameter of primary coil: $r_{inner}$
            2. Initial displacement of projectile, which adds a phase shift when system transitions from $state\ 1$ to $state\ 2$: $Disp_{initial}$
            3. Projectile height: $Height$
            4. Width of primary coil: $Width_{primary}$
            5. Width of secondary coil: $Width_{secondary}$
            6. Width of projectile: $Width_{projectile}$
    b. Outputs of the simulation:
        i. $L(x)$
            1. Includes a continuous inductance change, and a sudden jump between state changes
        ii. $R$: system's resistance
2. Simulation including the physics discussed above. This includes a differential equation model, modelled through the use of lumped elements whose derivation will be discussed in the chapters to come $(study_2)$
    a. Inputs of the simulation:
        i. Initial and operating conditions:
            1. Initial inductor current
            2. Power supply (capacitor bank etc.)
        ii. Contact analysis to better describe the value of the resistance during state change
        iii. Electrical characteristics, output of $study_1$(inductance, resistance etc.)
    b. Outputs:
        i. Ohmic losses
        ii. Projectile's velocity
        iii. Accelerating force (in the axial direction)
3. Simulation to find the disconnection resistance as a function of contact pressure (during the change between states where the secondary coils is disconnected, Paragraph 4.3.1)
4. $Magnetic\_force\_study$ which derives the radial force density acting on the structure, as well as its distribution. Also, the distribution of the axial accelerating force is derived. This study is done for both states before and after switching (to describe the conditions before and after the projectile). The output results are fed to a structural analysis where the stresses and displacements are investigated.
    a. Input:
        i. Axial force from $study_2$
    b. Output:
        i. Radial force density distribution
        ii. Axial force density distribution
5. Structural analysis:
    a. Input:
        i. Axial force from study_2
        ii. Force distributions from $magnetic\_force\_study$
    b. Output:
        i. Stresses

ii. Displacements

6. Finally, a thermal analysis coupled with a fluid flow for cooling, is done to investigate the thermal loads acting on the structure due to ohmic heating, as well as to extract the heat from the system.
    a. Inputs:
        i. Resistance and current (to simulate heat source) from $study_1$, $study_2$
        ii. Fluid inlet velocity
        iii. Fluid type
    b. Output:
        i. Temperature distribution
        ii. Heat extracted from system.

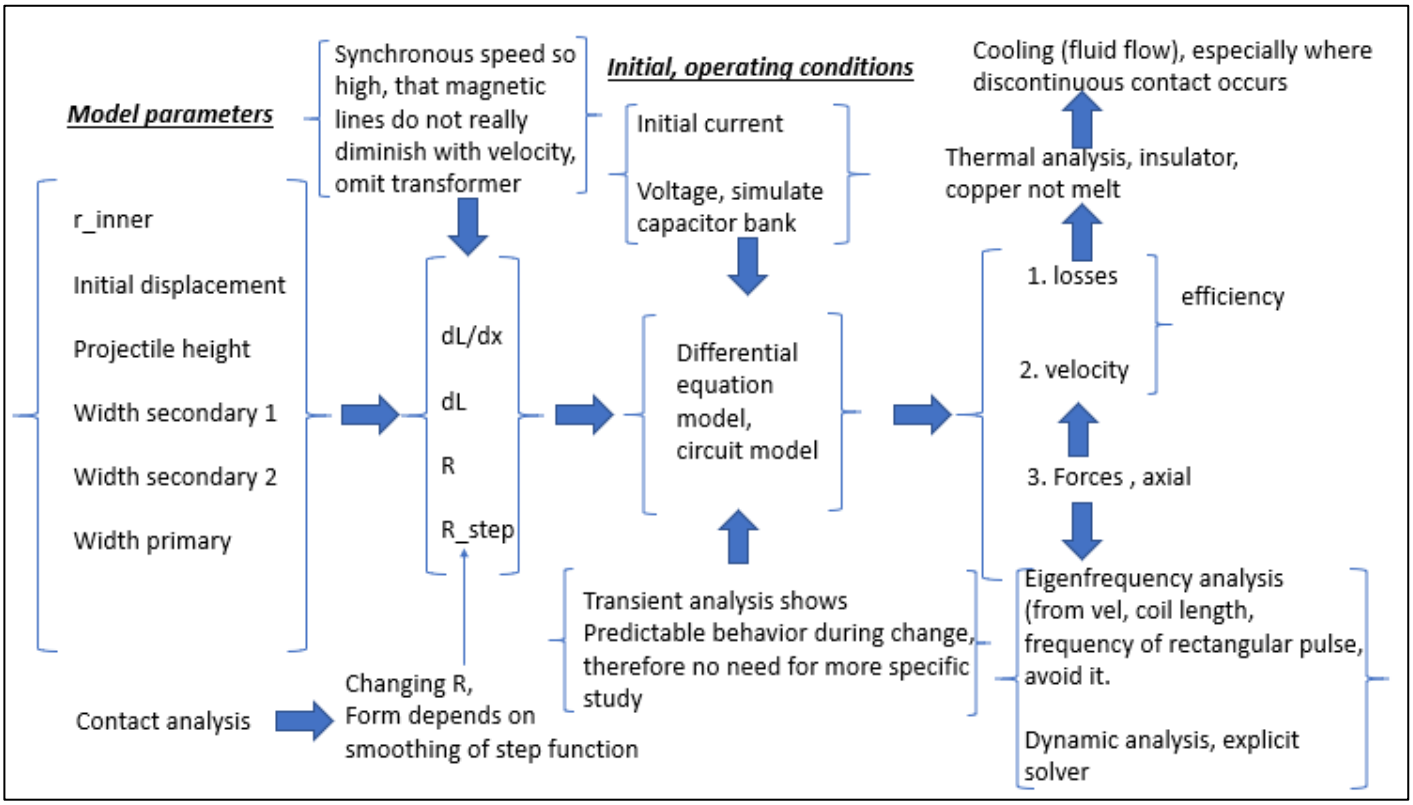


*Figure 41: Workflow of the simulations needed to show the operation of the proposed launcher*

This design caters to two different operating modes. The first, is the one seen above, where all coils are made in such a way as to allow for uniform current distribution along their cross-section. The second, is a design where coils are made of solid copper material, and due to skin and proximity effects have a non-uniform current distribution. Of course, many other possible configurations exist, with an iron core for example etc. these will also be discussed later on. The first design will now be explored, and the others later.

Firstly, parameters of this design need to be extracted, in order to simulate the physics in action. This is done in a parametric way, where all dimensions affecting the design act as input parameters. These include:

1. Inner diameter: $R_{innner}$
2. Primary coil width: $W_{primary}$
3. Stationary secondary coil width: $W_{secondary}$
4. Projectile width: $W_{projectile}$
5. Individual stationary secondary coil height: $L_{secondary}$
6. Displacement, relative to the start of individual stationary secondary coils, at which they become disconnected (like phase shift): $disp$

The desired output properties include:

1. Inductance as a function of projectile displacement
2. Inductance jump when stationary secondary coil goes disconnected
3. Resistance of the system

And are calculated with a frequency analysis for a frequency $f_{analysis}$ [Paragraph 6.1.4], which is also a parameter of the simulation. Below the equivalent inductance of the system as a function of projectile displacement will be calculated.

*Inductance as a function of displacement, for simple 3 coil scenario:*

In this chapter the inductance change of the system will be investigated. Before analyzing the complex system however, it would be wiser to tackle the simplest possible scenario, that is associated with the operation of the device. This consists of three axisymmetric coils, two of which are stationary and the third moves towards them. Firstly, an analysis was done without any change in the conductance of the coils, and the switching process was implemented later on.

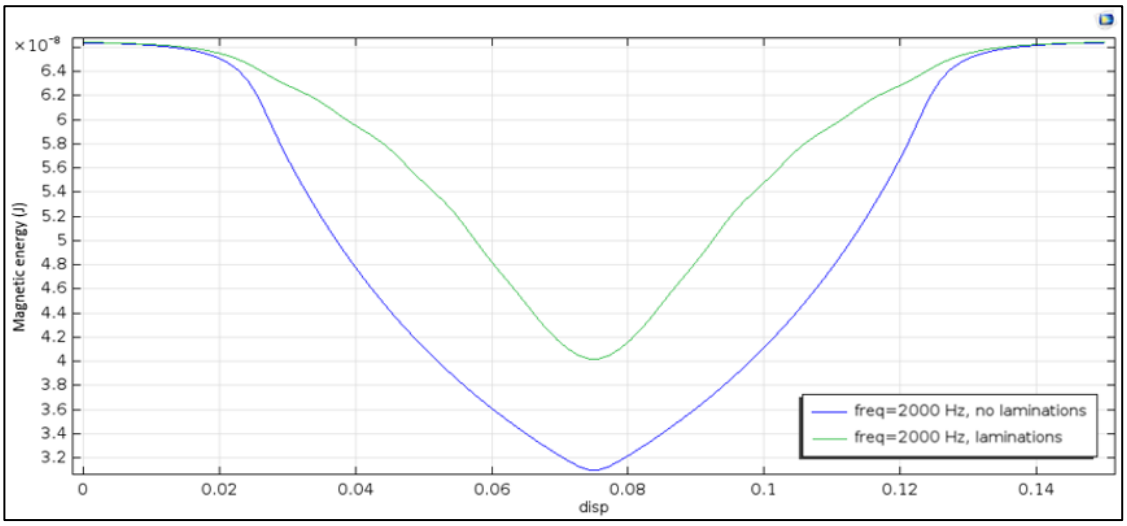


*Figure 42: Magnetic energy as function of displacement for coils with and without axial lamination*

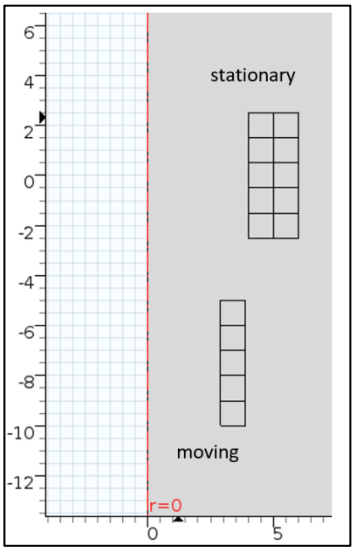


*Figure 43: simulated model's design, with axially placed laminations*

1. Both waveforms are symmetric around the displacement of 7.5 [cm]. This was expected since the geometry of the model is symmetric.
2. Inductance is very low in both systems, which is to be expected since essentially the stationary secondary coil always cancels out the magnetic field created by the primary
3. Lowest energy value is reached when all three coils are aligned. This is also logical, since all three coils form an even better transformer as a system.

*Simple switching between two conductive states*

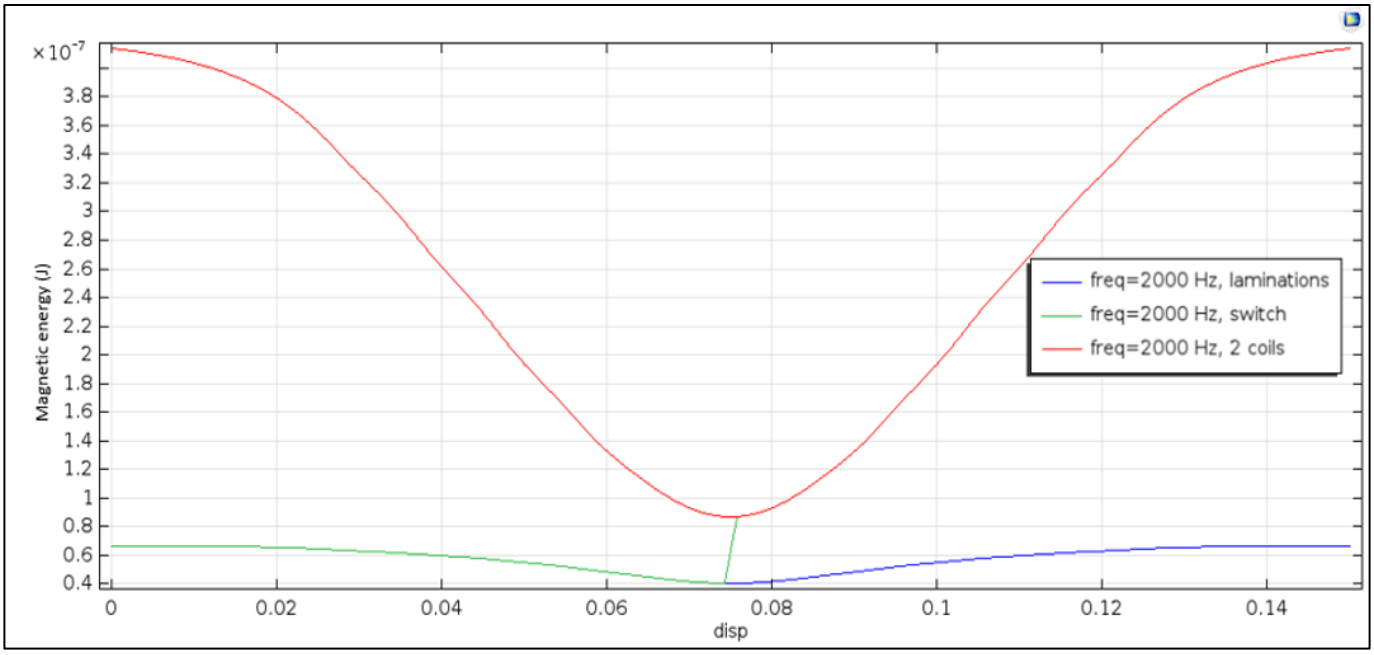


*Figure 44: Inductance jump, and states with and without secondary being disconnected*

It can be seen from the graph above, where the switch of the stationary secondary coil was implemented, that the complex system's inductance is equal in part with the system's inductance before and after the sudden change. This was expected but nevertheless the graph helps a lot in visualizing this point. A few things can be observed in the graph above.

1. An inductance jump exists when stationary secondary switches from conducting to non-conducting state
2. Inductance as a function of displacement is almost constant before the switch occurs, and rises linearly afterwards.
3. At a certain displacement, inductance gradient drops off and tapers to 0. This occurs for a large displacement of the moving secondary, when it is located far from the rest of the coil assembly.
4. Inductance jump, like the one seen above, is of great importance for the operation of the device for two reasons
    a. Energy associated with inductance jump is dissipated as heat, and thus lowers the efficiency of the launcher.
    b. Energy dissipated in the form of heat could cause problems in the operation of the launcher.

## 5.3 Geometry based parametric studies

### 5.3.1 Parametric study with primary coil's inner diameter $R_{inner}$

For reduced simulation time, in all simulations below, an analysis was done before and after switching occurs, and not in any intermediate projectile positions. Since no inductance jump occurs in any intermediate position, and thus the accuracy of the simulation does not get compromised, (what is of importance is the total system's inductance change, like in all conservative fields what matters is initial and final position, dynamic energy etc.). Furthermore, as the simple study done earlier illustrates, this change anyways is almost linear. Thus, the decision was taken, to run the smallest number of simulations possible. This is the reason why in all graphs, the change seems to occur in a perfectly linear way, when in reality this is not the case.

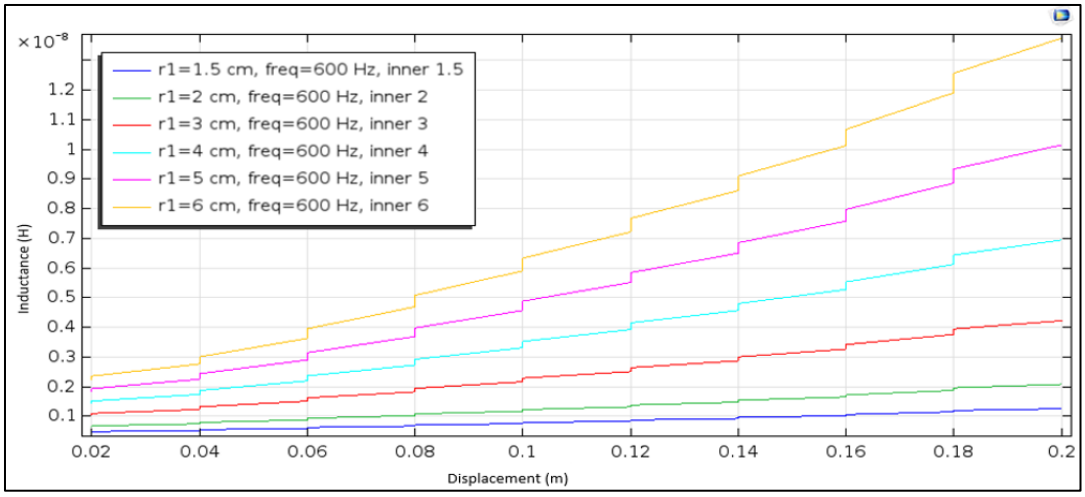


*Figure 45: Total system inductance as a function of displacement and inner radius of primary coil*

For a better comparison between the multiple studies, the ratio of the total inductance jump due to secondary coil's disconnection, to smooth inductance change is plotted for all parameter values:

$$R = \frac{\sum L_{sudden_{jump}}}{\sum L_{smooth_{force}}} \tag{38}$$

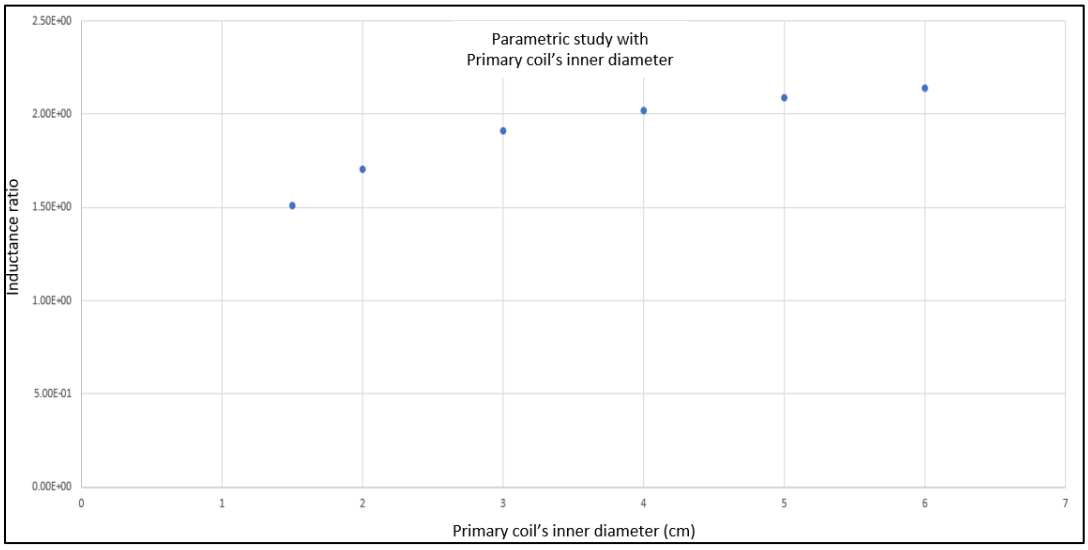


*Figure 46: Graph of inductance ratio, as a function of the inner radius of the primary coil*

From the graph above it can be seen that as the inner coil radius increases, so does the desired ratio. This was expected, since the mutual inductance(coupling) between coils gets larger, the higher the ratio of the coil's outer diameter to its inner, for a constant coil width.

### 5.3.2 Initial projectile displacement, effectively introduces phase shift to coil's switching

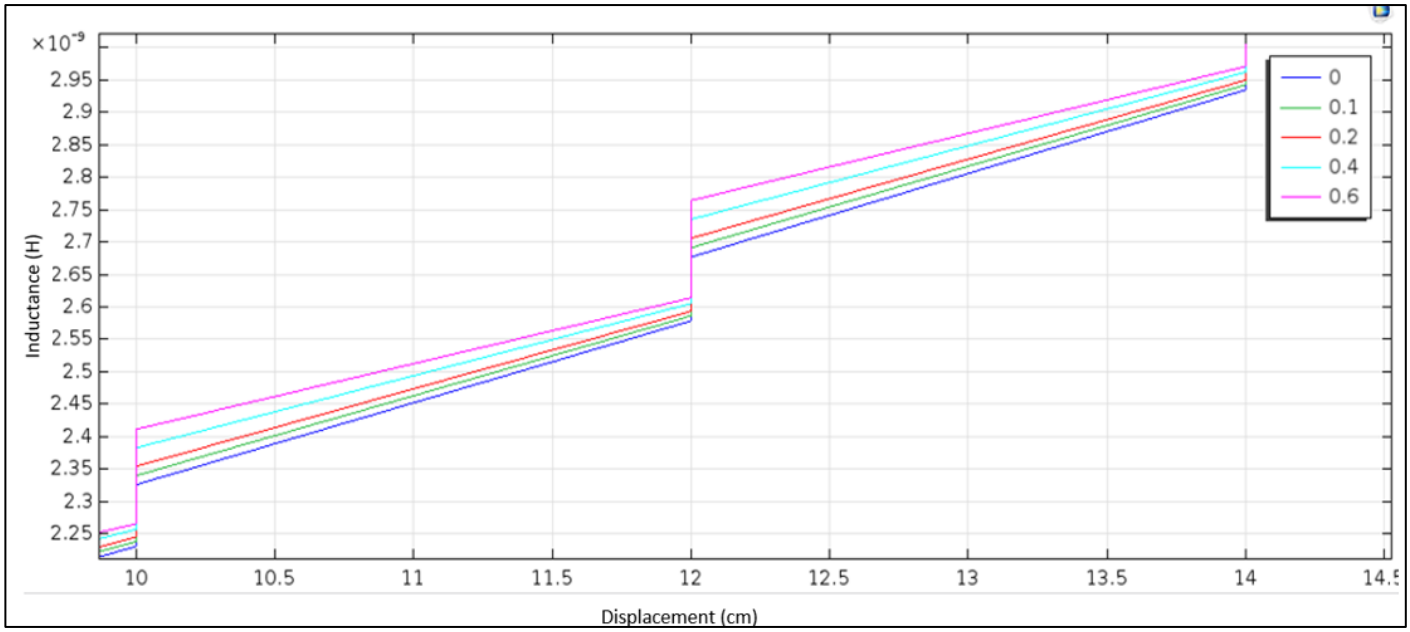


*Figure 47:Total system inductance as a function of displacement and initial projectile displacement (phase shift)*

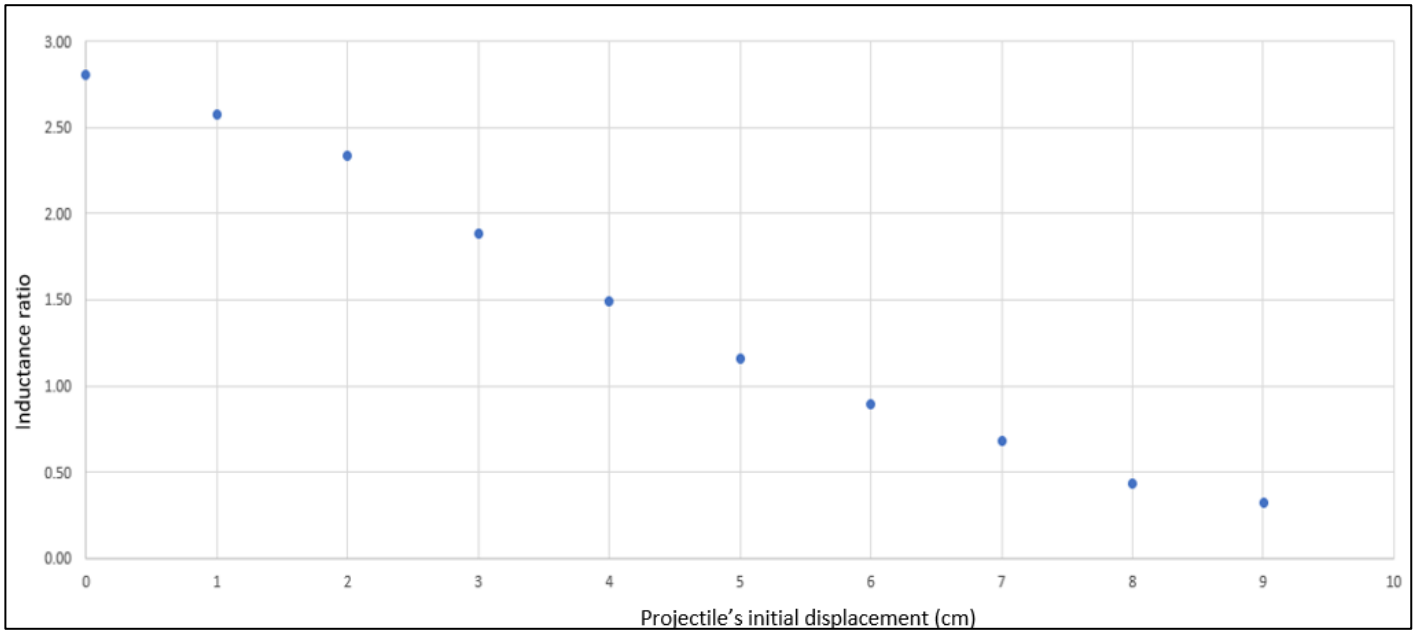


*Figure 48: Graph of inductance ratio, as a function of initial projectile displacement*

From the graph above it can be seen that as phase difference increases, the desired ratio decreases. This was expected since coupling between projectile and primary coil gets worse. As coupling, or mutual inductance gets worse, inductance jump increases, thus desired inductance ratio decreases. It is clear that this effect has a large impact on the operation of the device. Therefore, the position and mechanism that switches the coils off, needs to be implemented in such a way as to not undermine the smooth operation of the device.

### 5.3.3 Projectile length (stationary secondary coil's length constant)

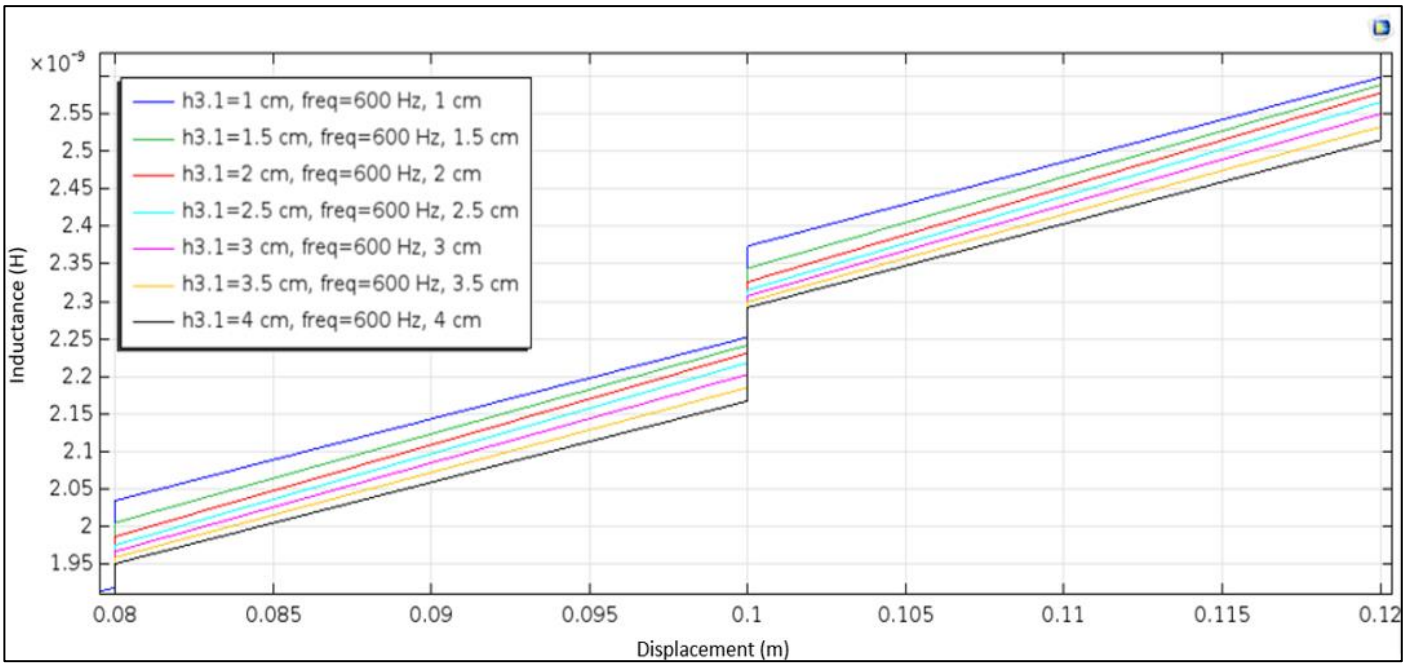


*Figure 49: Total system inductance as a function of displacement and height of projectile, individual secondary stationary coil.*

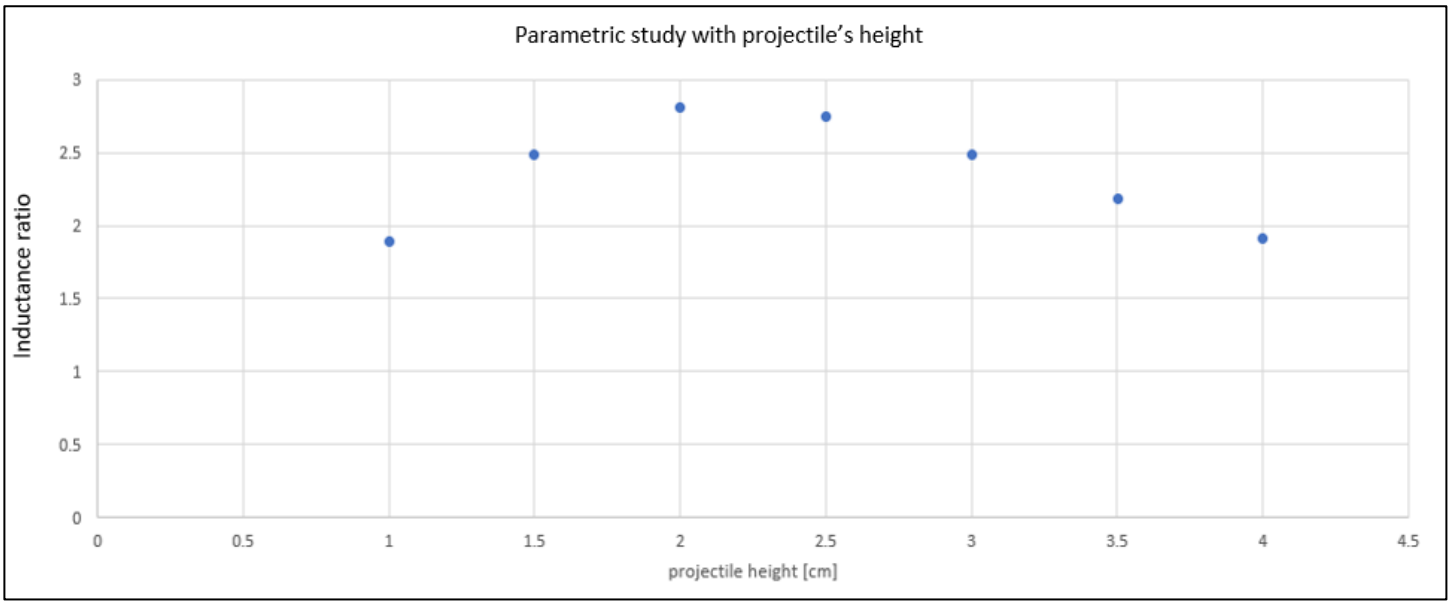


*Figure 50: Graph of inductance ratio, as a function of projectile height*

From the graph above it can be seen that the desired ratio becomes maximum when the height of the projectile is equal to that of the individual stationary coil. This happens, because effectively by changing the projectile's length and keeping the switching position constant, a phase difference was implemented (as in Paragraph 5.3.2].

### 5.3.4 Primary coil width

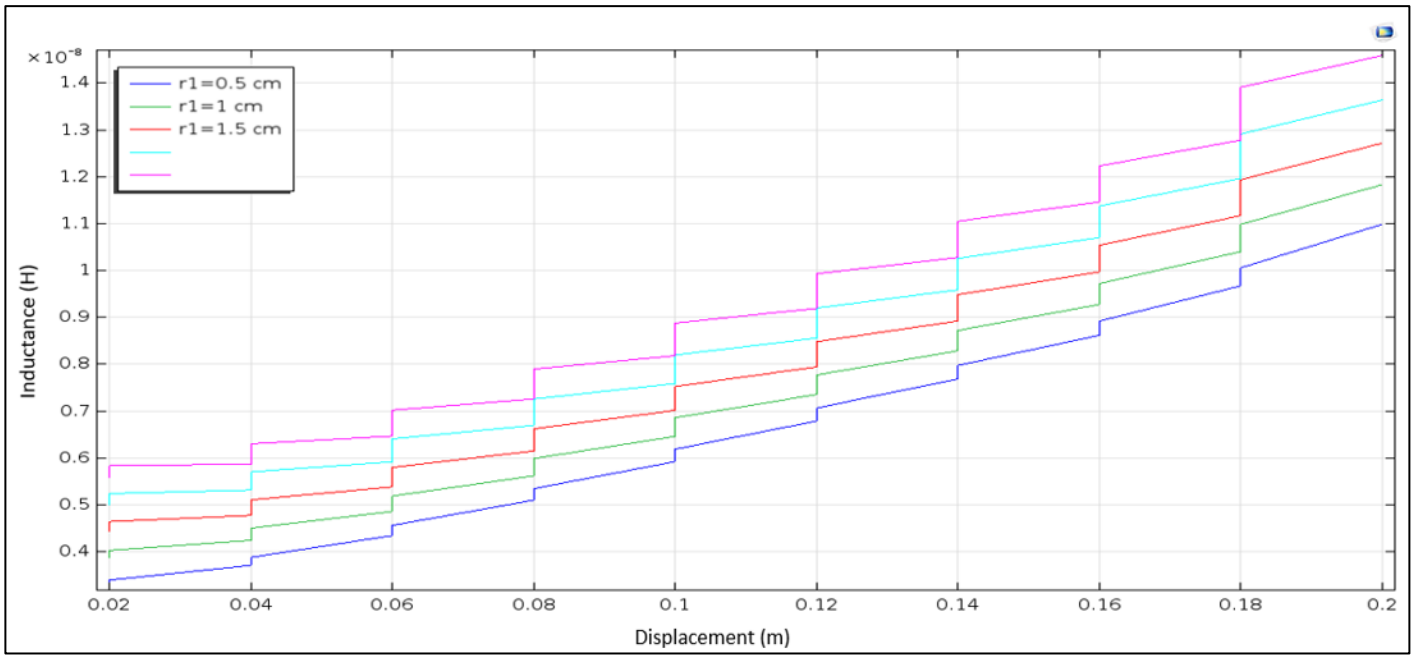


*Figure 51: Total system inductance as a function of displacement and width of primary coil*

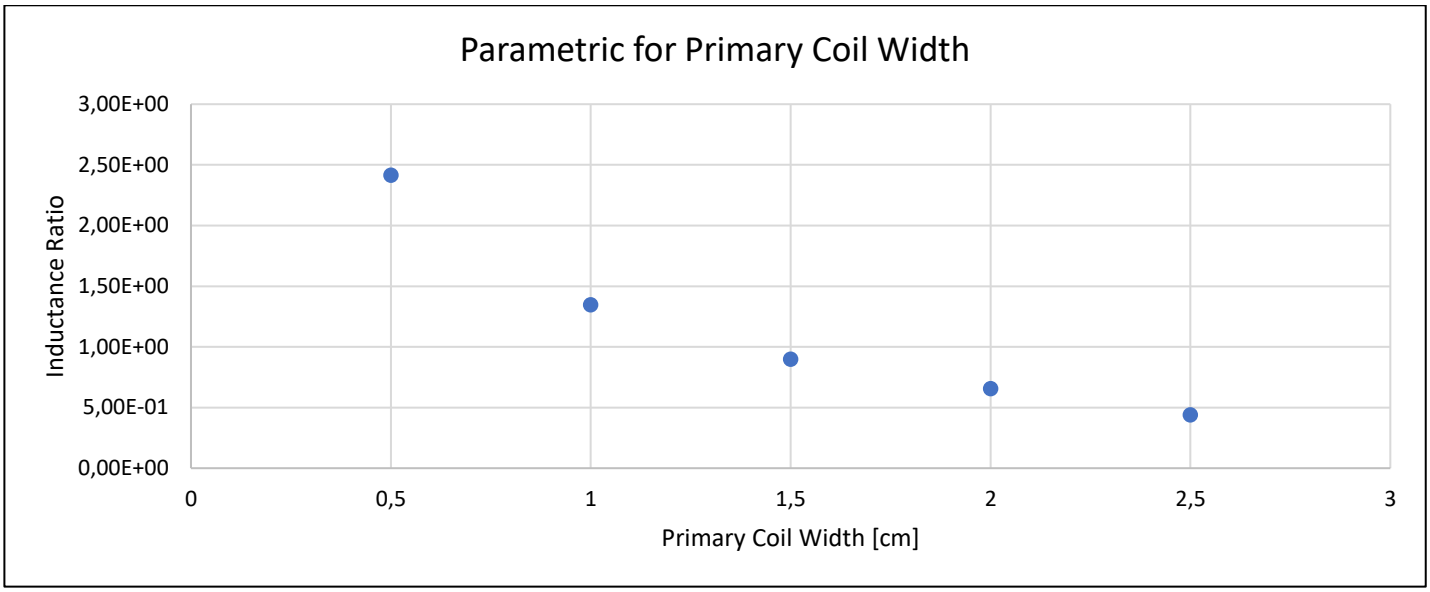


*Figure 52: Graph of inductance ratio, as a function of primary coil width*

It can be seen from the graphs above that the smaller the width of the primary coil, the smaller the inductance jump, and thus the better the operation of the motor. This is due to the fact that coupling between primary and stationary secondary coils is better. The configuration making use of the skin effect is so efficient due to this reason, because the effective coil width of the primary is reduced greatly due to the skin effect [as seen in Paragraph 6].

### 5.3.5 Secondary coil width

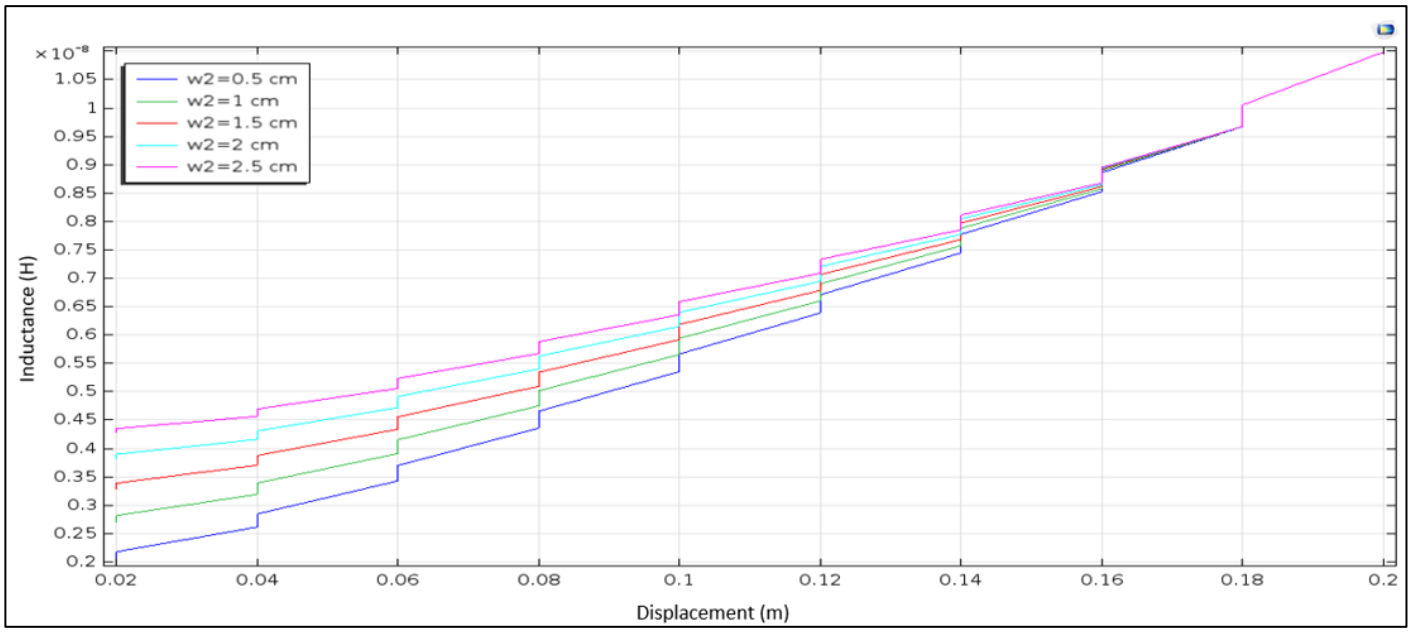


*Figure 53: Total system inductance as a function of displacement and width of secondary coil*

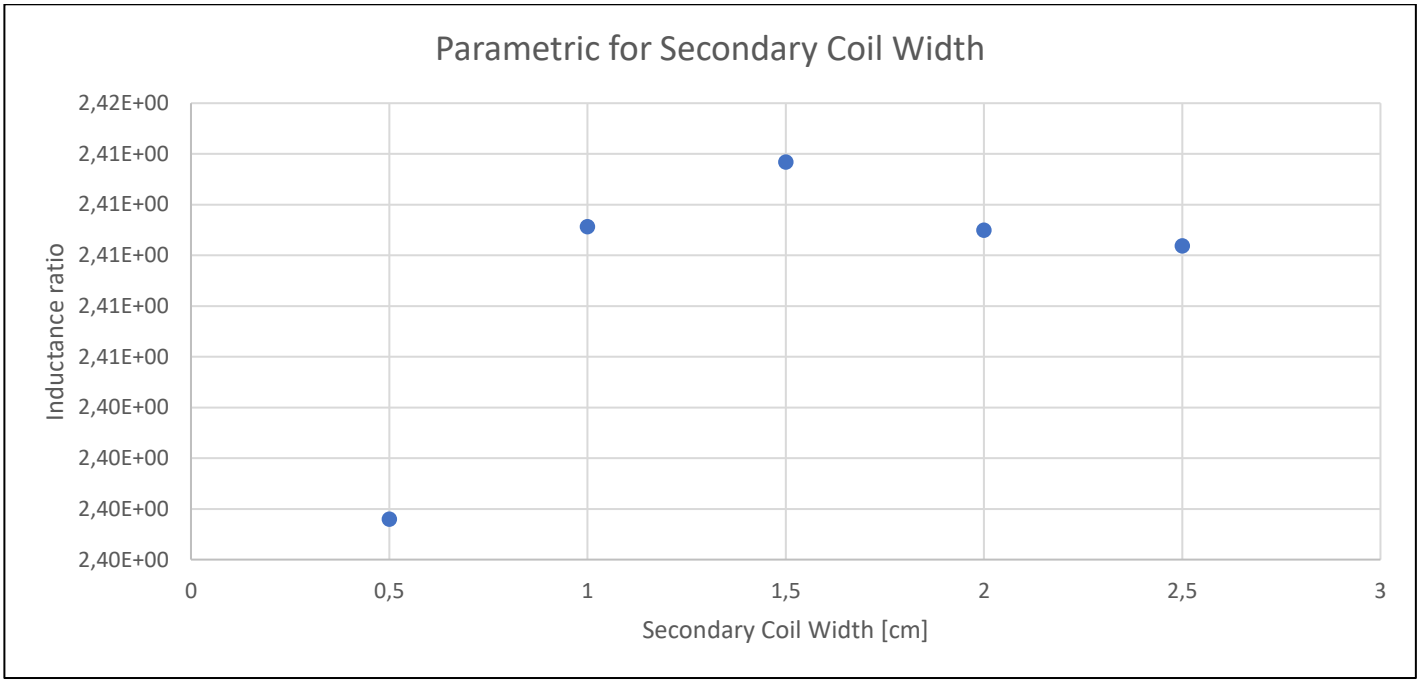


*Figure 54: Graph of inductance ratio, as a function of secondary coil's width*

It is observed that the desired ratio remains almost constant regardless of the secondary coil's width. From the first figure however, it can be seen that a larger total inductance change exists for a smaller secondary coil width ($L_{final} - L_{initial}$), which is desired since for the same barrel length, energy given to the projectile will be higher. This happens because the final kinetic energy is proportional to the total inductance change of the system, subtracting the inductance jump. The total efficiency of the system however, will be the same, since it only depends on the total inductance jump and the resistance of the system which changes only slightly due to the increased width of the secondary coils.

From the analysis done above, it can be seen that for the homogeneous coils' configuration, inductance jump relative to smooth inductance change is very high. This however could be made much smaller, according to the thought experiment explained here. It is obvious that the final magnetic field is the summation of all individual magnetic fields from the coil assemblies. The assumption can be made that each coil assembly does not interact with another (they are spaced far apart), then the simulation can be simplified greatly, since a study for only one of the coil assemblies can ensue, and the magnetic field will simply be the superposition of this assembly with itself, with a phase shift according to the projectiles displacement. This can be illustrated in the figure below, where for simplicity no inductance jump is plotted. To be more exact, the figure below corresponds to the total system inductance for an induction coil-gun. (this is closely related with inductance change rule 3) [see Paragraph 6.1.3 as well]

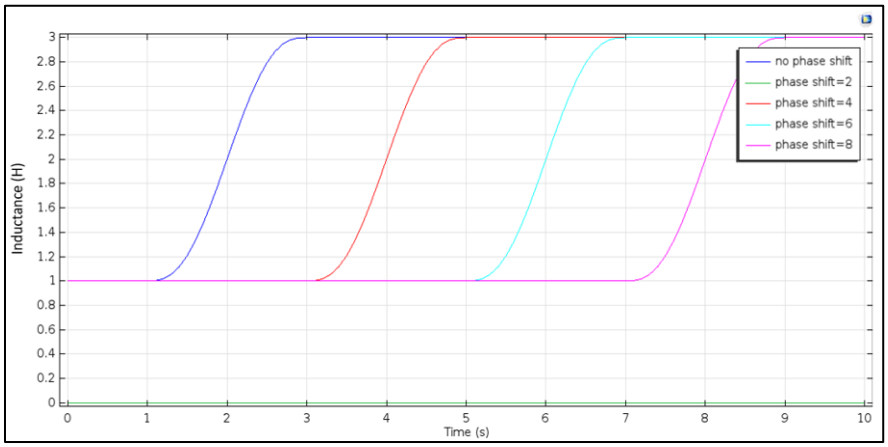


*Figure 55: Superposition of individual inductances, as the model above states*

| Coil configuration, depends on projectile displacement | $Energy\ (inductance), (J)$ |
|---|---|
| Coil assembly without projectile (far away) | 107 |
| All three coil are active and aligned | 47 |
| Stationary secondary disconnected | 94 |
| Projectile displacement high, located far away from primary | 280 |

*Table 5: Possible coil states for one coil subassembly*

Desired energy ratio: $ratio = \frac{280-94+47-107}{94-47} = \frac{126}{47} = 2.68$, much larger than previously seen, and was calculated for a primary coil width of $1[cm]$.This hypothesis can be verified, with an analysis whose results are presented below. In this way effectively edge effects can be ignored.

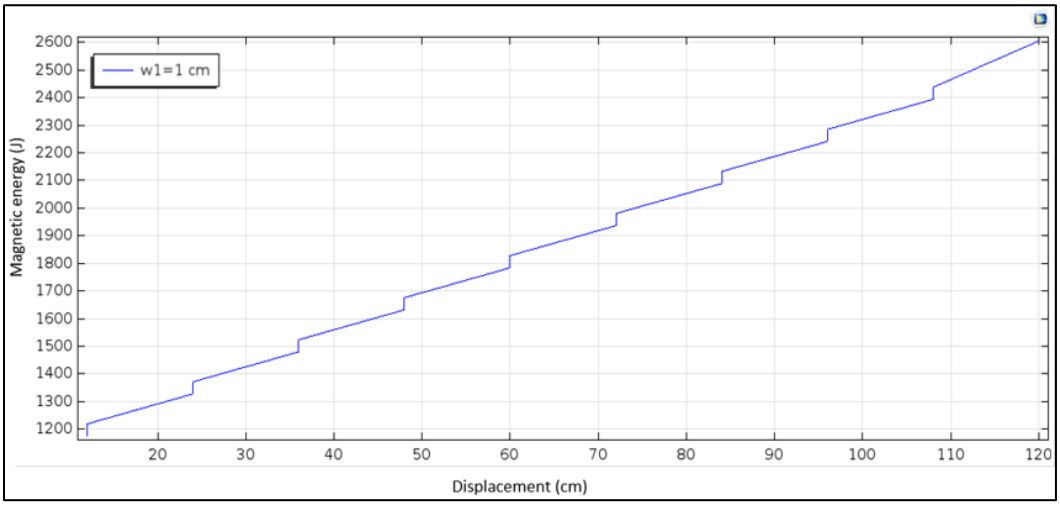


*Figure 56:inductance as a function of displacement for the homogeneous coil configuration, with a gap of 12 [cm] between the coil subassemblies. Here average inductance ratio is 2,67 almost similar with the theoretically calculated above.*

# 6 MODEL EXPLOITING THE SKIN EFFECT

As previously stated, the device presented here can operate at two different configurations. The one, which was examined above consists of highly laminated coils, which do not allow for skin and proximity effects to be noticeable. The other configuration exploits the skin effect to improve the coupling between the coils. In this simulation apart from the geometric parameters of the model, what is of great importance is a simulation in the frequency spectrum as well, in order to examine the effect, the skin effect has in the device's operation. The results from the simulations done above for the homogeneous configuration apply here as well.

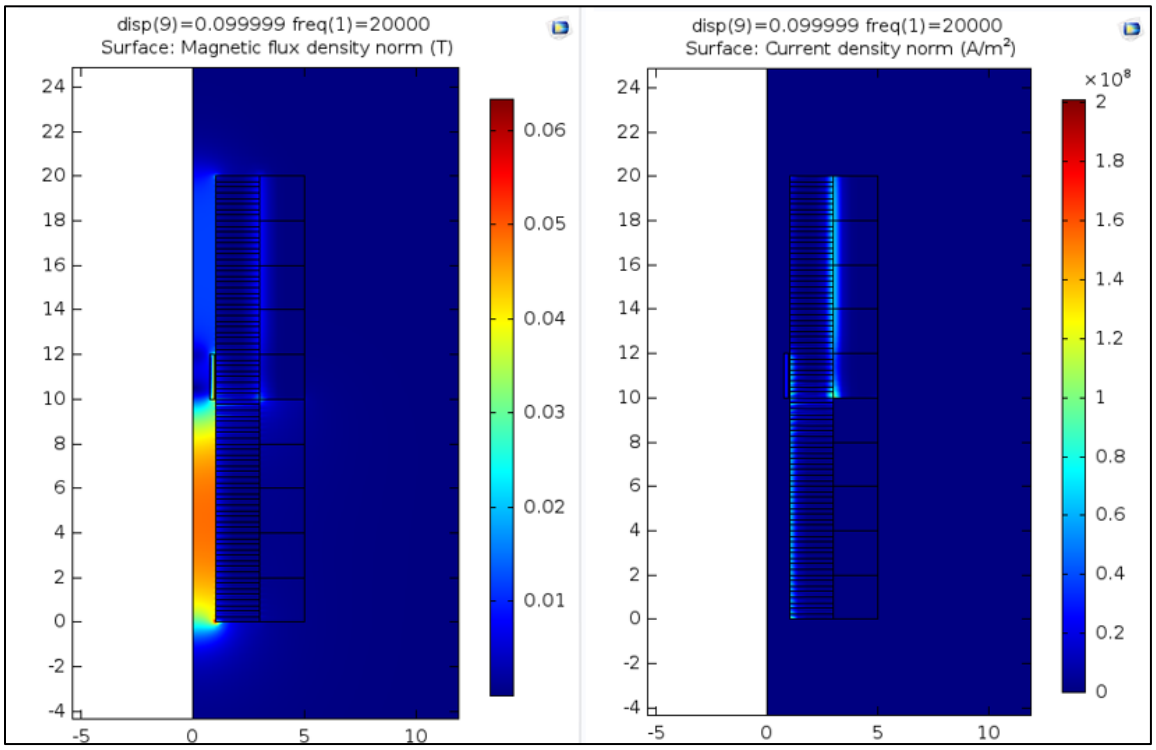


*Figure 57:Left magnetic field, Right: current density, for projectile at intermediate displacement*

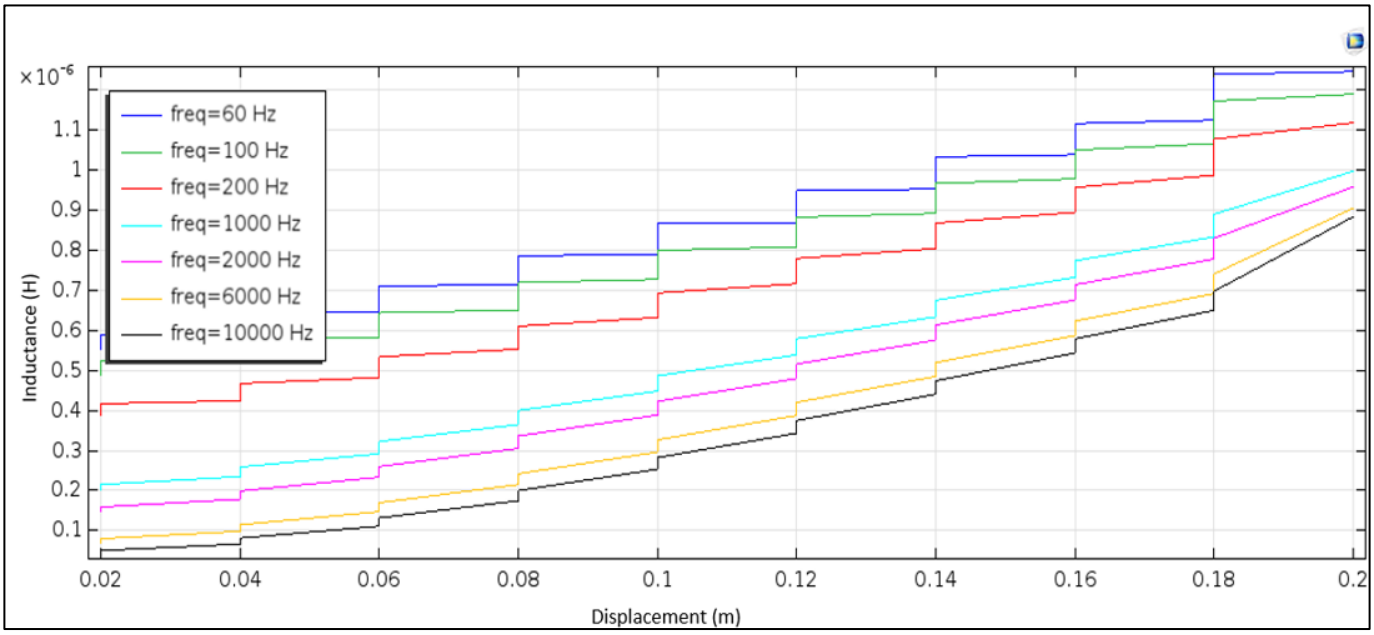


*Figure 58: System inductance for skin effect model, as a function of frequency and projectile's displacement*

### 6.1.1 Primary coil width

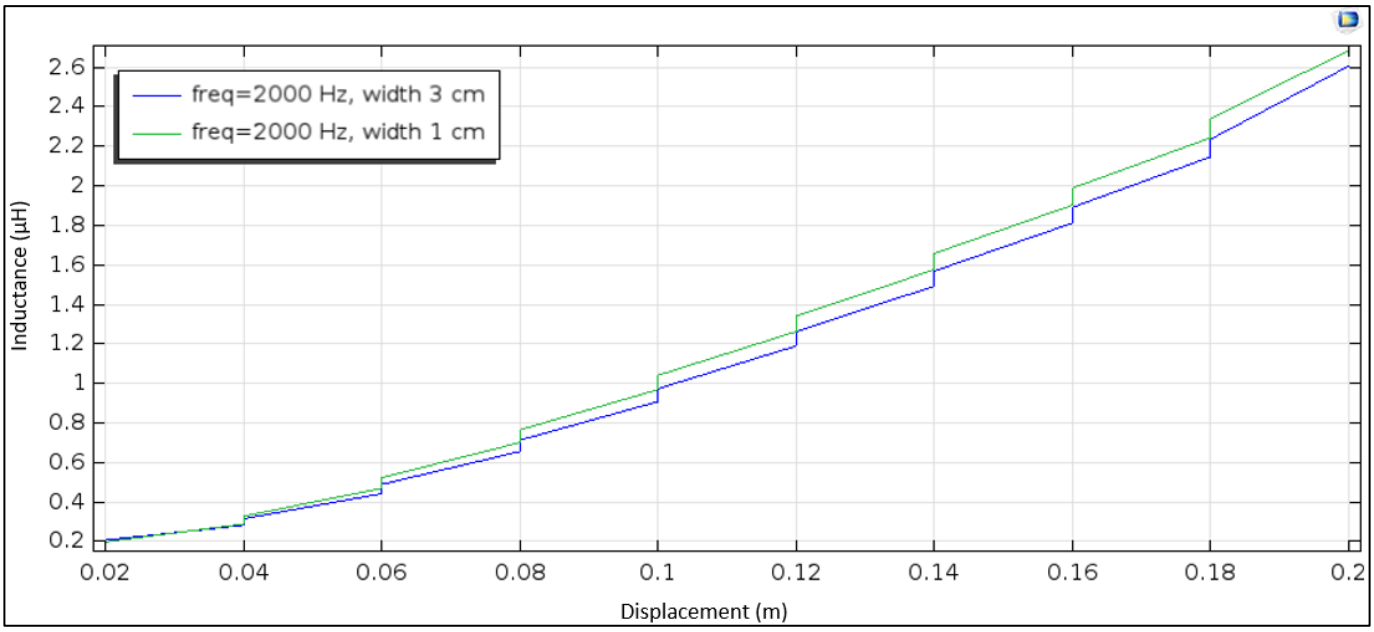


*Figure 59: Comparison for different primary coil widths*

Due to skin effect being present, the effect of a larger primary coil width is mitigated as the figure above shows. This is positive because conductors of larger width can be used, which would lead to better structural integrity.

### 6.1.2 Effect of primary lamination thickness (same frequency)

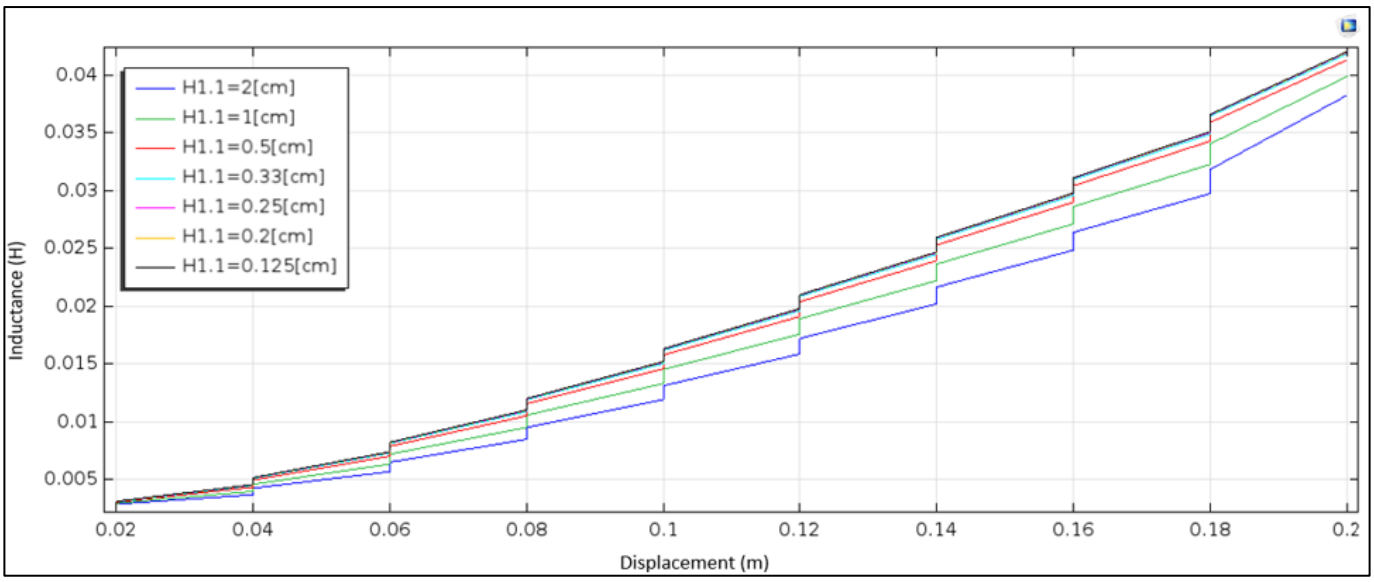


*Figure 60: Graph showing system inductance as a function of projectile displacement, and axial lamination of primary coil*

It can be seen that for smaller axial laminations [ as in Fig. 43] inductance jump is smaller. This however requires a more complex construction, which needs to be taken under consideration. Nevertheless, even with no axial laminations, inductance jump is greatly reduced.

### 6.1.3 Spacing between individual coils, which form the primary coil of the device

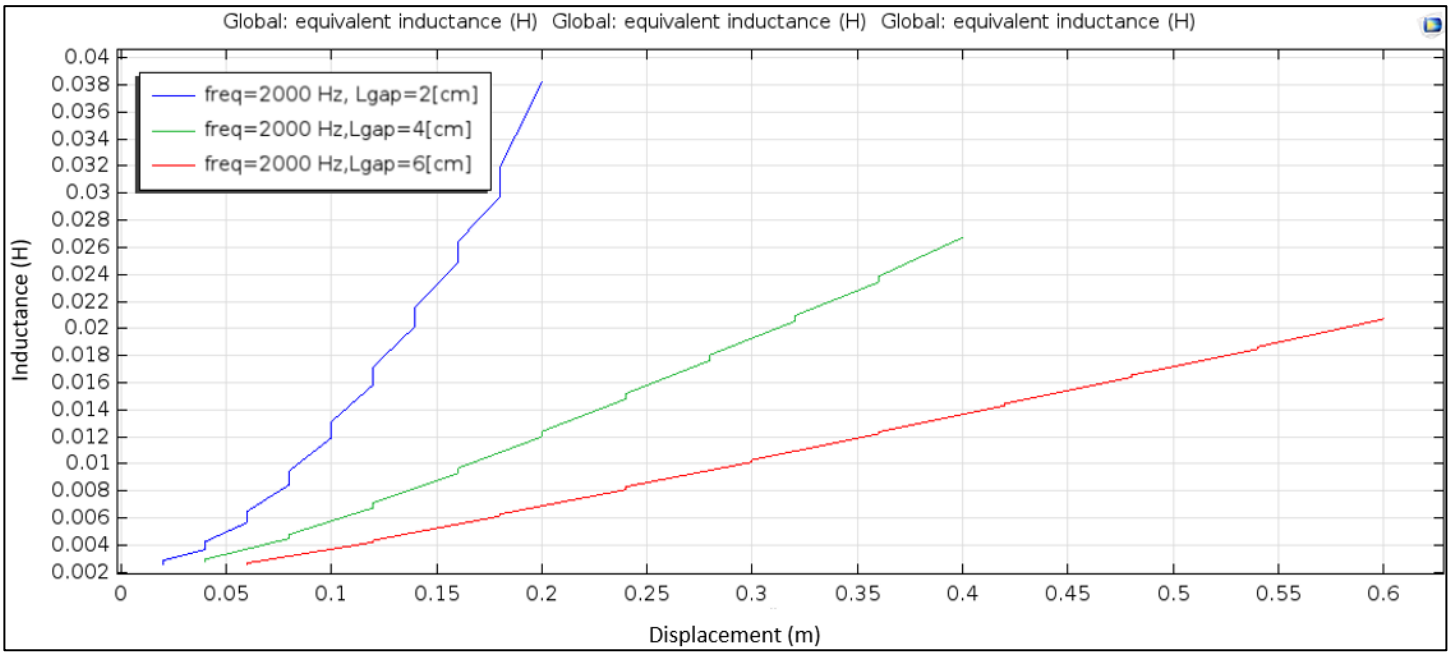


*Figure 61: System's inductance as a function of projectile's displacement, and spacing between individual coils*

Another parameter of the model is the axial distance between the individual coils, as discussed earlier. It can be seen from the graph above that the bigger the axial distance, the smaller the inductance jump. With an intermediate gap between the coils the construction is easier, cooling gets better, positioning of switches in the middle, and supports are better. On the other hand, if the coils are spaced too far apart, the approximation made earlier that primary and secondary current is almost the same does not apply.

All inductance graphs above, are qualitative rather than quantitative. To be more exact, the shape of the graph is accurate, but the values on the $y$ $axis$ are not. This however does not pose a problem, since the aim of these studies is to extract the form of the inductance function, and not its exact values. This can be done by finding the lower and upper inductance value, and retrofitting the graphs above to these values.

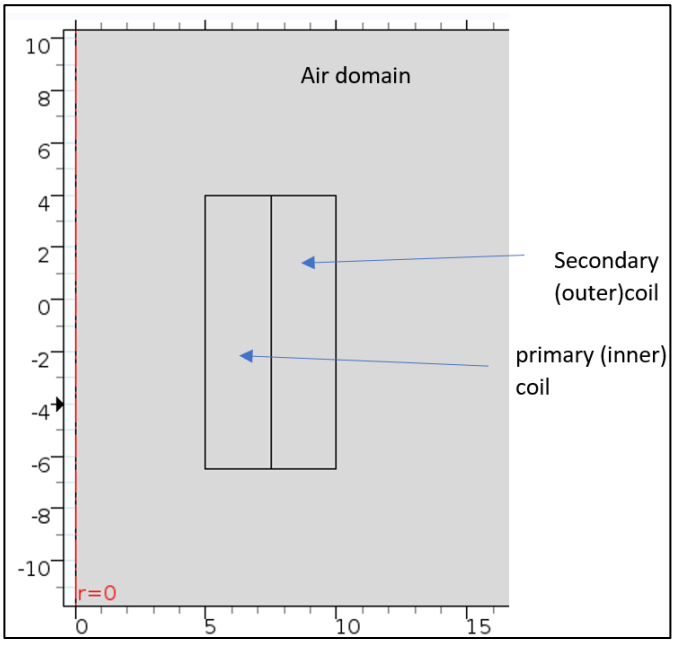


*Figure 62: Model where current shift during switching was calculated*

*<u>Current shift when inductance jump occurs:</u>*

Below, the current at the skin depth of the primary coil (for its inner and outer diameters) is graphed, as a function of time. It can be clearly seen, that when the secondary (outer coil) gets disconnected, the current density in an extremely quick manner moves from the outside diameter to the inside. The graph also shows that no unpredictable phenomena occur. The exciting current of the primary coil was $1\ [A]$.

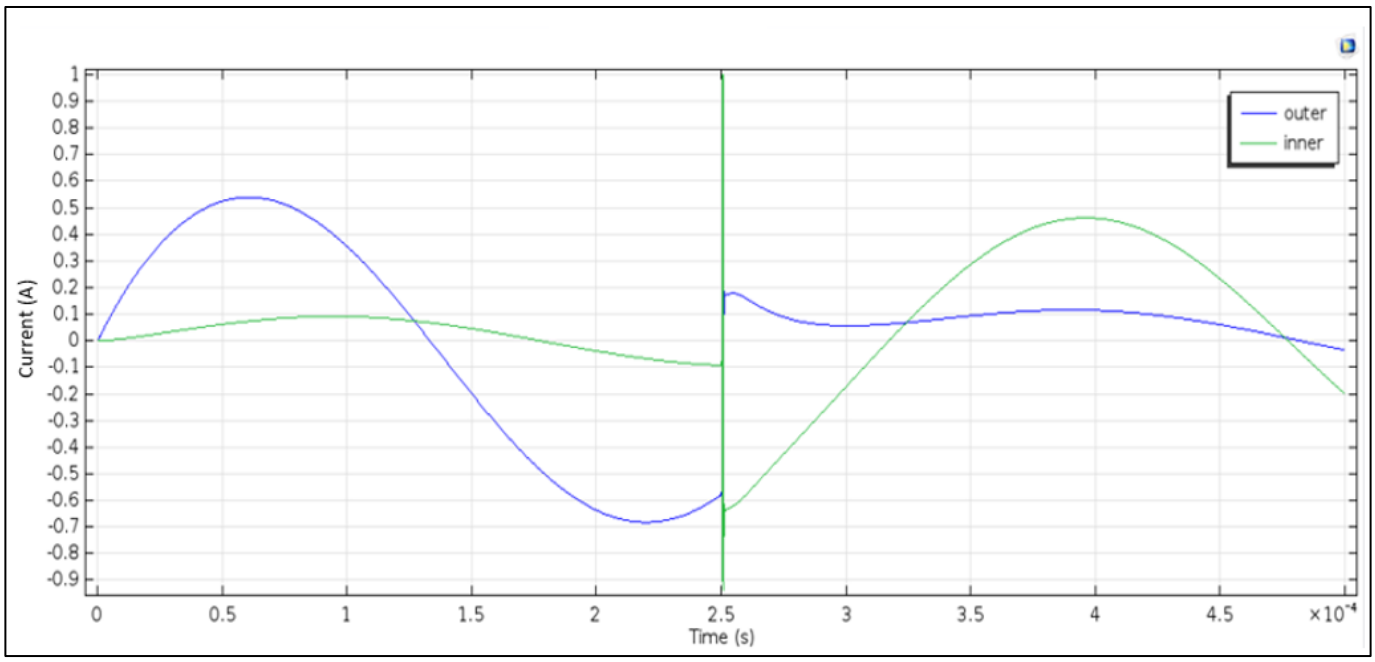


*Figure 63:Current waveforms during switching, close the inner and outer boundary of the primary coil*

### 6.1.4 Frequency selection

Like the studies above indicate, the frequency at which the study is simulated, is of great importance. In this segment, a rough estimation of a frequency at which the device is expected to operate takes place. If a capacitor bank power supply is used, which is the most common for this kind of application, then the above frequency will be the natural frequency of the occurring $LC$ circuit. Since the inductance of the system changes, and so does its natural frequency, the worst-case scenario for the operation of the device needs to be considered, which occurs for the lowest frequency [highest skin depth]. Thus, the frequency used, is associated with the system's highest inductance, which occurs as the projectile leaves the primary. Below, a frequency calculation ensues, as well as a graph which demonstrates the importance of the system's inductance for its natural frequency.

| ***Capacitance (F)*** | ***Inductance (μH)*** |
|---|---|
| 0.032 | 0.01 |
| | 0.02 |
| | 0.03 |
| | 0.04 |
| | 0.05 |
| | 0.06 |
| | 0.07 |
| | 0.08 |
| | 0.09 |
| | 0.1 |
| | 0.11 |
| | 0.12 |
| | 0.13 |
| | 0.14 |
| | 0.15 |
| | 0.16 |
| | 0.17 |
| | 0.18 |
| | 0.19 |
| | 0.2 |

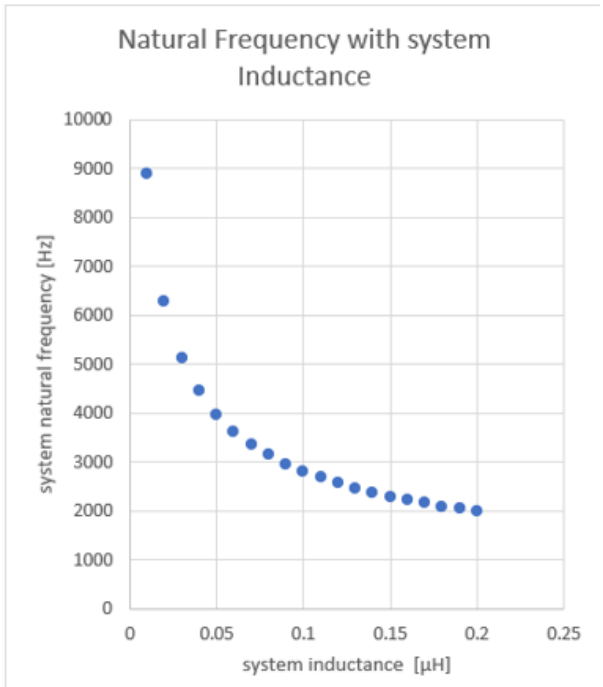


*Figure 64:Frequency dependency on system's inductance*

*example:*

1. $L_{max} = 0.1\mu H$
2. $C_{capacitor\ bank} = 32mF$
3. $omega = \frac{1}{\sqrt{LC}} = 17677$
4. $f = \frac{omega}{2\pi} = 2800Hz$

Things however are not as simple as they appear. Inductance of a solid copper coil, depends on the width of the skin effect, which in turn depends on frequency. Furthermore, to find the natural frequency of oscillations for the device, its inductance should be known. This creates a two-way coupled problem, which could be solved iteratively. It should be said however, that dependence of inductance on skin effect is not that high.

*Model with capacitor, natural frequency:*

In this chapter, the effect of the power supply's capacitance is integrated in the study.

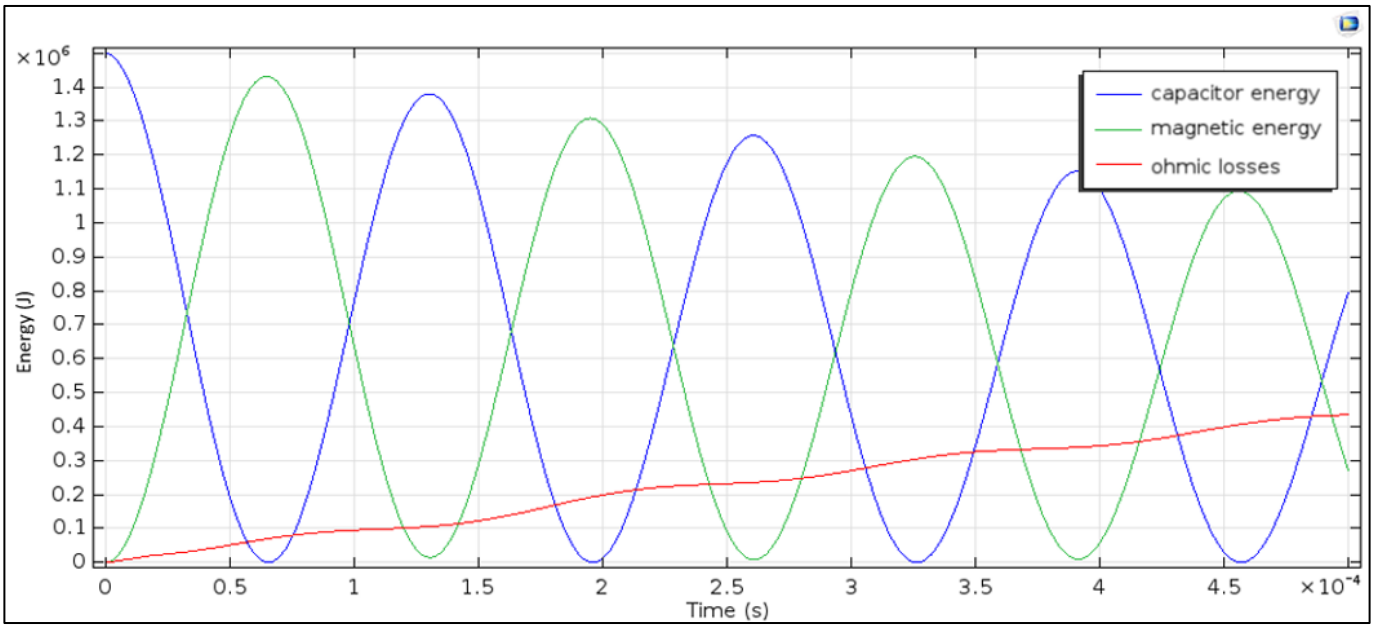


*Figure 65: Oscillatory behavior due to capacitor, inductor, resistor ($RLC$) system*

The tuning of the natural frequency of the system, as a function of the power supply's capacitance to achieve both low resistive losses (bigger skin effect depth), and good coupling (high frequency, small skin effect depth) according to the highest efficiency (lowest losses) criterion is desired.

## 6.2 Parametric study with capacitance

In this simple study, the effect of capacitance in ohmic losses was investigated. A connection between capacitance and ohmic losses exists due to the skin effect which depends on the system's natural frequency.

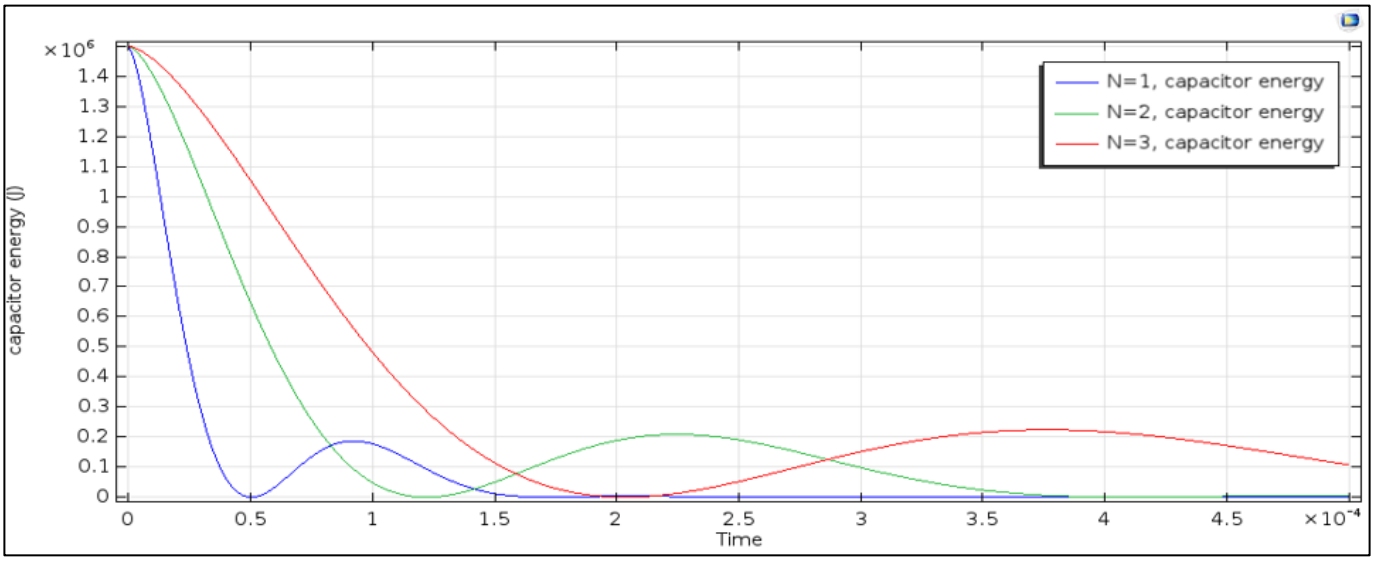


*Figure 66: Energy stored in the capacitor as a function of time, for different system capacitances*

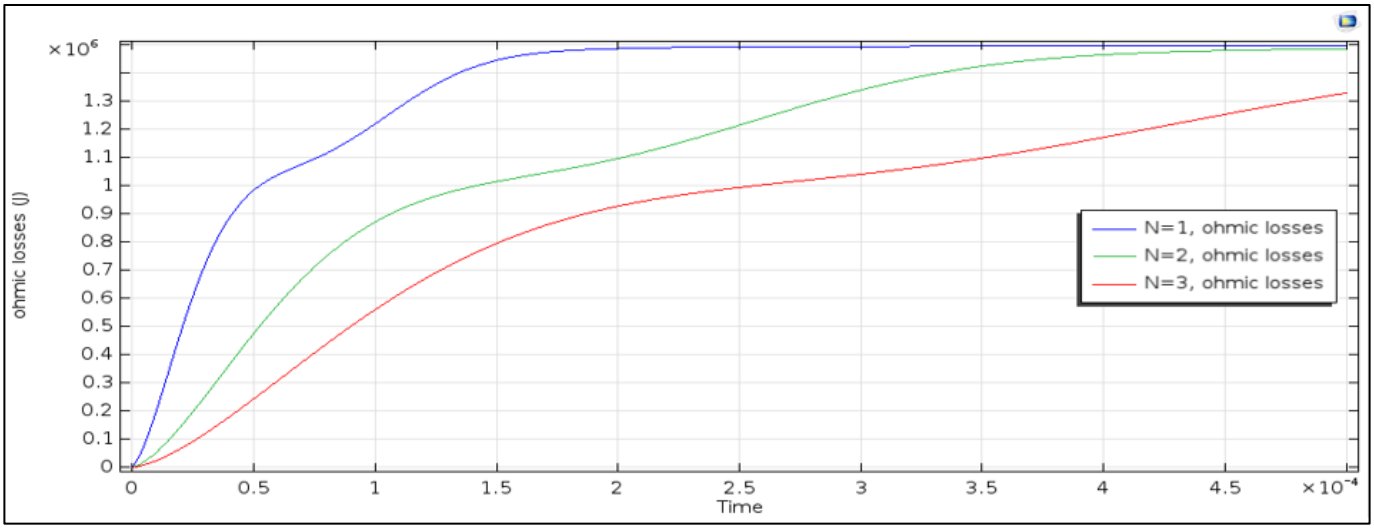


*Figure 67: Comparative ohmic losses for different frequencies, due to varying skin depths*

$$R \propto f$$

$$L \propto f$$

Damping ratio for an $RLC$ circuit: $$\zeta = \frac{R}{2}\sqrt{\frac{C}{L}}$$

*For same natural frequency:*

$$\omega_n^2 = \frac{1}{LC} \tag{39}$$

$$C = \frac{1}{\omega_n^2 L} \tag{40}$$

$$\zeta = \frac{R}{2}\sqrt{\frac{\frac{1}{\omega_n^2 L}}{\frac{L}{1}}} = \frac{R}{2}\sqrt{\frac{1}{\omega_n^2 L^2}} = \frac{R}{2}\frac{1}{\omega_n L} \tag{41}$$

In general, in all electromagetic devices, their efficiency boils down to the ratio :$\frac{R}{L}$, and more specifically, $\frac{R}{L_g}$, where if $L_{final}$ is high, with a low $L_0$, it equates to a high inductance gradient, $L_g$.

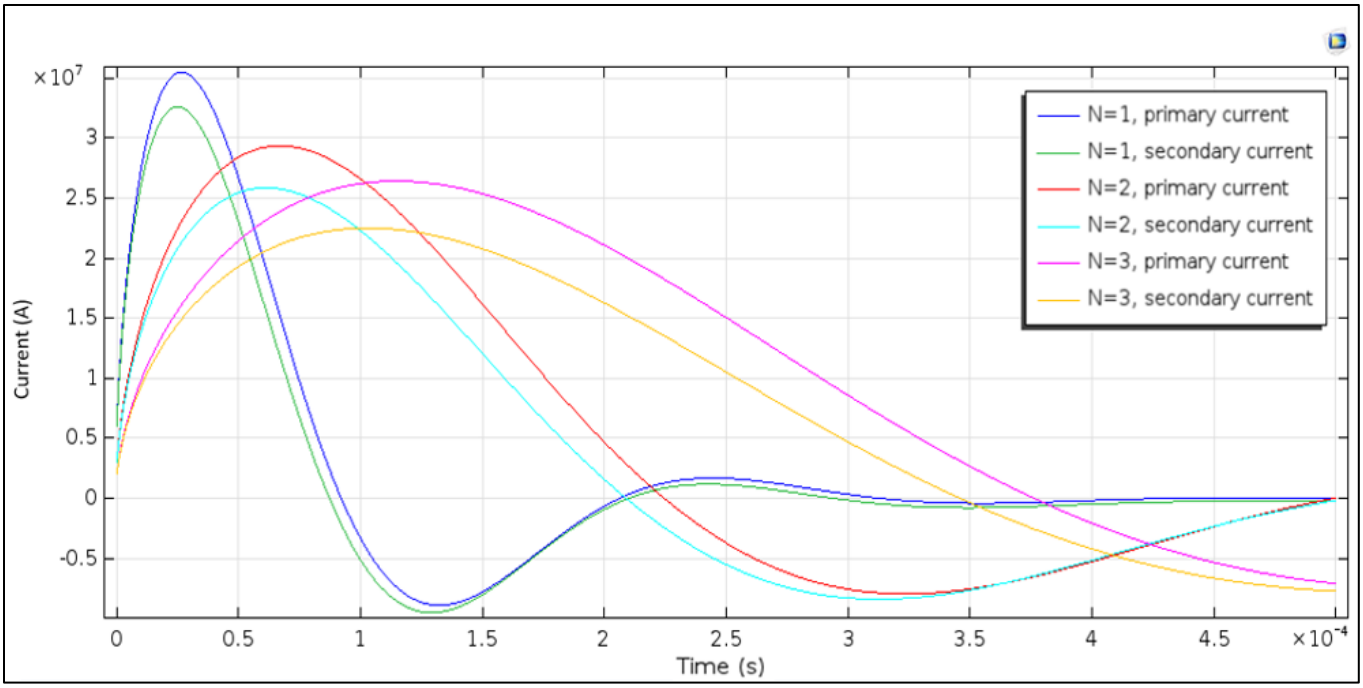


*Figure 68: Graph of primary and secondary currents for different power supply capacitance, and natural frequency*

***Skin effect with different capacitance, and therefore different natural frequency:***

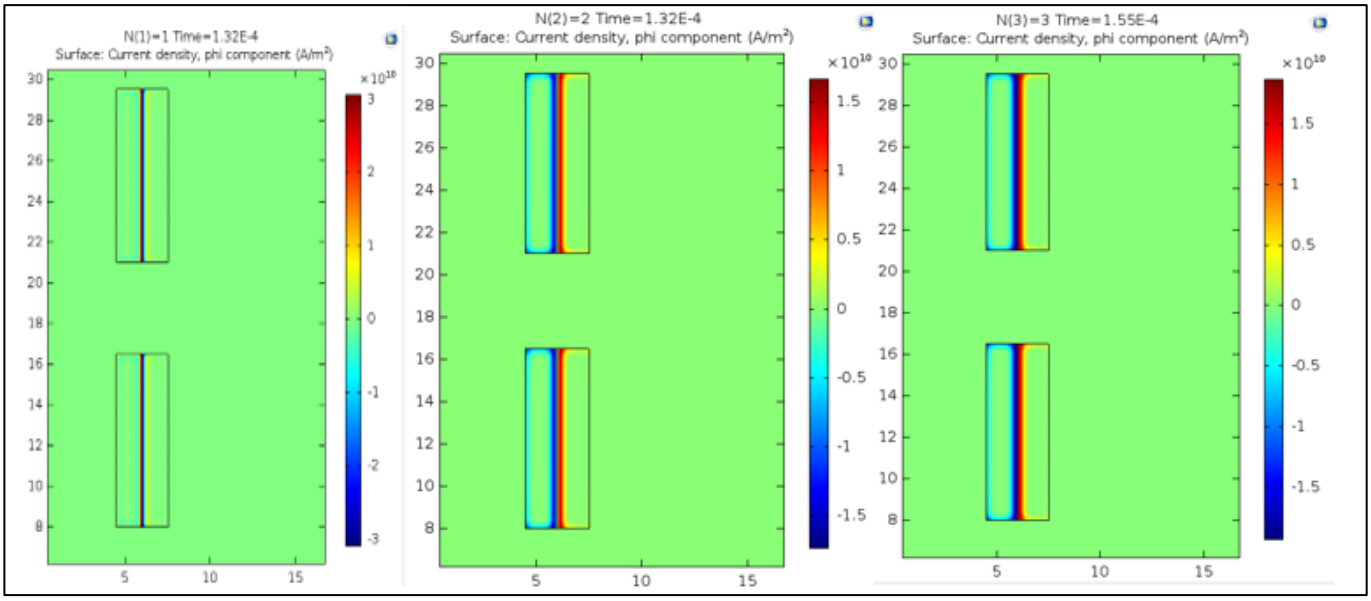


*Figure 69: Graph showing skin depths for different operating frequencies*

Changing the capacitance of the power storage assembly, to affect the natural frequency of the system, and thus the skin depth, to lower the system's resistance (skin effect width gets large) can be seen in the figure above. It is thus evident that natural frequency affects not only the magnitude of the inductance jump but also the resistance of the system. Tuning of this frequency could be done to achieve the highest possible efficiency for a given configuration, by minimizing the sum of the losses due to ohmic heating and sudden inductance jumps.

## 6.3 Efficiency

What needs to be investigated is ways of minimizing the damping ratio of the system: $\zeta = \frac{R}{L_g}$

$$R = \rho\frac{A}{L}, A = conductor\ surface, \tag{42}$$
$$L = conductor\ length, \rho\ specific\ resistance\ and\ depends\ on\ material\ properties,$$
$$L \propto number\ of\ turns\ of\ coil$$

*For coil inductance:*

$$L_{coil} = \mu_r\mu_0\frac{N^2A}{l} \tag{43}$$

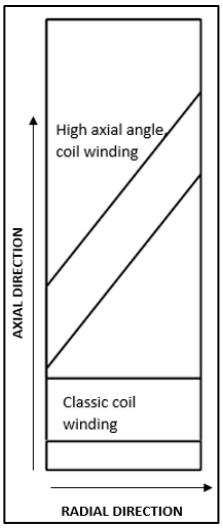


*Figure 70: Alternative coil winding*

The only way of changing the damping ratio, is by changing the inner diameter of the primary coil, since inductance changes by the square of the radius, whereas resistance changes linearly with the radius. In other words, the larger the inner radius of the primary coil, the more efficient the design. It would therefore make sense, the launcher to be used to propel large objects, since it would do so in a much more efficient way than for smaller projectiles. By changing the length of the coil, one can change the acceleration of the projectile (damping factor remains the same), and thus impose a desired acceleration profile to the projectile [Paragraph 7.6]. For small currents and relatively smaller final velocities, an iron core and outer sleeve can be used, which increase the inductance of the system, keeping the system resistance constant (or even lowering it, since homogenized coils can be used). Such a design is presented later [Paragraph 7]. To achieve higher efficiencies, the launcher's primary coil should have as big an area as possible. The simplest way of enlarging this area, is by making the inner radius of the coil bigger, as mentioned above. Another not so straight forward method is to wind the coils with a bigger axial angle, as the figure to the left shows, effectively transforming the coil's cross section to an ellipse. This is equivalent to having a second coil subassembly placed vertically to the first (its axis parallel with r axis of cylindrical system).

| freq (Hz) | Total magnetic energy (J) | Total electric energy (J) |
|---|---|---|
| 100.00 | 1.1689E-8 | 3.8806E-22 |
| 200.00 | 1.1017E-8 | 1.7467E-21 |
| 300.00 | 1.0704E-8 | 4.2100E-21 |
| 400.00 | 1.0510E-8 | 7.8214E-21 |
| 500.00 | 1.0373E-8 | 1.2609E-20 |
| 600.00 | 1.0269E-8 | 1.8596E-20 |
| 700.00 | 1.0186E-8 | 2.5798E-20 |
| 800.00 | 1.0118E-8 | 3.4223E-20 |
| 900.00 | 1.0061E-8 | 4.4866E-20 |
| 1000.0 | 1.0013E-8 | 5.5815E-20 |
| 1100.0 | 9.9705E-9 | 6.8001E-20 |
| 1200.0 | 9.9335E-9 | 8.1428E-20 |
| 1300.0 | 9.9007E-9 | 9.6100E-20 |
| 1400.0 | 9.8714E-9 | 1.1202E-19 |
| 1500.0 | 9.8451E-9 | 1.2921E-19 |
| 1600.0 | 9.8212E-9 | 1.4766E-19 |
| 1700.0 | 9.7994E-9 | 1.6738E-19 |
| 1800.0 | 9.7795E-9 | 1.8838E-19 |
| 1900.0 | 9.7612E-9 | 2.1067E-19 |
| 2000.0 | 9.7444E-9 | 2.3426E-19 |

*Figure 71:Comparative values of magnetic and electric energy stored in the coil's capacitance*

*Capacity analysis:*

Since the operating conditions of the device are of high energetic nature, the self-capacitance of the system needs to be examined, to ascertain that it does not interfere with the operation of the device. To do so, a simple frequency analysis was established for a simple single turn coil. the study was simulated for many frequencies to examine the effect of frequency on the model. It can be seen that the energy stored in the system as electric energy (in the capacitance of the system), is many orders of magnitude smaller than the one stored as magnetic energy. Therefore, all capacitive effects can from now on be ignored, except from the capacitance of the power supply of course which plays a huge role in the operation of the system. This study was done to mainly investigate the electrical forces due to the system's capacitance on the projectile, and it can be seen that nay electric forces can be neglected.

## 6.4 Circuit analysis (physical model)

The circuit used to simulate the physical processes in action will now be explained. As mentioned earlier, the operating principle behind all kinds of electromechanical devices is an inductance gradient which produces a force. To simulate the inductance jump that the figures above show, the circuit used earlier (chapter inductance jump) will be used. COMSOL software in circuit analysis does not allow for the use of a variable inductance (in contrast with simscape software which does allow for its use). The voltage term caused by the variable inductance however can be simulated by a voltage source, whose voltage equals that of the inductance change.

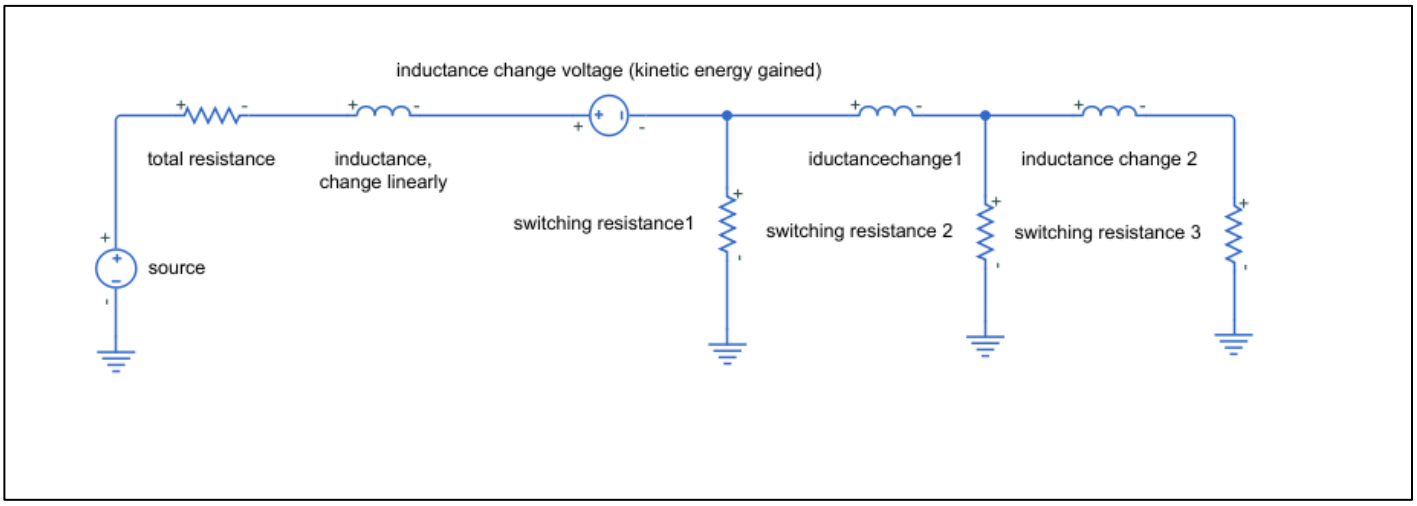


*Figure 72: Lumped parameter model, where with two inductance jumps are implemented through the use of three variable resistances.*

Switching (to trigger disconnection of secondary) is accomplished with the use of variable resistances, like the one seen below.

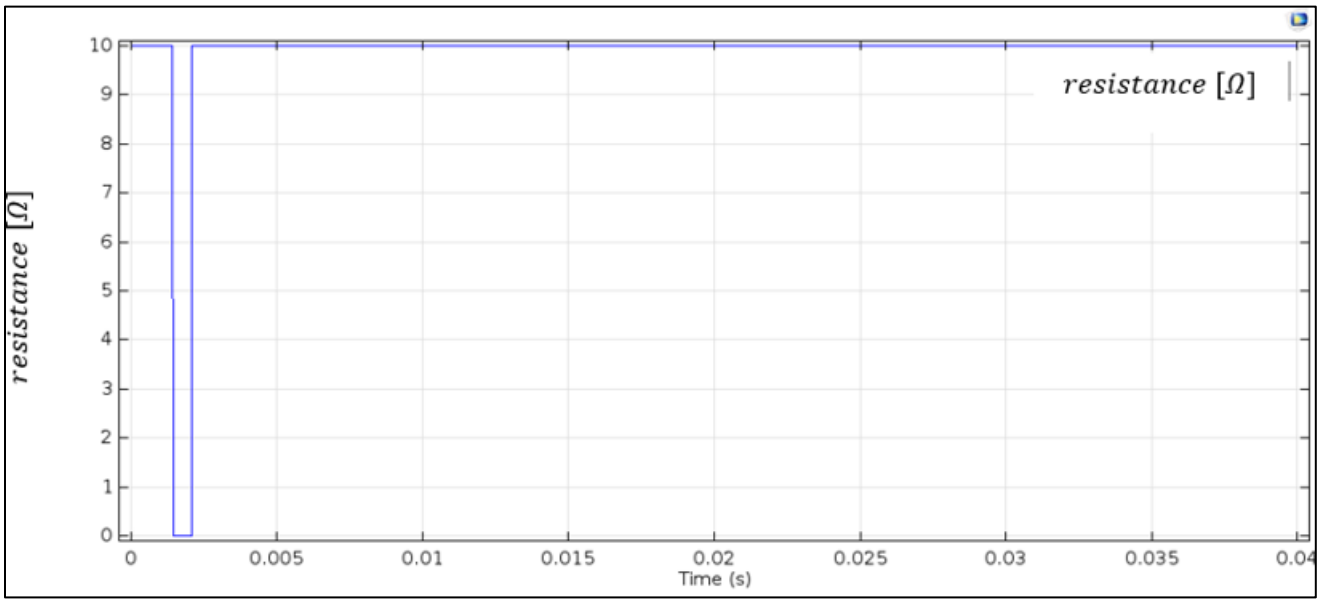


*Figure 73: Resistance profile to trigger switching in lumped parameter model mentioned above*

| PARAMETER NAME | PARAMETER VALUE | PARAMETER DESCRIPTION |
|---|---|---|
| $dl$ | $0.05[mH/N]$ | *Sudden inductance jump* |
| $Res$ | $0.01[\Omega]$ | *System's resistance* |
| $X1$ | $0.14286[m]$ | *Distance where switching occurs* |
| $L0$ | $10[mH]$ | System's initial inductance |
| $Lg$ | $0.2[mH/cm]$ | *Inductance gradient* |
| $mass$ | $1[kg]$ | *Projectile's mass* |
| $I\_0$ | $1000[A]$ | *Initial current* |

*Table 6: Properties of simulated system*

In the simulation performed below, the power supply was a voltage source and not a capacitor bank. The capacitor was integrated in the simulation in later studies. his simulation however serves mainly as a proof of concept, and not to simulate a real-life design.

General results before the presentation of a realistic scenario:

*Energy conservation/conversion*

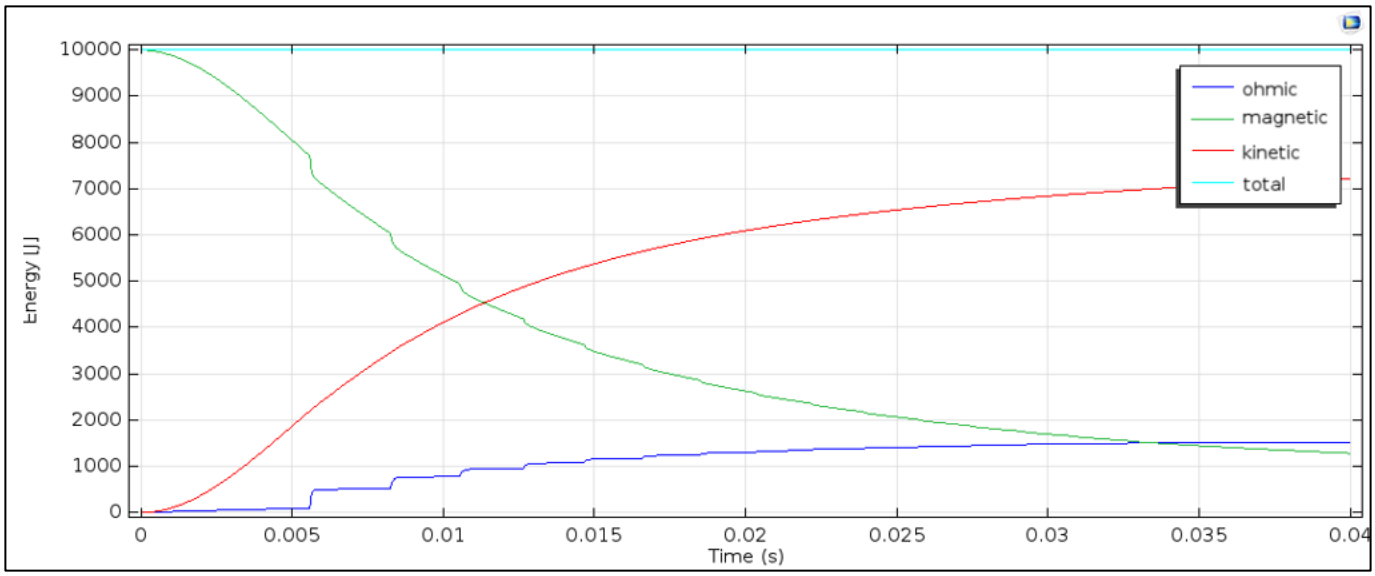


*Figure 74: Graph showing the total, magnetic, kinetic and lost energies for the above simulated system*

1. Energy is conserved (total energy in the system remains the same), which means that probably the analysis is correct.
2. Energy lost during inductance jump is the same gained by resistive losses
3. Gradient of magnetic energy gets smaller, as time passes since inductance gets larger

The force produced by the device, as previously stated is proportional to the current squared, and for an initial current and no other voltage source in the circuit, decays as the graph above shows, having its maximum value at time zero.

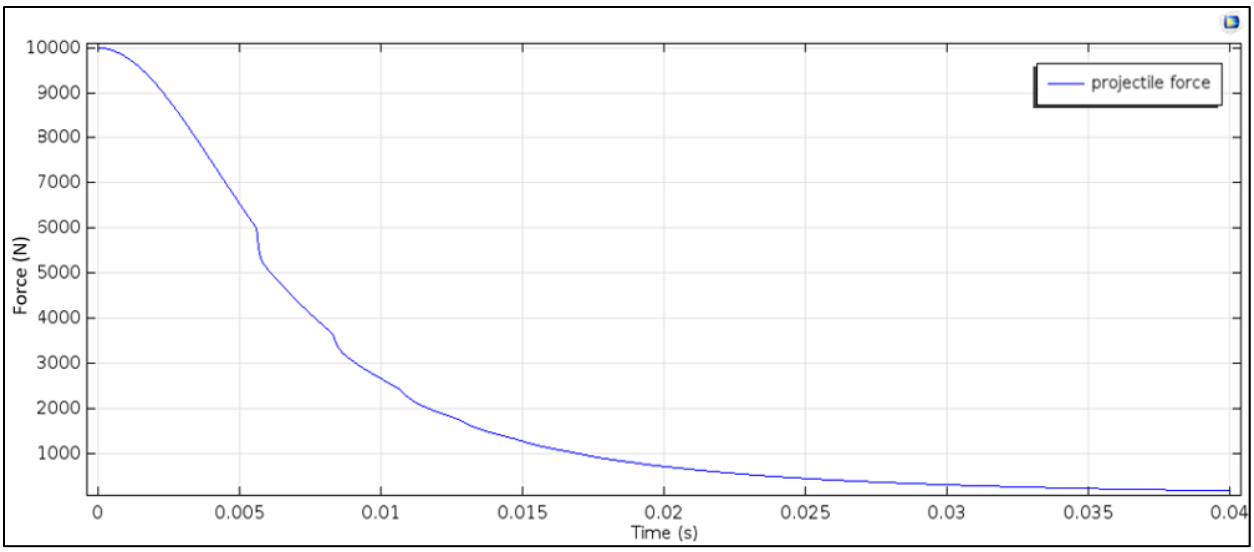


*Figure 75: Force as calculated from lumped parameter model*

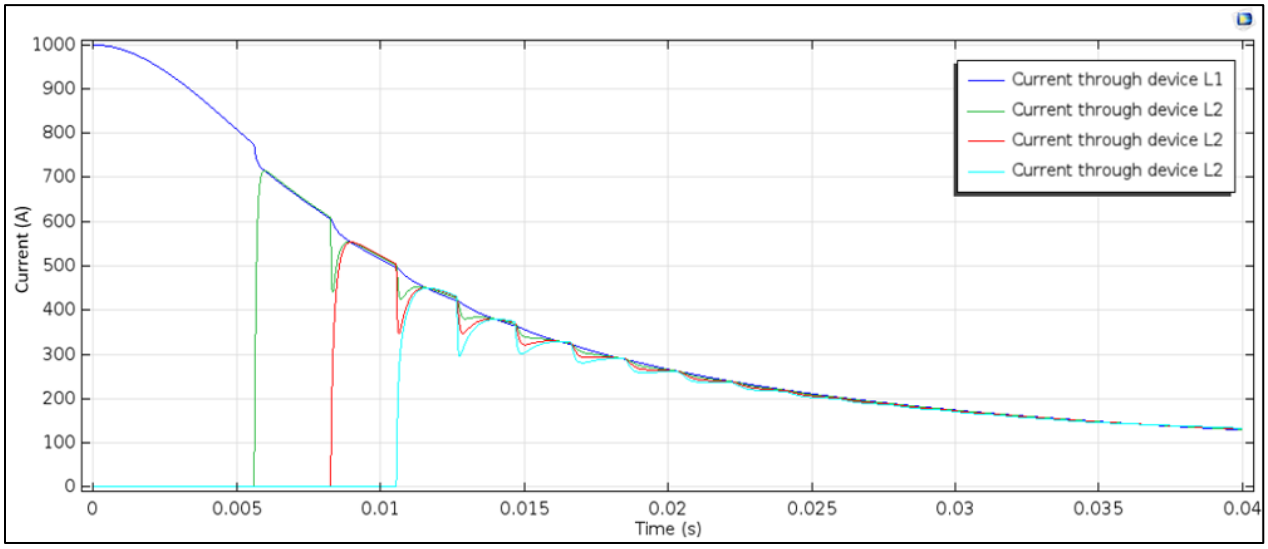


*Figure 76:Current for multiple inductors, as calculated from lumped parameter model*

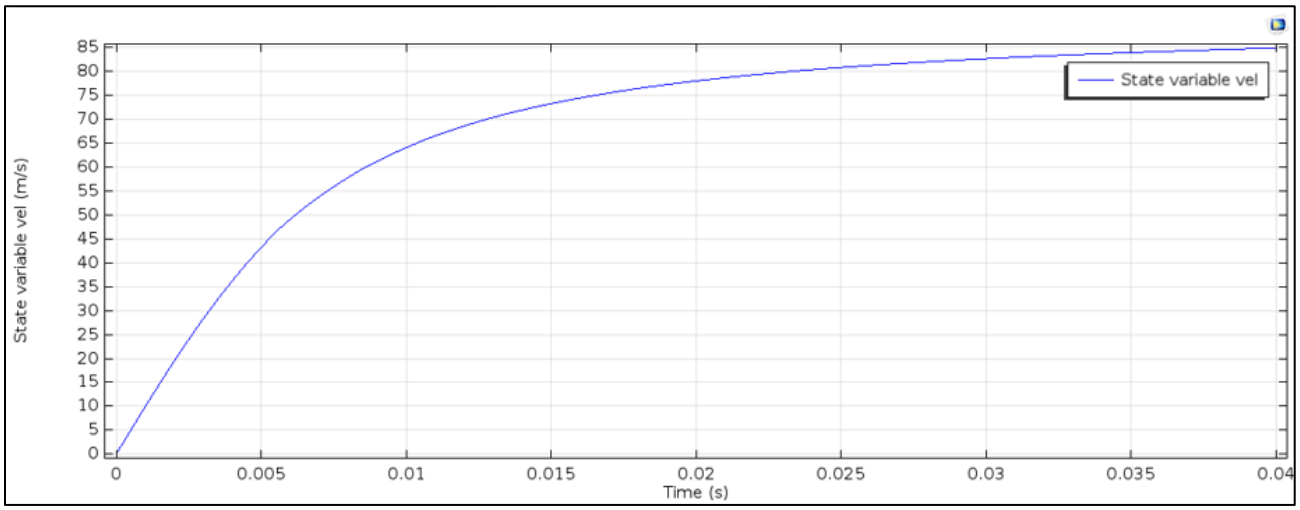


*Figure 77: Projectile velocity as calculated from lumped parameters model*

The final attained velocity is not that high, because the initial stored energy in the inductance of the system as magnetic energy was low. The efficiency of this design is around 80%.

## 6.5 Final configuration 1

1. $R = 0.0035[\Omega]$
2. $r_{inner} = 14[cm]$ (thick configuration), $primary\ width = 1.5[cm]$

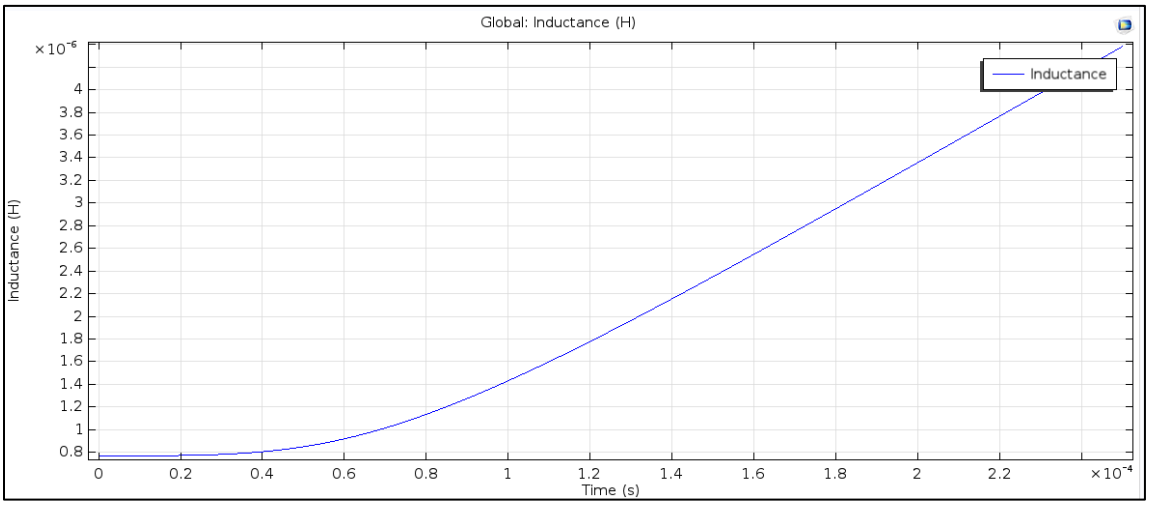


*Figure 78: System's inductance as a function of time, excluding inductance jumps*

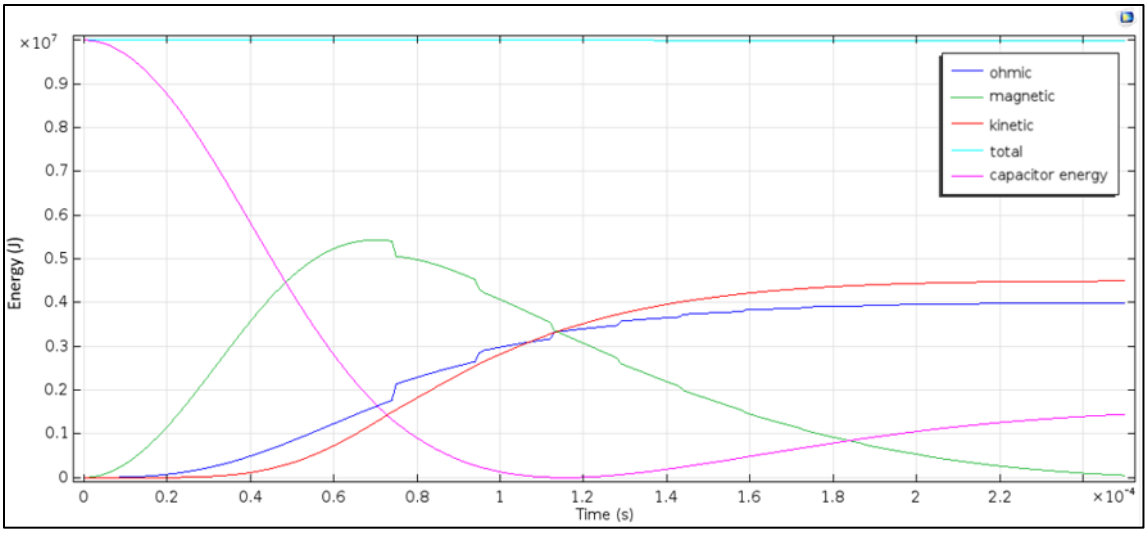


*Figure 79: Energy equilibrium for the system. Total, kinetic, capacitive, magnetic and ohmic energies are plotted*

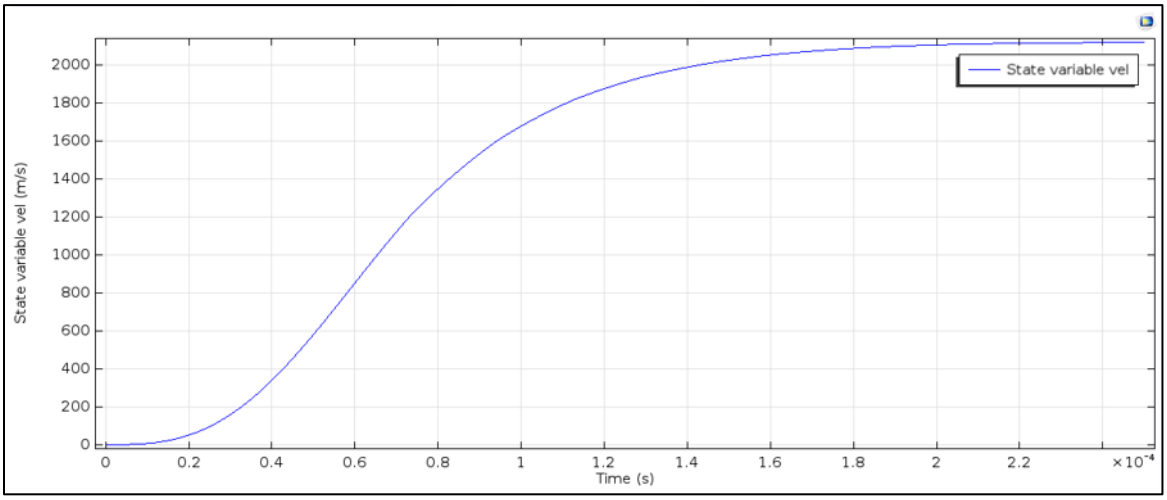


*Figure 80: Projectile's velocity as a function of time*

## 6.6 Final configuration 2

1. $R = 0.0017[\Omega]$
2. $r_{inner} = 6[cm]$ (slim configuration), $primary\ width = 1.5[cm]$

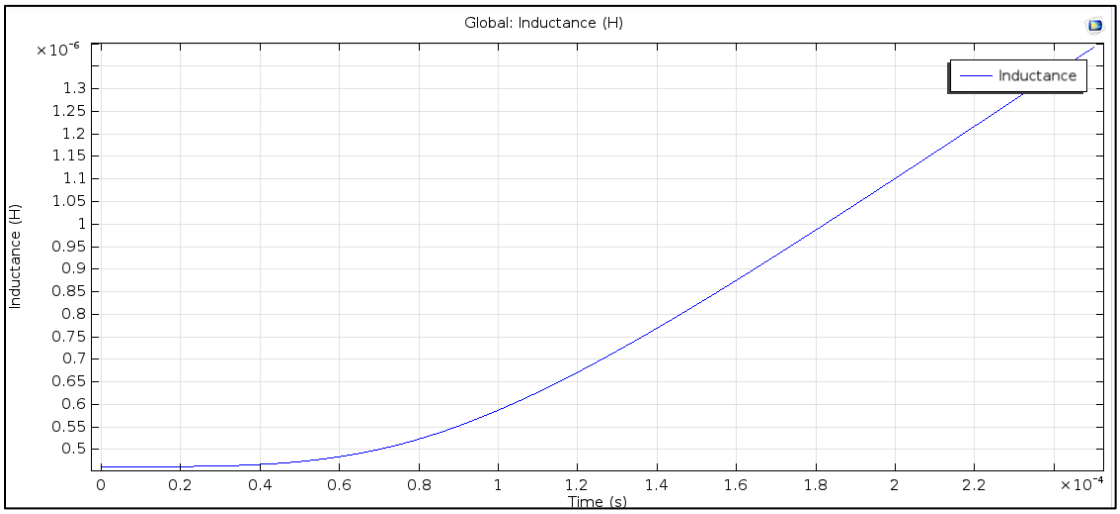


*Figure 81: System's inductance as a function of time, excluding inductance jumps*

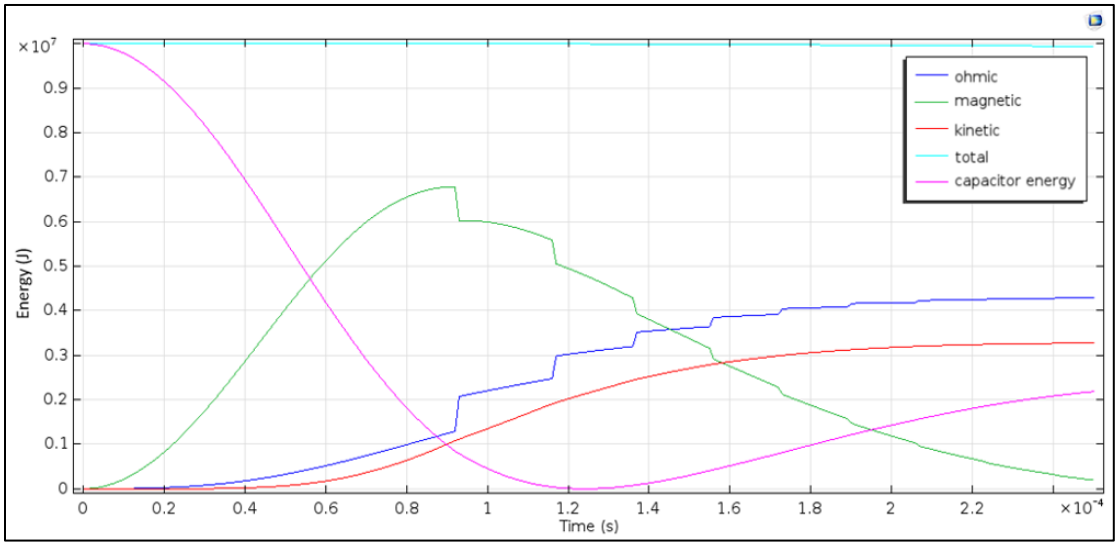


*Figure 82: Energy equilibrium for the system. Total, kinetic, capacitive, magnetic and ohmic energies are plotted*

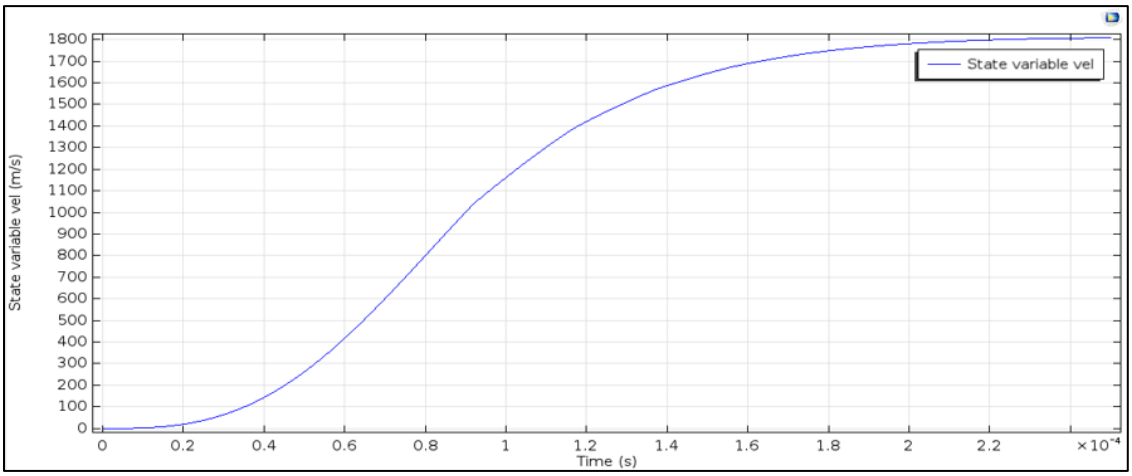


*Figure 83: Projectile's velocity as a function of time*

## 6.7 Final configuration 3, homogeneous coils spaced far apart

1. $R = 0.00016[\Omega]$
2. $r_{inner} = 4[cm]$ , $primary\ width = 1.5[cm]$

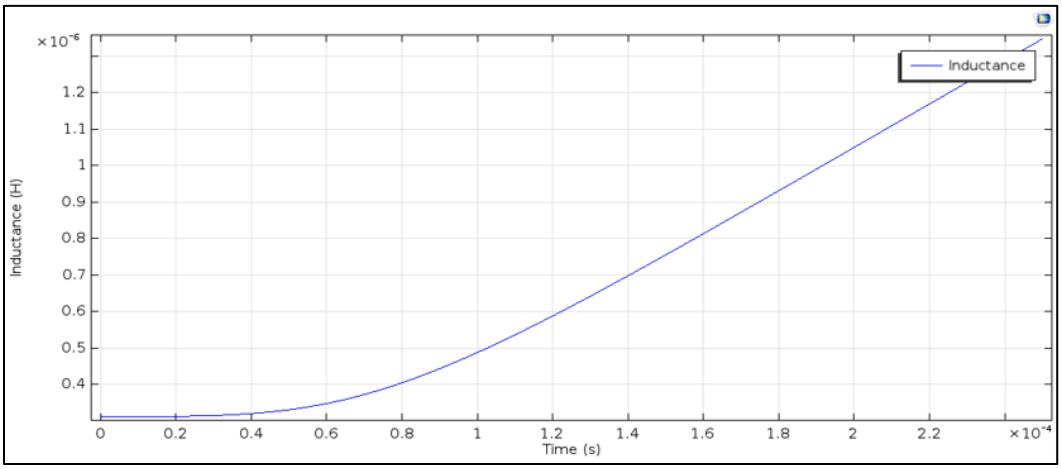


*Figure 84: System's inductance as a function of time, excluding inductance jumps*

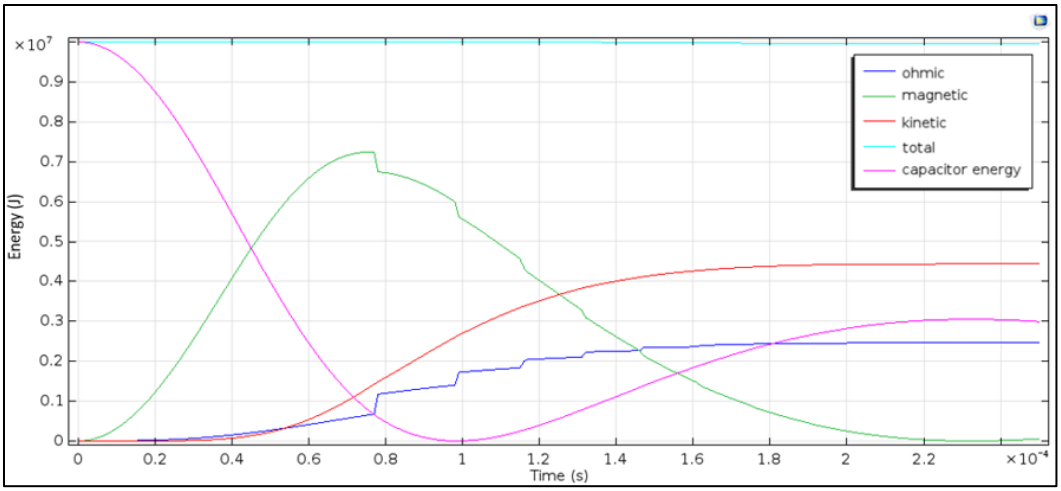


*Figure 85: Energy equilibrium for the system. above total, kinetic, capacitive, magnetic and ohmic energies are plotted*

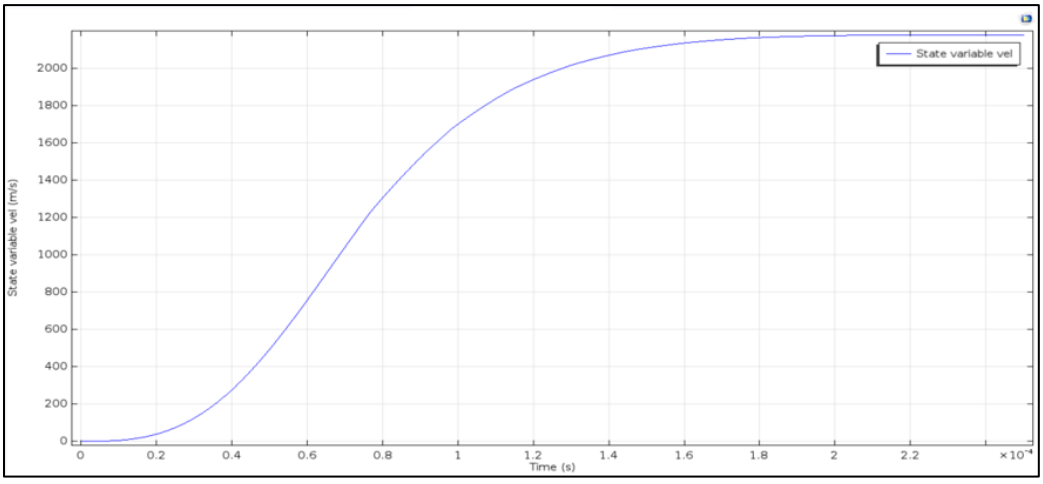


*Figure 86:Projectile's velocity as a function of time*

From the diagrams above it can be seen that the operation for the homogeneous configuration is similar if not more efficient than that of the skin effect configuration. Of course, other than efficiency, this configuration does not present any other advantages over the skin effect design. More specifically, the skin effect design has a much smaller inductance jump, larger inductance gradient and easier construction. Of course, on the other hand due to homogeneous current density, the homogeneous design presents lower ohmic losses, and structural loads are distributed over a bigger volume due to the elimination of the skin effect.

# 7 DESIGNS WITH FERROMAGNETIC MATERIAL

## 7.1 Design with stationary iron core and sleeve

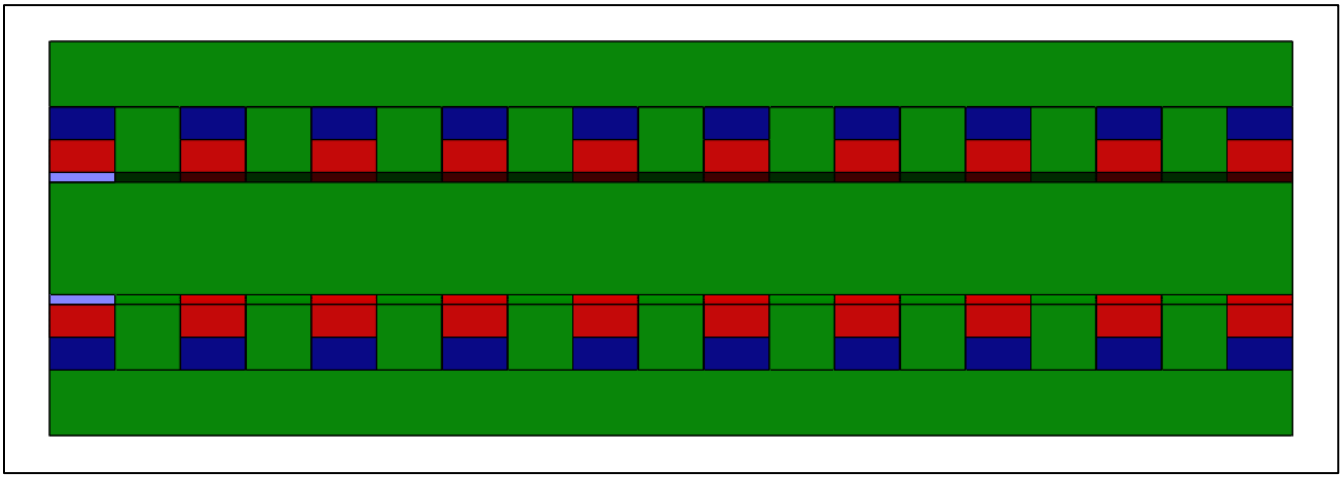

*Figure 87: Simple schematic of configuration with iron core and sleeve*

1. Green: iron core, sleeves
2. Deep blue: stationary secondary coils
3. Light blue: projectile (moving secondary)
4. Red: primary coils

Disadvantages of iron core design:

1. Hollow projectile
2. Magnetic fields lower, as not to lead to the saturation of the magnetic material. As a consequence, force acting on the projectile will also be smaller

Advantages:

1. Efficient design, since damping ratio of equivalent circuit is much smaller, as compared to a design of the same dimensions but without the ferromagnetic material.
2. This design especially fits for the acceleration of small diameter projectiles.

*Simulation with iron core and sleeve:*

1. Normally, a ferromagnetic material such as iron would be selected for an analysis like this. The frequency simulation however for magnetic fields in COMSOL dos not allow for a material with a B-H curve like iron to be simulated. Thus, a material with magnetic permeability of 1000 was selected.
2. Stimulating current: $I_{primary} = 10.000 \cdot \sin(2 \cdot \pi \cdot 100 \cdot t)$, frequency was selected this low, to simulate a homogeneous coil (where skin effect is eliminated).

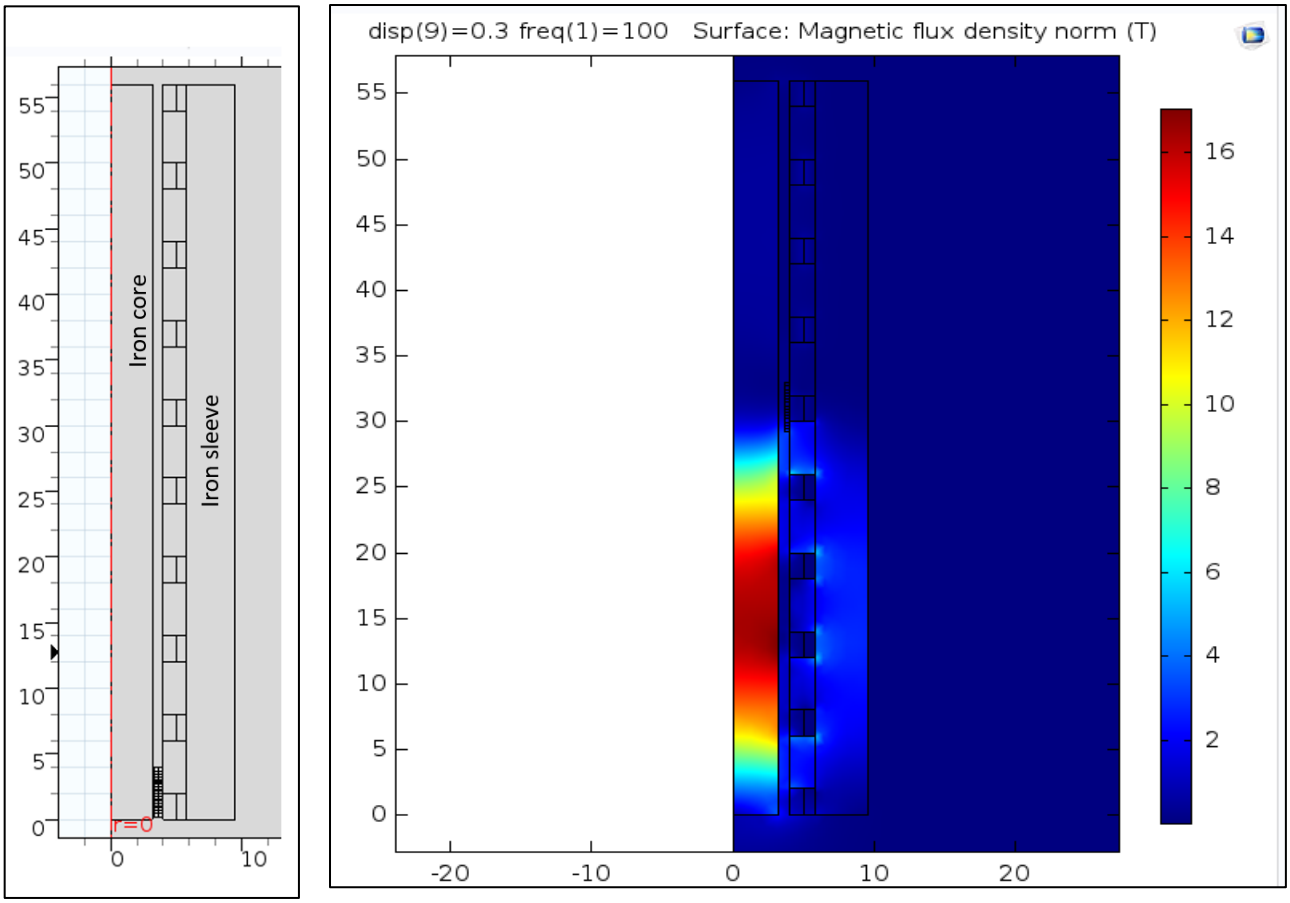


*Figure 88:Simulated system to the left, to the right: magnetic field present at configuration with stationary iron core and sleeve*

Magnetic field for configuration with iron core and sleeve. This design is very helpful, since it facilitates modelling because it requires much smaller currents (due to the iron core) for its operation.

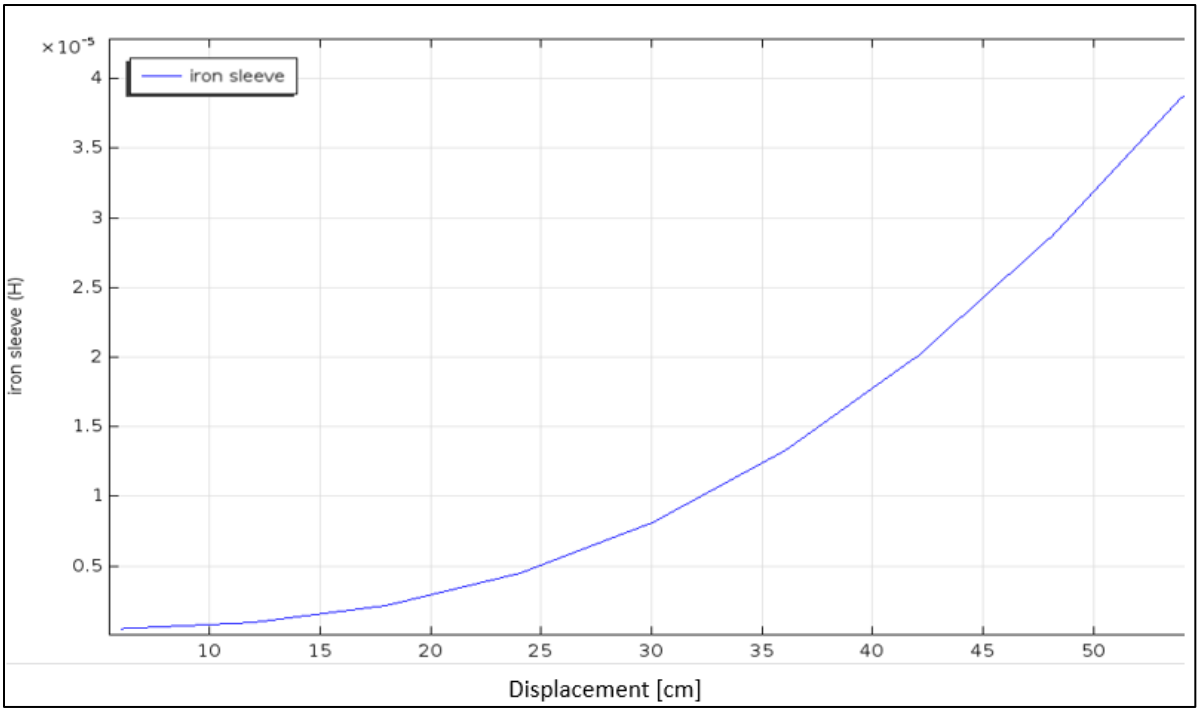


*Figure 89:Inductance as a function of displacement for configuration with iron core and sleeve*

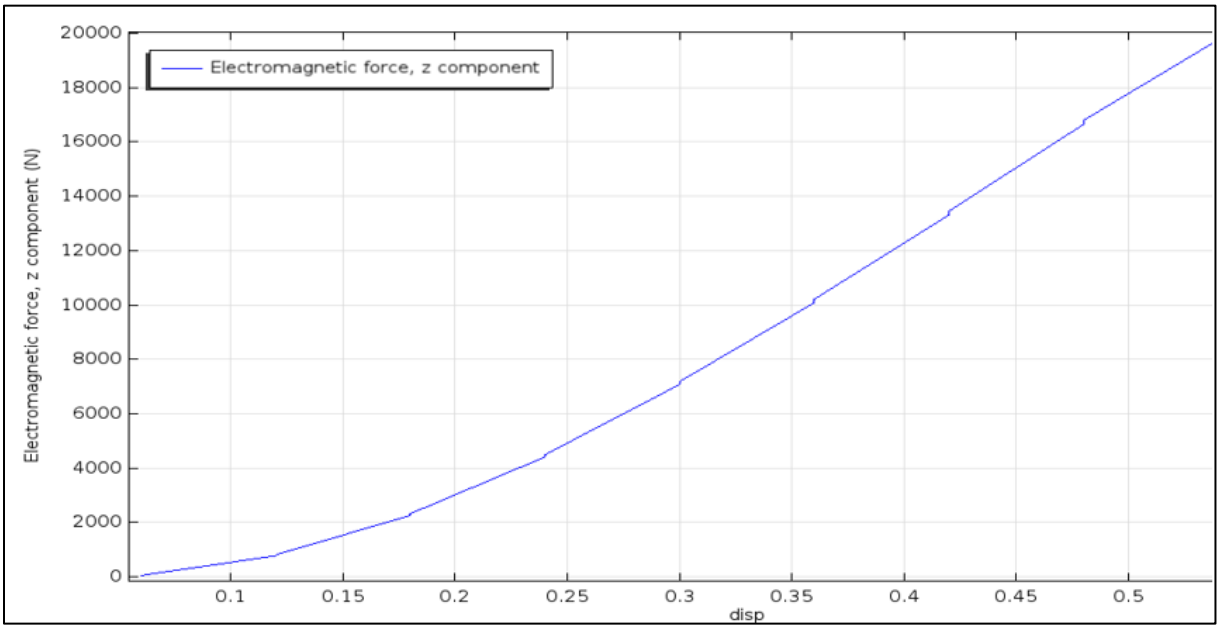


*Figure 90: Force as a function of displacement for configuration with iron core and sleeve*

In reality due to magnetic saturation of the core and sleeve, inductance will not change in a parabolic way, but rather linearly. Nevertheless, before saturation occurs, the graph above is valid, and the configurations manages to reduce total system resistance, while simultaneously increasing system inductance. Furthermore, magnetic hysteresis phenomena were not accounted for in the model. Nevertheless, their effect will not be very noticeable because magnetic saturation plays a much more significant role.

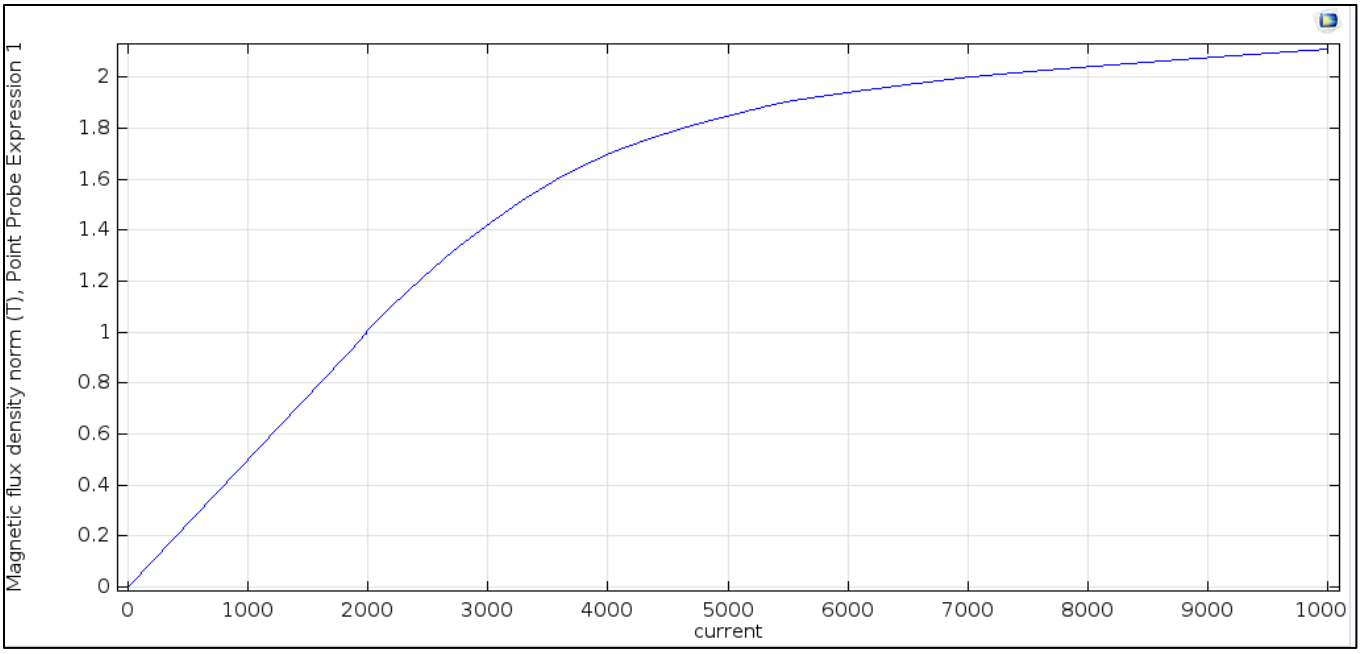


*Figure 91: Magnetic field as a function of current, for simple coil with iron core configuration. It can be seen that saturation is beginning to be reached at around 2 Tesla.*

## 7.2 Configuration with no inner stationary iron core, only with outer sleeve

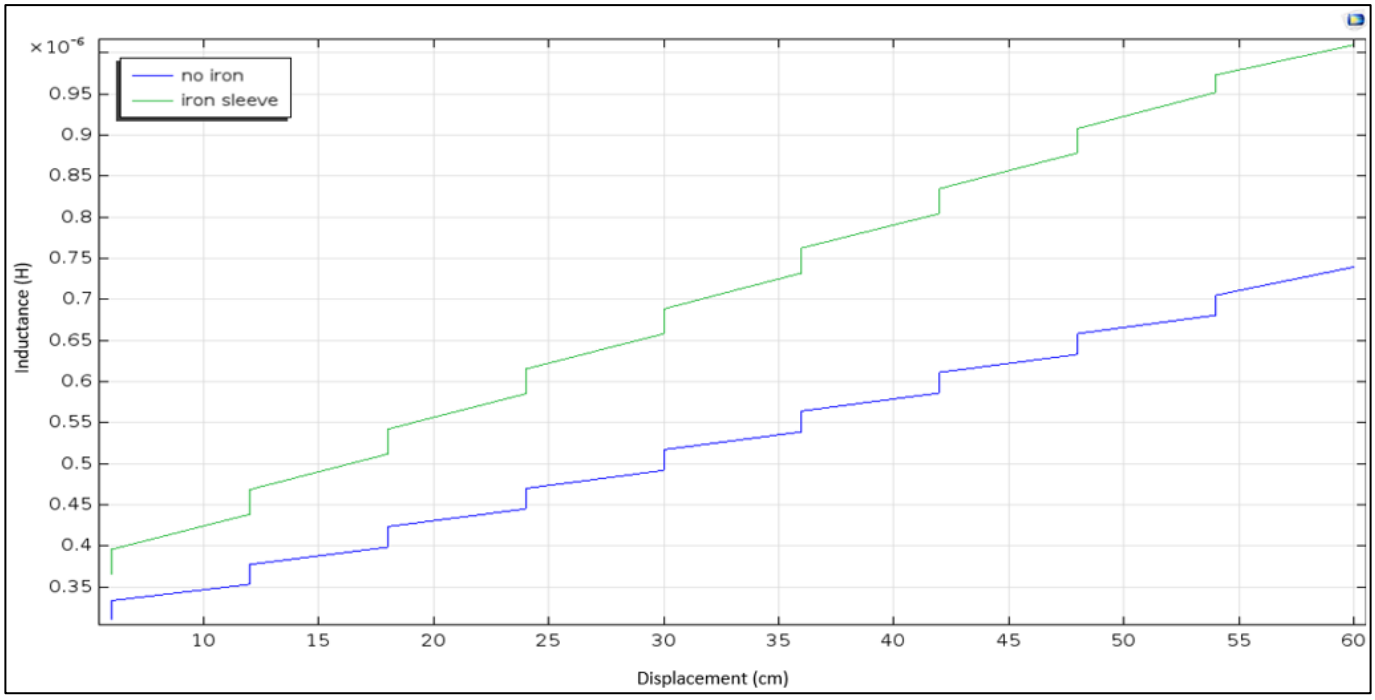


*Figure 92: Comparative diagram for configurations with and without iron sleeve*

Inductance remains the same, but inductance jump is reduced. In this design, the total resistance of the system as compared to the total inductance of the system is much smaller, making the design more efficient (since homogenized coils are used, whose resistance is at least 10 times smaller). The inductance jump can be reduced even further if a moving iron core is used, which can be seen in the following figure [Paragraph 7.3].

## 7.3 Configuration with iron sleeve and moving iron core as part of projectile

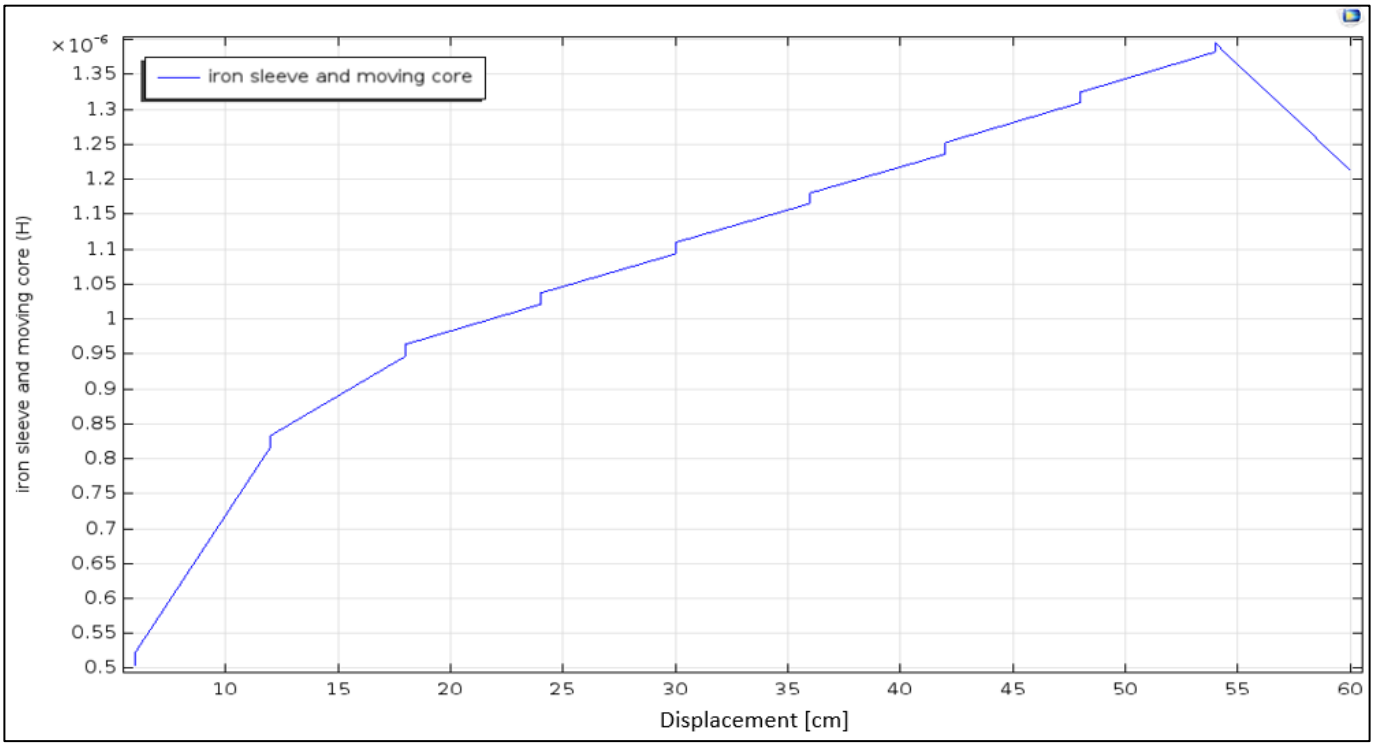


*Figure 93: Inductance graph as a function of projectile displacement for configuration with moving iron core and stationary sleeve*

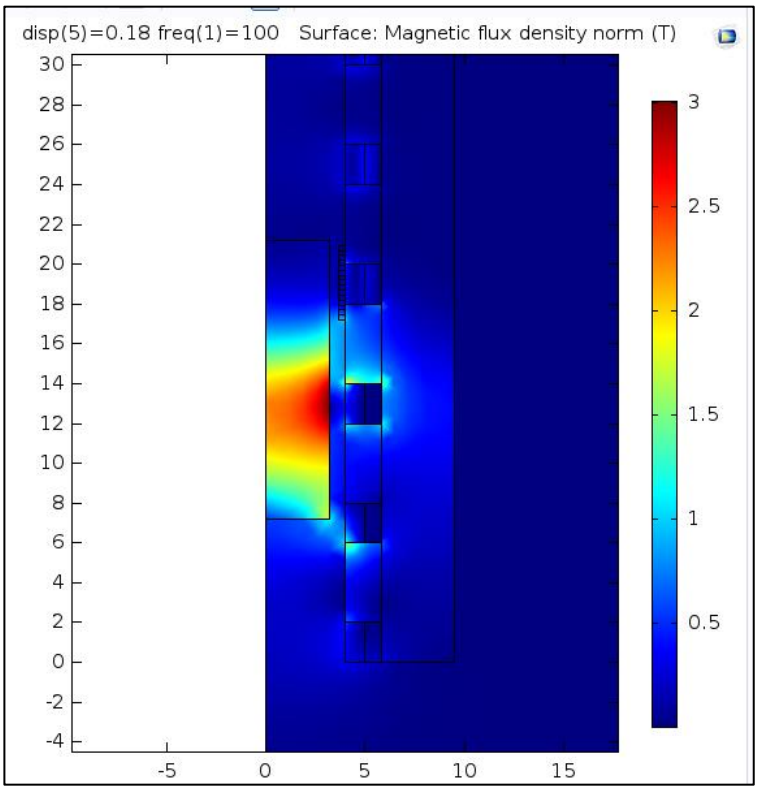


*Figure 94:Magnetic field formed in the configuration with moving iron core and stationary outer sleeve*

Total inductance change is the same for the model with and without the iron core. The inductance jump however is much smaller, because with the iron core and sleeve when change occurs, coupling is better between primary, projectile, and stationary secondary coil, due to the addition of the ferromagnetic material. A sudden rise and fall in inductance can be seen as the projectile enters and leaves the primary coil. this happens due to the ferromagnetic core, which effectively multiplies the system's inductance.

## 7.4 Comparison between homogeneous, solid conductor and iron core and sleeve configurations

| ***PROS*** | | |
|---|---|---|
| ***HOMOGENEOUS DESIGN*** | ***WITH IRON CORE AND SLEEVE*** | ***SOLID CONDUCTOR DESIGN*** |
| Low damping ratio | Low damping ratio | Low initial inductance |
| High output velocity | Low inductance jump | High inductance ratio |
| Low ohmic losses | Easy construction | Easier construction |
| More predictable behavior | High inductance ratio | High output velocity |
| High dependence on geometry, thus easier to optimize for | Low ohmic losses | Low inductance jump |
| | Very predictable behavior | |
| ***CONS*** | | |
| High initial inductance | Low output velocity | High damping ratio |
| Low inductance ratio | Magnetic saturation occurs | High ohmic losses |
| High inductance jump | Hollow projectile | Less predictable behavior |
| | | Less dependency on geometry, thus more difficult to optimize |

*Table 7: comparative table for homogeneous design, skin effect and with iron core configurations*

*Power supply capacitance:*

The capacitance of the power supply needs to by such that:

1. Natural frequency of system is small, and thus energy is transferred in a rapid manner from capacitor bank to coils [Paragraph 6.1.4].
2. Allows for both polarity currents, if energy retrieval is desired. Usually, polarized capacitors are cheaper than unpolarized, and this is why they are often used. Other than that, they offer no significant advantage over unpolarized capacitors.
3. Able to recharge (retrieve energy that would have been lost as breech voltage)
    a. Breech voltage (energy): energy lost when projectile leaves rails (in railgun operation), thus opening the circuit. Due to inductance and sudden change in current a high voltage is produced which also produces arcs. In the design here, breech energy can be simply defined as the energy still remaining in the circuit, in the form of magnetic energy (stored in inductance), which in contrast with the railgun operation will not be lost.

The simulations above where done with a power supply capacitance such that, the requirements above were met. This is not to say that capacitance was optimized for every scenario as to achieve the highest possible efficiency, but rather merely satisfied the above requirements.

## 7.5 Final construction for skin effect configuration

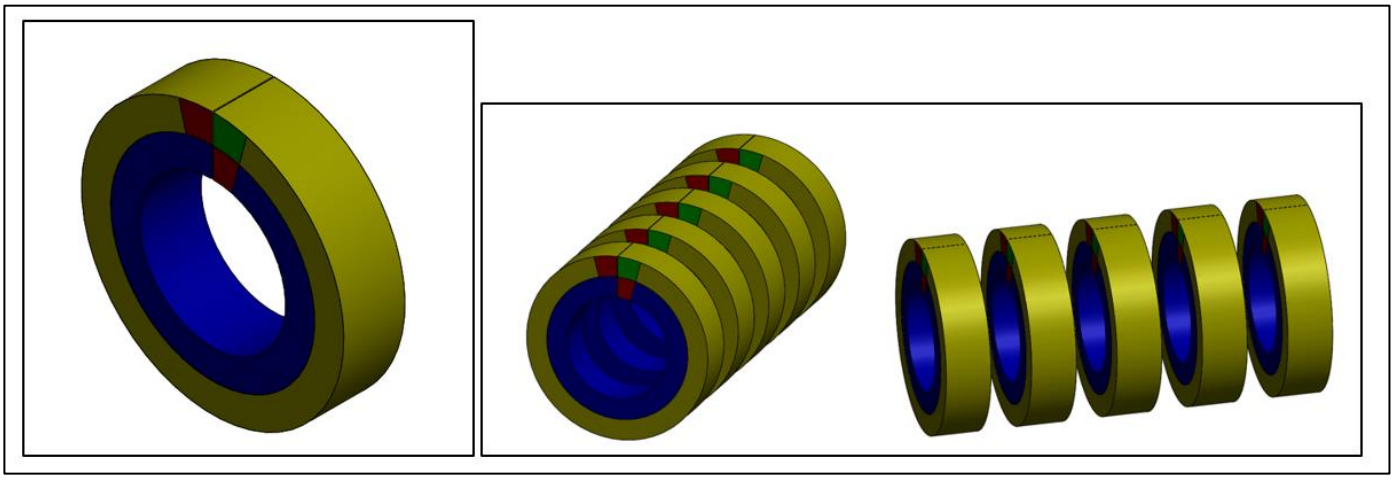

*Figure 95: Views of coil subassembly and assembly with 5 linearly patterned coils, for proposed accelerator*

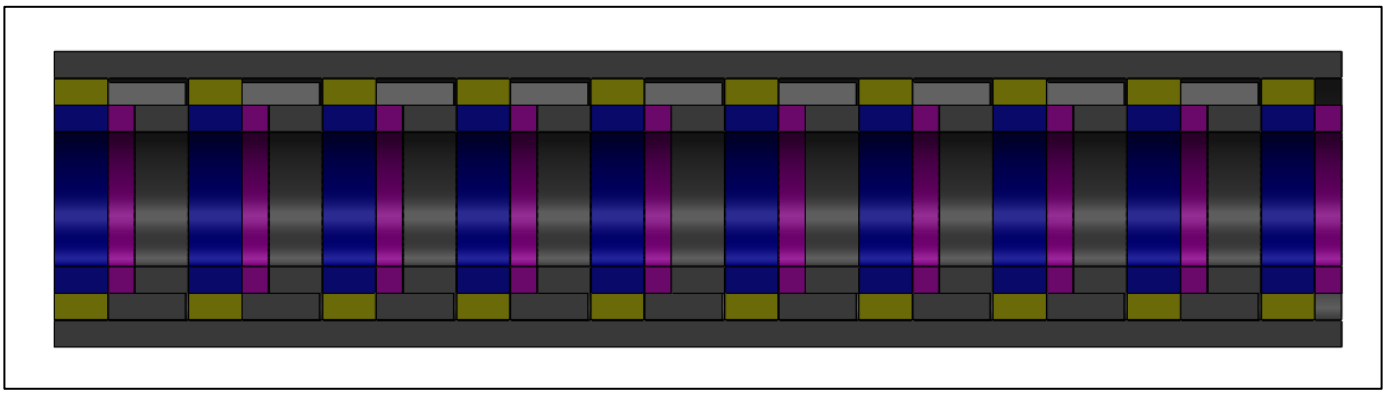

*Figure 96: Section view of the proposed mass accelerator, where coil subassemblies as well switches and structural supports can be seen*

1. *Green*: current inlet
2. *Red*: curernt outlet
3. Yellow: stationary secondary coil
4. *Blue*: primary coil
5. *Gray*: strutural support
6. *Purple*: switch

Above some figures can be seen of the proposed launcher's construction, which consists of linearly repeating coil subassemblies as seen above. The primary as well as the secondary can be made from either multiturn coils [Paragraph 7.6], or single turn, according to the device configuration. The switch can be located either coaxially in-between successive coil subassemblies, or they could all be placed one in front of the other, to the side of the rest of the device. structural support material is placed between coil subassemblies and as an exterior sleeve surrounding the whole launcher. Doing so increases the system's stiffness and keeps everything tightly in place in spite of the high forces. Each secondary coil is connected to a switch, and all primary coils are connected to each other, forming a larger single coil. Power supply would be connected to the "current inlet" of the first primary coil, and the "current outlet" of the last.

## 7.6 Final construction for homogeneous coil configuration

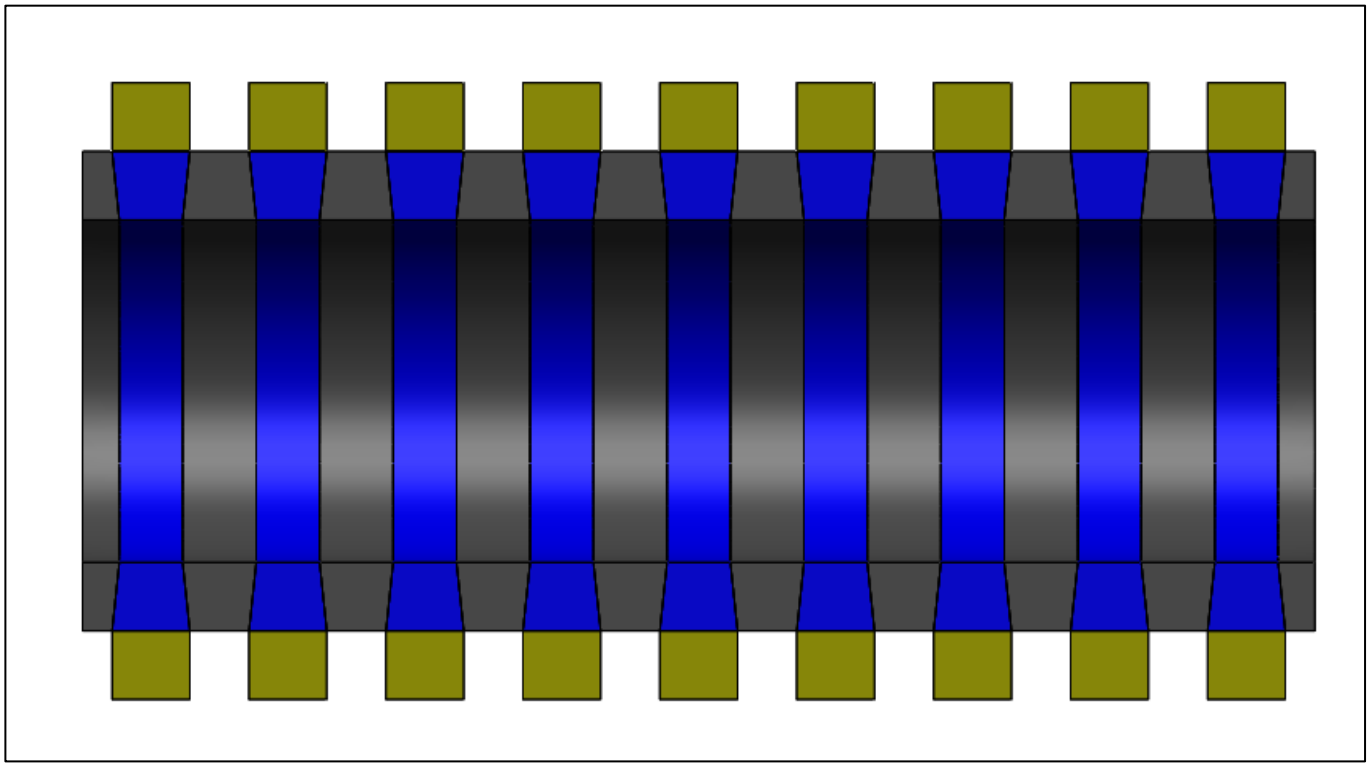

*Figure 97: Design of the homogeneous coil configuration*

In this configuration, the structural supports (gray) are wedge shaped at the place they contact the primary coil. As electromagnetic force pushes the coils inwards, due to small contact angle, contact force cancels out the radial electromagnetic force, thus keeping the coils in place. Structural supports for the secondary coils as well as the switches are not pictured, since they are exactly the same as for the previous configuration [Paragraph 7.5]. As previously mentioned, in this configuration individual coils forming the primary coil are spaced far apart, in contrast to what is shown in the figure above. For better visualization however, of the relative dimensions of the individual parts, they were positioned closer to each other (mainly for the wedge shape to be visible). Some type of axial clamping should be used to keep all components in contact, as well as to add rigidity and stiffness to the system. The projectile could either be a homogenized coil, or simply a thin sleeve of conductive material.

From the graphs above (page 66-68) it can be seen that basically one third of the projectile's final velocity is gained as the projectile leaves the first coil subassembly (when first switching action occurs). In the homogeneous coil configuration this could be easily mitigated by axially varying the inductance gradient of the device (not linear change as explained in Paragraph 5.3.1, but parabolic for example), by having more or fewer coil turns per coil subassembly. This could be done for the skin effect configuration as well, but not as easily.

*Difference with induction coil-gun [Paragraph 1.1]:*

1. The design presented here consists of one primary circuit, which is supplied with power, whereas induction coil-gun consists of multiple unconnected circuits, all connected to a different power supply
2. In a coil-gun, coils are switched on as the projectile passes them, whereas here they switch off
3. A coil-gun is an actively powered design (has a simple feedback loop), whereas the design here is operated passively like a railgun, this is the biggest drawback of an induction coil-gun, since it restricts the max velocity of the launcher, which the design here solves.

*Comparison between proposed launcher and conventional railgun:*

The advantages of each configuration are clear. On one hand, the homogenized coil configuration offers much lower system resistance, thus increasing the efficiency of the device. However, it produces a very significant inductance jump, and poses some construction as well as structural issues. It also adds complexity to the design of the device. On the other hand, the solid conductor configuration, due to the skin effect, produces a very small inductance jump. It is also very simple in its construction and much more robust and structurally sound (in the presence of high loads) than the homogenized coil configuration. However, the resistance of the system is increased, due to the skin effect. The design which seems to prevail is the solid conductor design, due to its simplicity and small inductance jump. The increased resistance however, will pose some problems, which need to be solved. It is also of value to compare the skin effect depth during the railgun operation and of the device at hand.

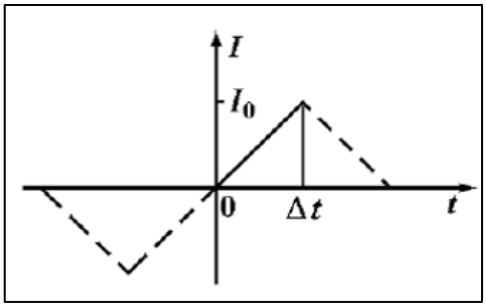

*Figure 98: Diagram calculating equivalent frequency of railgun*

In the figure to the left, the following can be seen. Pulse current climbs from 0 to $I_0$ in a typical rail cross section for a time interval $\Delta t$ while armature runs across the section (solid line). The current form can be regarded as a section of a sawtooth (dashed line). The sawtooth form can also be approximately regarded as a sine waveform with a period of $4\Delta t$ according to Fourier series analysis. The equivalent vibration frequency is $f = \frac{v}{4l}, l = length\ of\ rail.$ The skin depth can be calculated as $\delta_v = k_e \sqrt{\frac{4\rho l}{\pi \cdot \mu \cdot v}}$. [8]

| armature velocity, $v$ in m/s | equivalent frequency, $f = v/(4l)$ in kHz | velocity skin depth, $\delta_v$ in mm |
|---|---|---|
| 50 | 0.625 | 2.680 |
| 100 | 1.25 | 1.894 |
| 200 | 2.5 | 1.339 |
| 400 | 5 | 0.9477 |
| 800 | 10 | 0.6695 |
| 1600 | 20 | 0.4739 |
| 3200 | 40 | 0.2379 |

*Figure 99:Table showing skin depth as function of projectile velocity for the railgun*

Thus, in the railgun operation the frequency causing the skin depth can be as high as $40\ kHz$. In the device here however, the natural frequency (which is the frequency causing the skin effect) is around $3000\ Hz$, which means that the resistance of the device will be much smaller, even for the skin effect configuration. In the railgun however, current does not flow in all of the rail length (stops at the displacement of the projectile), whereas here current flows through all of the device, which once again increases the system's resistance. Overall, it is fair to say that the damping ratio for a railgun and a similarly sized launcher will be similar.

## 7.7 Comparison of proposed launcher with railgun and induction coil-gun

| ***RAILGUN PROS*** | ***INDUCTION COIL-GUN PROS*** | ***PROPOSED LAUNCHER PROS*** |
|---|---|---|
| Simple construction | Efficiency | efficiency |
| High output velocity | Structural integrity | Structural integrity |
| Structurally sound design | Electrical isolation | No electrical contact between moving and stationary components |
| 3 different configurations (augmented railgun, helical railgun etc.) | No inductance jump | High output velocity |
| Can operate with iron core | Low friction | Many different configurations, for specific purposes |
| | Retrieval of breech energy | Very low friction between moving and stationary components |
| | Smaller total resistance as compared with inductive launcher | Breech energy (energy when projectile leaves launcher), can be retrieved |
| | | Can operate with low currents, if the geometry of the launcher is such that produces high inductance gradient |
| | | Easier to turn coils off rather than on |
| | | Higher average fore than induction coil-gun, since current does not change as frequently (on-off as in induction coil gun) |
| | | Passive switching |
| ***RAILGUN CONS*** | ***INDUCTION COIL-GUN CONS*** | ***PROPOSED LAUNCHER CONS*** |
| Low efficiency | More complex design | More complex construction than railgun |
| Has reached its limits with the current material technology | Requires many switches | Requires more switches |
| Stationary and moving components are not electrically isolated | High forces perpendicular to projectile's displacement | High forces, perpendicular to projectile's displacement |
| High frictional losses | Requires many individual smaller power supplies, adds complexity | In general, this launcher's efficiency with the homogeneous coils is about 25% less than that of the induction coil gun |
| Breech energy is lost | Velocity limitation due to current rise time (without adding switching time) | |
| High forces, perpendicular to projectile's displacement | Complicated electronic circuit | |
| Operates only with very high currents | Active switching | |

*Table 8: comparative table between proposed design, induction coil-gun and railgun*

# 8 STRUCTURAL ANALYSIS

Next in line is the structural analysis of the linear motor. It is evident that the forces acting on the projectile, as well as the structure are very large, since the acceleration of the projectile is very high. Furthermore, the very nature of the system is such that the forces cannot be smaller, or the final velocity of the projectile would be smaller. Thus, since the operational forces are of such high magnitudes, and cannot be smaller, in order to mitigate for the extreme stresses, the structure of the motor needs to be such that can handle them. It needs to be said, that the time at which these forces act on the structure is very small, in the order of $10^{-4}$ seconds, so simple failure criteria cannot be taken into consideration when analyzing the stresses of the structure. In the analysis presented, the skin effect model was analyzed since it experiences larger forces than the homogeneous coil model [Paragraph 7.6].

From bibliographic sources it was found that, the max stress that a conventional railgun experiences is about 1000MPa and more [9]. Taking this into consideration, one could say, that here as well the maximum stress should be of the same order of magnitude. However, when analyzing the structure of a conventional railgun, and the motor presented in this thesis, it is clear that they have little in common, not only in the way of operation but also structurally. Nevertheless, for a preliminary study the max stress of the order a few 1000 MPa is a good starting point to act as a simple failure criterion.

*Magnetic forces:*

The forces acting on the projectile as well as the rest structure of the motor arise from electromagnetic phenomena. In the previous chapter, the model containing the physics of the operation was presented. From this model the axial force accelerating the projectile can be extracted. However, this study cannot calculate the distribution of this force, nor the radial force along the structure of the motor. This is why an extra study was created, where with the accelerating force as an input, the radial and axial force distributions can be calculated. This model is simple, but provides us with the insight needed to construct a more realistic structural analysis.

*Discrete states:*

In an operational cycle two discrete states occur. The first state occurs in front of the projectile, and the second behind it. More specifically, in front of the projectile, the stationary secondary coils are operational, whereas behind it they are not. This leads to two different force distribution states. The model presented here however accounts for both.

***State 1: in front of the projectile***

***State 2: behind the projectile***

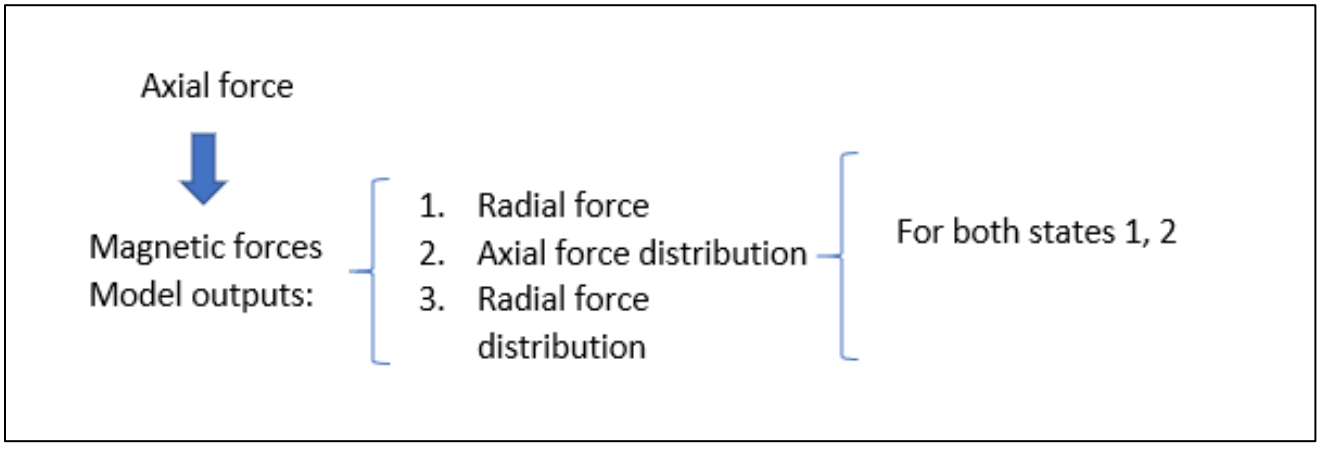


*Figure 100: Flow diagram to correctly and accurately determine radial and axial force density, with the only input being the axial projectile force*

*State 1:*

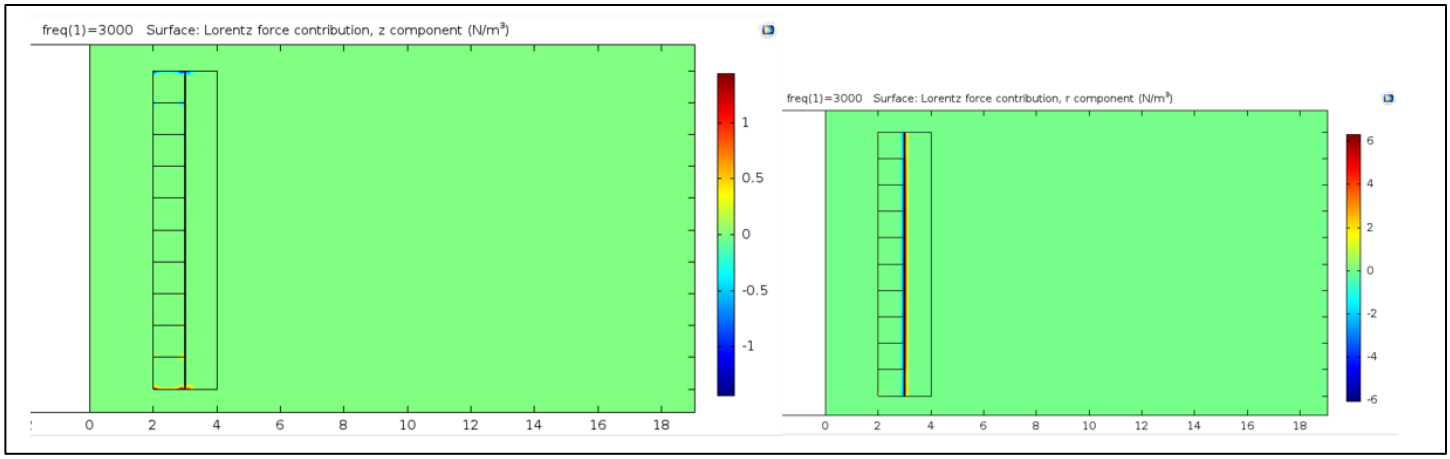


*Figure 101: Left figure: force density distribution along z axis, Right figure: force density distribution along r axis, for load state 1*

- Axial force distribution is almost zero, and negligible when compared to other forces, therefore it can be ignored.
- Radial force is concentrated at the outer boundary of the inner coil, and the inner boundary of the outer coil. This happens because current due to the skin effect, concentrates along these boundaries.
- Radial force density is almost uniform, for a zone around the common boundary of the primary and secondary coils.

*State 2:*

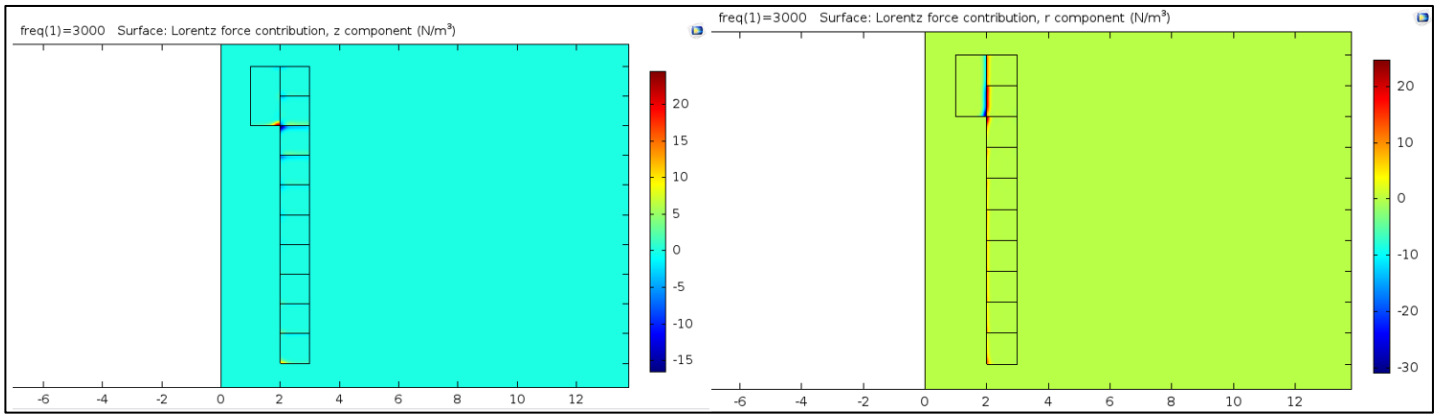


*Figure 102: Left figure: force density distribution along z axis, Right figure: force density distribution along r axis, for load state 2*

- In state 2, radial force has a similar distribution to state 1. The magnitude of the force distribution as a whole is also very similar to the one seen for state 1. The only difference is that here the force is concentrated at the inner boundary of the inner (primary) coil.
- Axial force is mostly concentrated behind the projectile and quickly tapers off to zero.

Electromagnetic forces depend on the geometry of the structure (since magnetic fields depends on geometry, and the path the current follows also depends on the geometry), and the magnitude of the flowing current. Therefore, combining the two studies seen above, one for the axial force magnitude and the other containing the geometric aspects of the device a full force profile can be derived, and thus an accurate enough structural analysis can take place.

*Simulation assumptions:*

- The current distribution does not change according to the magnitude of the current. More specifically, since the current magnitude changes, the current distribution for simplicity will be taken as constant. This is not the really the case however, since the skin effect depth fluctuates with time.
- Axial force distribution will be simulated as a rectangular pulse that follows the projectile, of width $W_1$, and magnitude $Axial_1$
- Radial force will be simulated as a step function that follows the movement of the projectile for state 2, and lags for state 1. Both forces are of equal magnitude, $Radial_1$
- Finally, the axial force will be assumed as constant, and the current associated with the force is $I_1$. This also is not the case for the true operation of the device. If, however the force is equal to the maximum for the whole discharge, then a worst-case scenario can be established.

*Notes:*

- W1 is the width of the skin effect, which depends on the frequency of the current. For simplicity here this width is assumed to be constant. This however will not always be the case. Since however the phenomena described occur at high frequencies, the differences in skin width can be neglected.

*Derivations:*

- For constant current, radial force density will also be constant.
- knowing the geometry of the structure, for any current, the ratio of the axial force density to the radial can be derived, from the "magnetic forces" simulation.
- This ratio clearly does not depend on the current, but only on the geometry of the structure
- Therefore, knowing this ratio and the axial force (which could vary with time) the auxiliary radial force density can be derived.

*Magnetic forces study explanation:*

$$\text{ForceDensity}_{\text{axial}} = \frac{Axial\ Force\ acting\ on\ structure}{volume\ upon\ which\ force\ acts}, \text{ForceDensity}_{\text{radial}} = \frac{Radial\ Force\ acting\ on\ structure}{volume\ upon\ which\ force\ acts} \quad (44)$$

This is a frequency domain analysis, and inputs of the study are the geometry of the device, the forward accelerating force, and a random current value since as stated earlier, the ratio $\frac{F_{axial}}{F_{radial}}$, does not depend on the current, but Is a characteristic constant of the system. This ratio however depends on the position of the projectile, because even though axial force remains almost the same for the same current since the inductance gradient of the system can be very well approximated by a straight line, radial force gets larger as projectile's displacement increases, since more area gets revealed for the force to act upon.

A better alternative, would be the ratio of force densities for the axial and radial force $\frac{ForceDensity_{axial}}{ForceDensity_{radial}}$, since it does not depend on either current or projectile position. Taking into consideration the simplifications made in the previous paragraph (simulation assumptions) the average value over the skin effect width of the radial force is calculated, as well as the average value of the axial force density, over the axial force pulse. Skin effect width remains almost the same, and for a long enough solenoid, axial force density height remains the same as well.

1. Ratio as stated earlier does not depend on current.
2. Knowing the axial pulse width (calculated by this study as Fig.102, Fig.103 show), which does not depend on projectile's motion, for every force, its accompanying force density can be derived.
3. From ratio, and axial force density, the radial force density distribution can be derived.
4. For a fuller analysis the domain over which the forces act could change shape (width) according to the projectile's motion.

## 8.1 Analysis definition

In the structural analysis the projectile is omitted, since the stresses present on the projectile are of low importance, in contrast to the ones present at the rest of the structure.

Model:

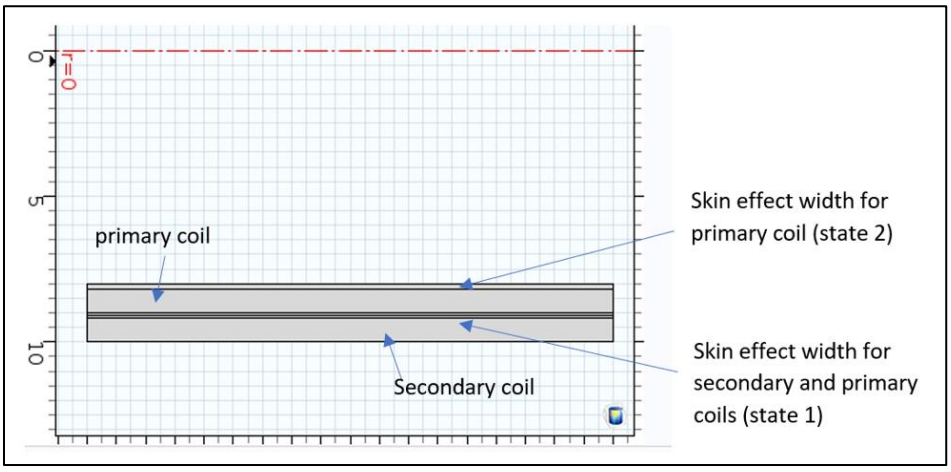


*Figure 103: model simulated in the structural analysis in the COMSOL Multiphysics software*

Dimensions:

| | |
|---|---|
| $Inner\ radius$ | $8[cm]$ |
| $Primary\ width$ | $1[cm]$ |
| $Secondary\ width$ | $1[cm]$ |
| $Skin\ effect\ width$ | $0.2[cm]$ |
| $height$ | $18[cm]$ |

*Table 9: simulated model's dimensions*

*Simulation of travelling loads:*

It is evident that the loads acting on the structure are not of stationary nature not only in time but also in space. This is to say that not only does their magnitude and direction change with time, but also the point at which they act. It belongs therefore to the family of travelling load problems.

*Travelling load background:*

In structural dynamics this is the load that changes in time the place to which is applied. Examples include vehicles that pass bridges, trains on the track, guideways, etc.

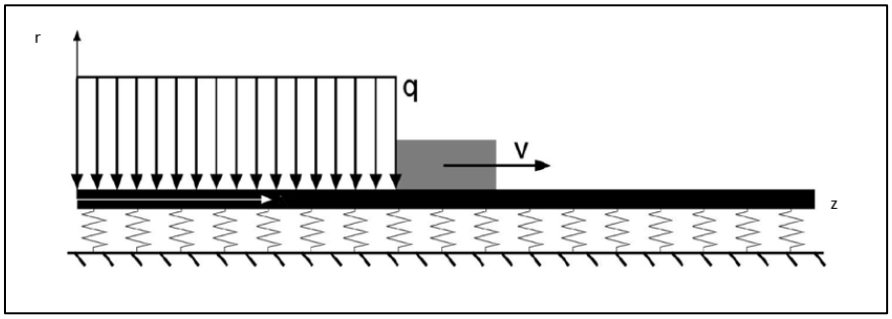


*Figure 104: Simple sketch that demonstrates the moving load problem.*

In a travelling load problem, the velocity as a function of time of the moving load needs to be known. For the simulation here, this graph can be seen below.

*Travelling load velocity:*

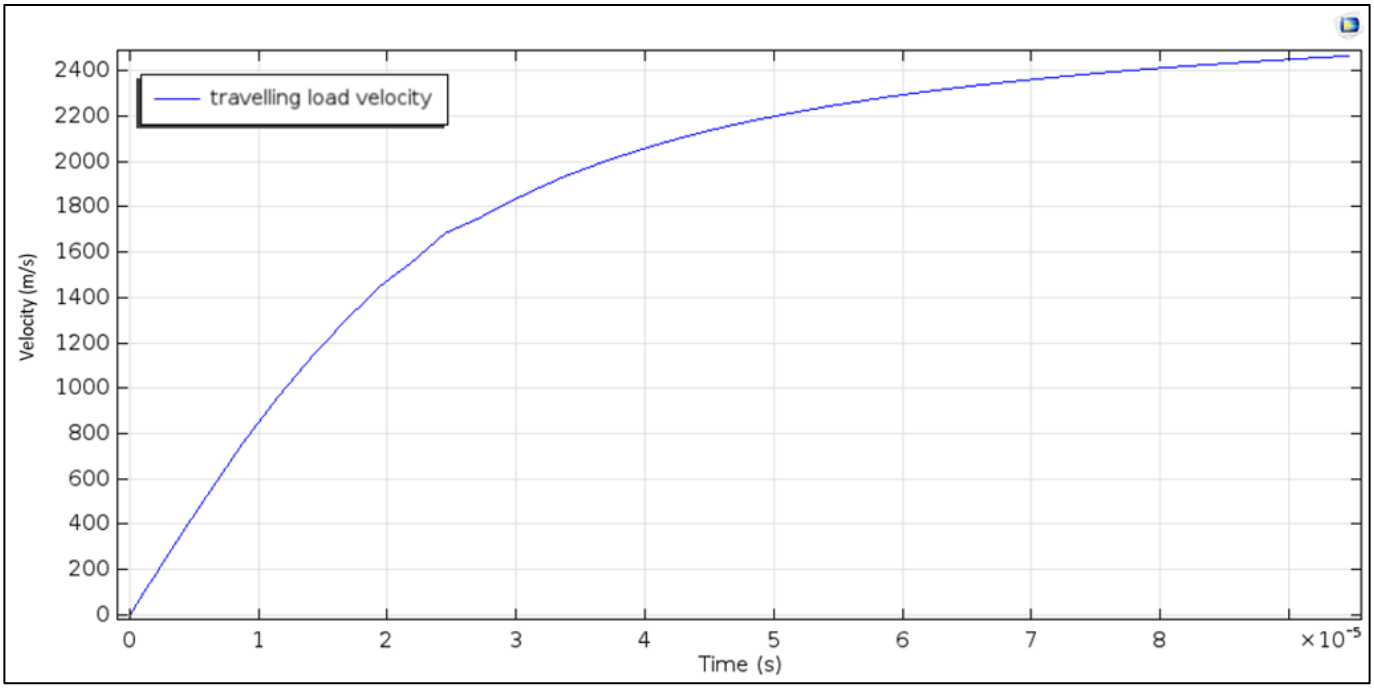


*Figure 105: graph showing the velocity of the travelling load, in the structural analysis, as a function of time*

### 8.1.1 State 1

- Constant axial force $of\ F_{axial} = 5000000[N]$, implemented as a volume force density, in the form of a rectangular pulse.

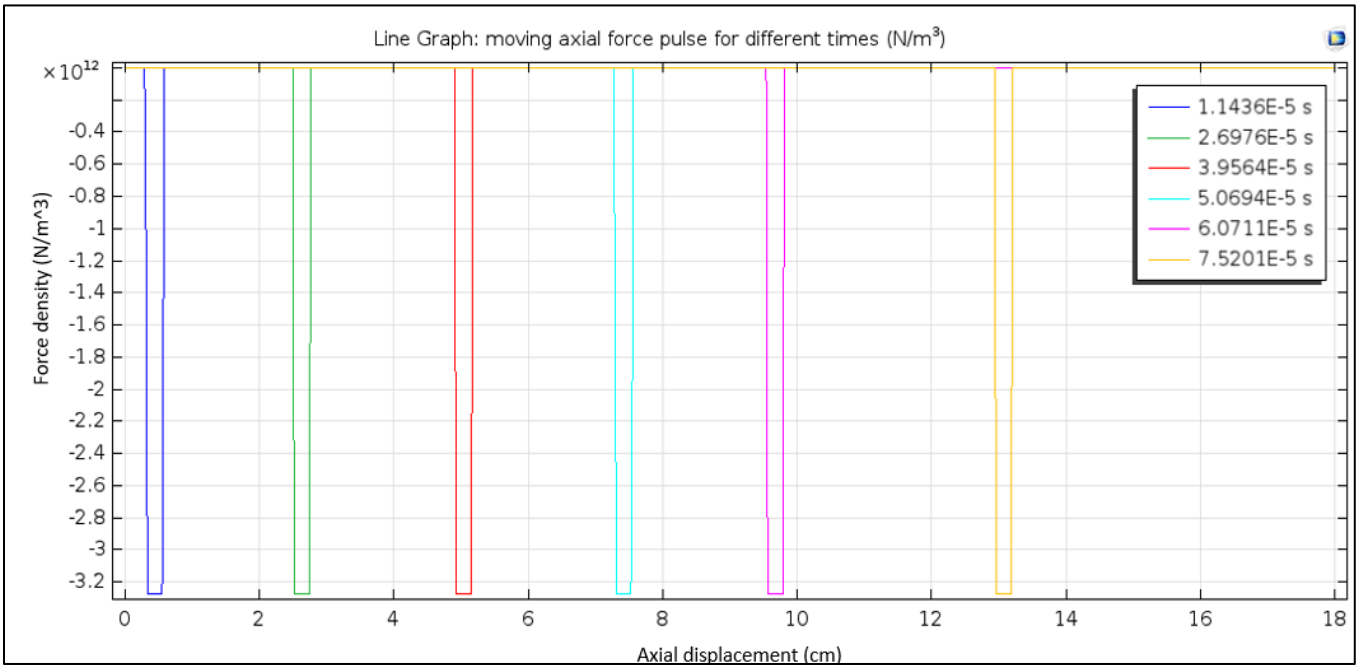


*Figure 106: In the figure above, the travelling axial force can be visualized for different times*

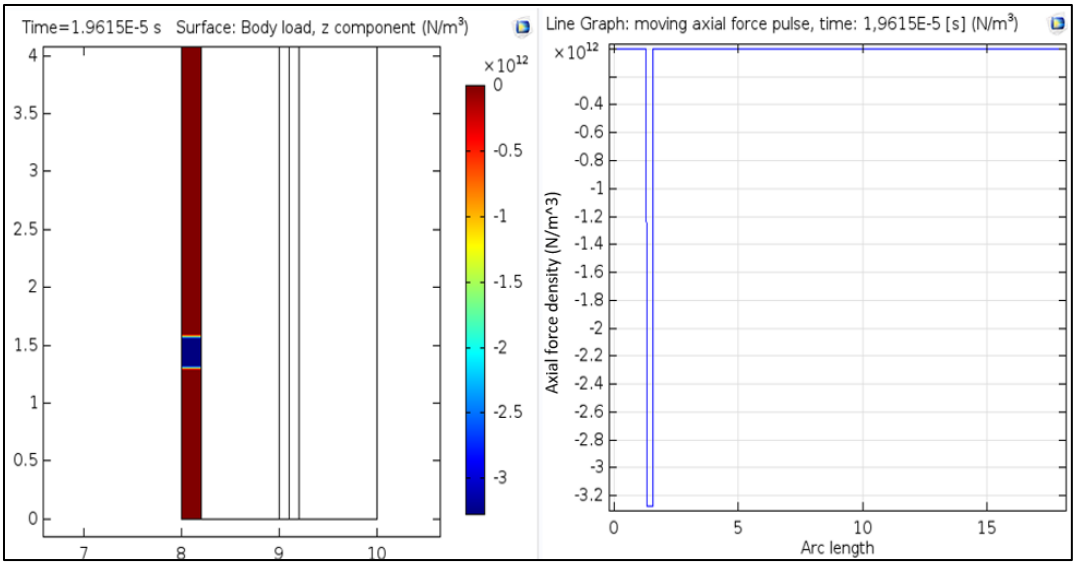


*Figure 107: In the figure above, axial force density distribution can be visualized*

Constant Radial volume force density, whose magnitude remains the same regardless of the axial displacement of the projectile, and is implemented through the use of a Heaviside function

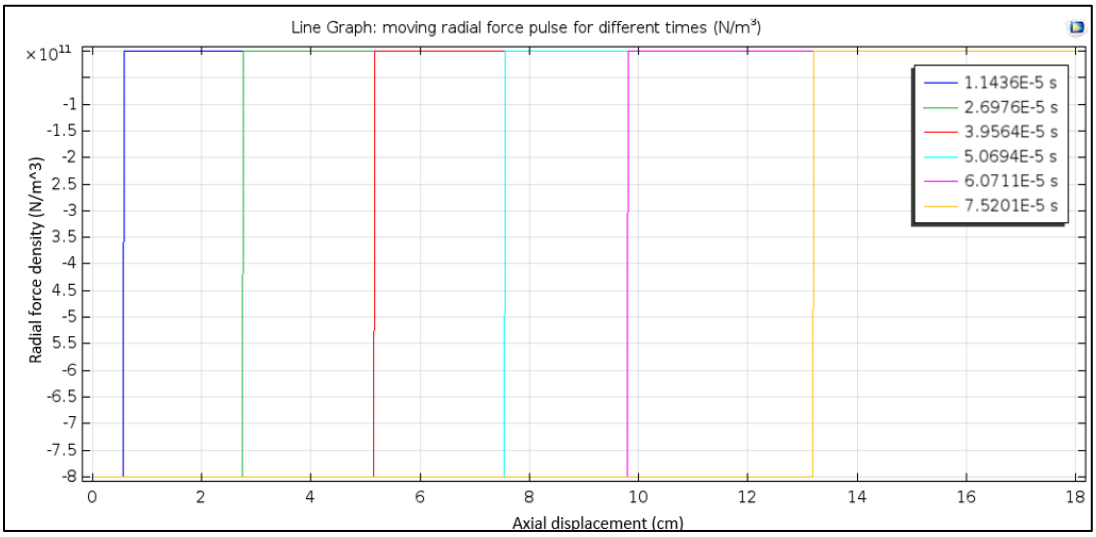


*Figure 108: In the figure above, travelling radial force can be visualized*

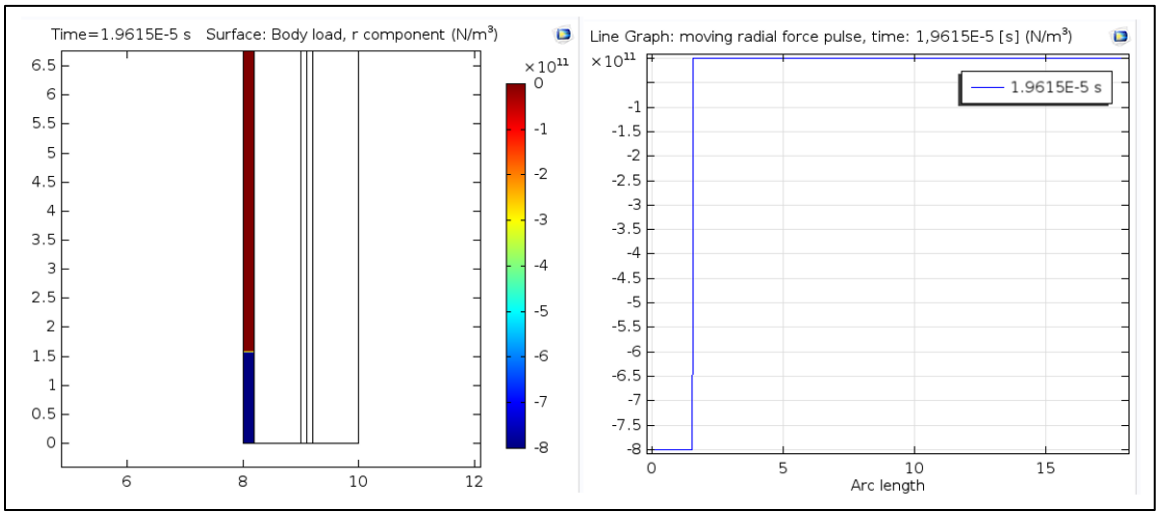


*Figure 109: In the figure above, radial force density distribution can be visualized*

### 8.1.2 State 2

- Axial force is zero
- Two opposing radial force densities acting (at the primary and the secondary), whose magnitudes are the same, but have opposing directions. These too are implemented through the use of a Heaviside function. In contrast however with the radial force density at state 1, they precede the projectile.

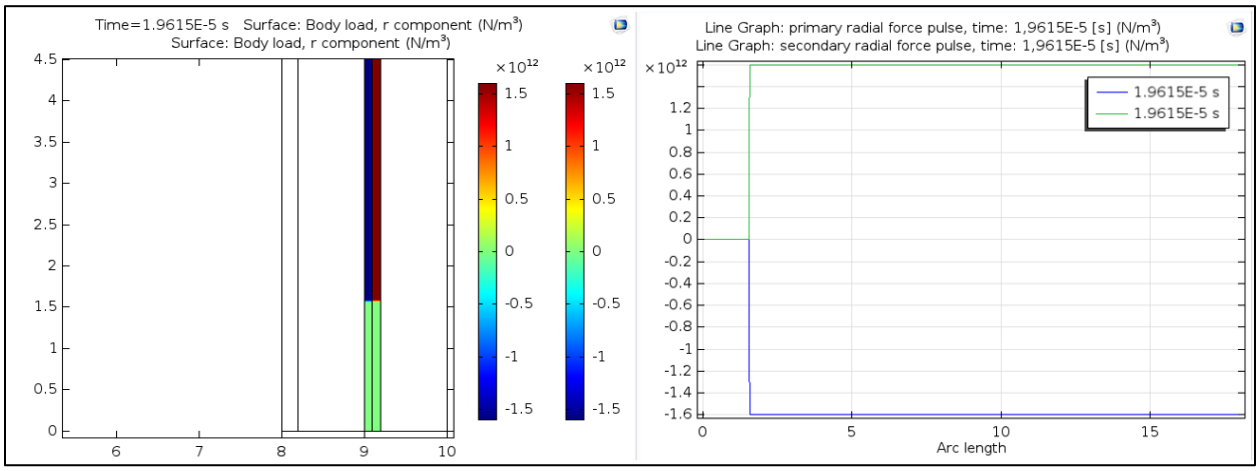


*Figure 110:radial force density for state 2.*

*Supports:*

- Both circular surfaces of hollow cylinder have a roller support
- Outer surface of cylinder has a spring foundation support, with a spring constant K=10e11[N/m]

## 8.2 Results

Usually in travelling load problems, a critical velocity exists that stimulates the first eigenfrequency of the structure, bringing it to resonance. This velocity, which corresponds to the first eigenfrequency depends on the geometry of the structure, the way it is supported and the direction of the force. Here since the geometry is axisymmetric, the equivalent radial spring is very stiff, thus increasing the critical velocity. Furthermore, as the spring constant of the spring foundation increases, so does the critical velocity. Thus, here a situation exists that not only the structure itself has a very high stiffness, but also the supports are such that allow for even higher velocities, before resonance occurs. This is evident from the graph below, where the total displacement of the middle point of the structure is plotted.

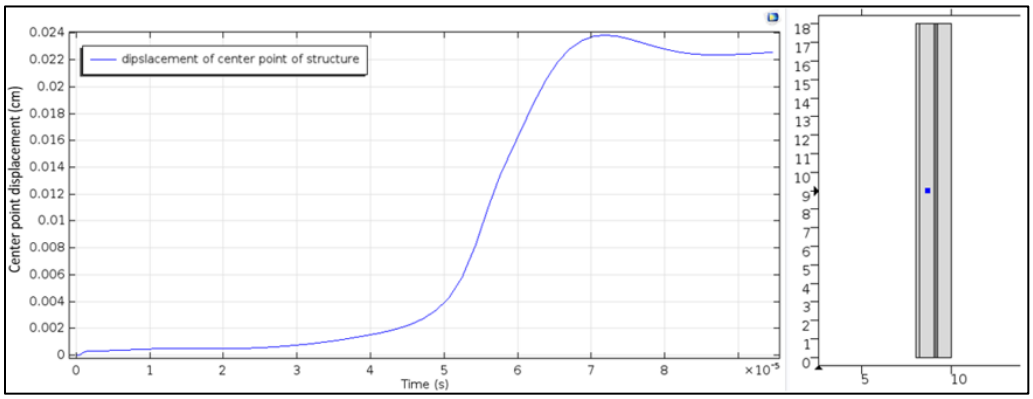


*Figure 111: Total displacement of point located at the middle of the structure*

It can be seen that no evidence of resonance exists. This however can be attributed to the excellent supports, which envelop the structure completely.

*Stresses:*

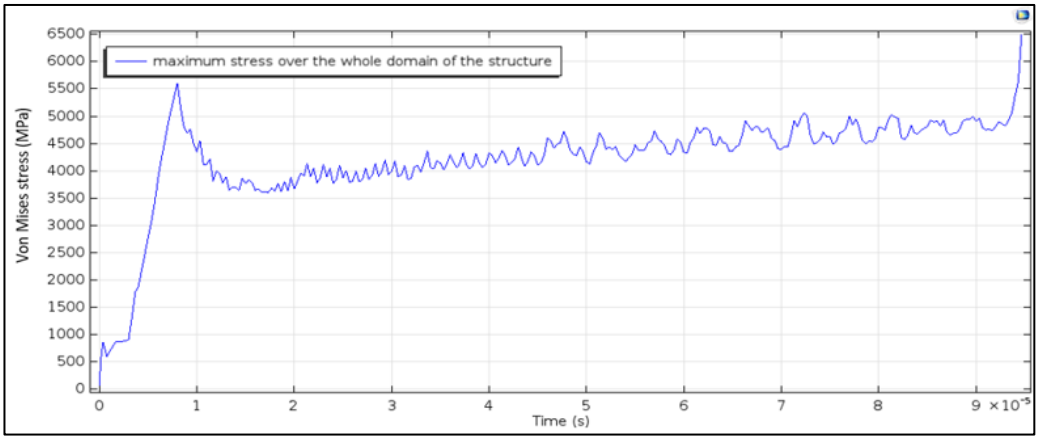


*Figure 112: maximum Von Mises stress as a function of time, over the whole domain of the structure*

In the graph to the left the maximum stress over the domain of the structure is plotted. It can be seen that this value is very high, and many times higher than the ultimate tensile strength of copper) and even steel). However, this maximum stress is concentrated to small areas, as the graph below shows.

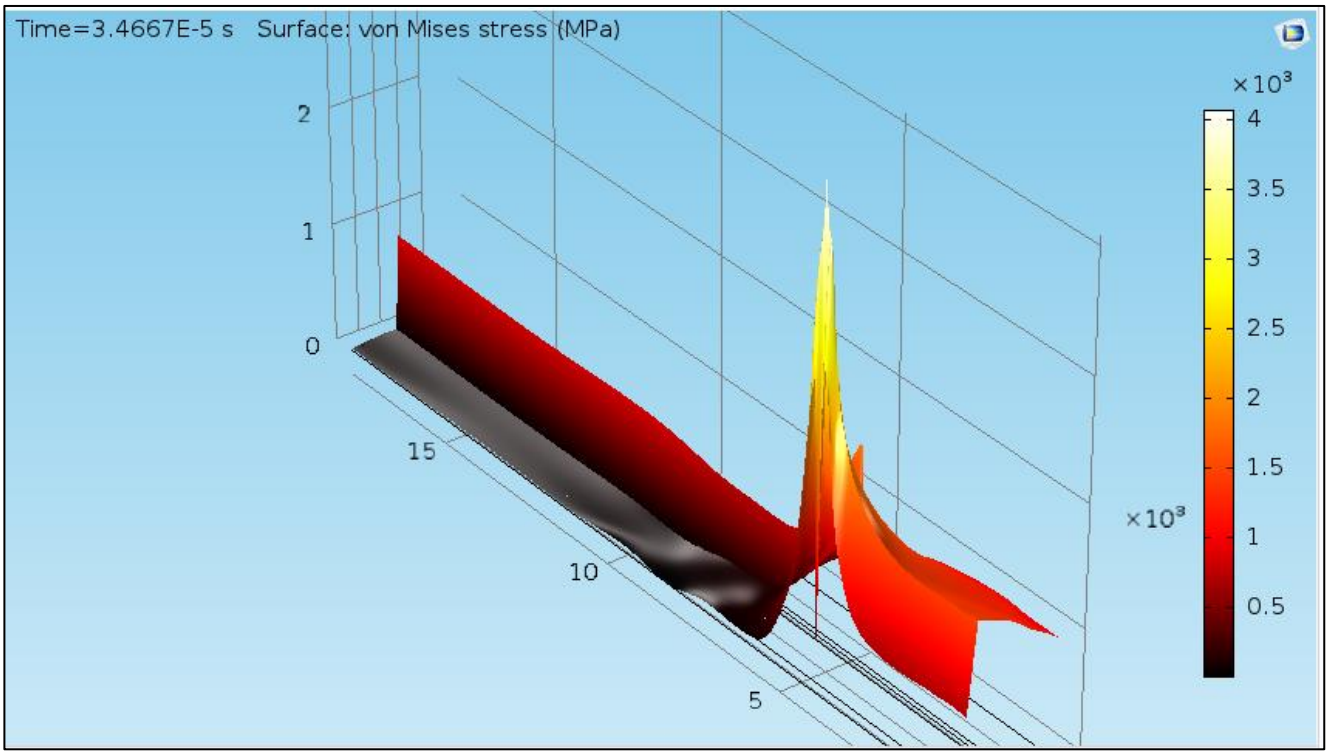


*Figure 113: 3D graph illustrating the narrow regions where the equivalent Von Mises stress is very high*

The scope of this analysis is very broad, and mainly serves to show the stress levels to be expected during the operation of the device. The force, in the simulation although chosen as constant in magnitude, does not represent a real operational scenario. It is however the most extreme case of loading for the device, and serves as a case study against which more accurate analysis will be compared. If a simulation with the real force magnitude was to be carried out, the same comsol simulation could be used, since the results from the "magnetic forces study" have already been incorporated (derivation of radial force etc. from magnitude of axial force).

## 8.3 Material selection

1. As the inner diameter gets bigger, force also increases for the same current, since inductance gradient is larger. The volume at which this force is distributed however grows at the same rate, thus maximum stresses will remain at the same overall level.

| ***MATERIAL*** | ***Yield Strength (MPa)*** | ***Ultimate Tensile Strength (MPa)*** | ***Density (g/cm^3)*** |
|---|---|---|---|
| *structural steel* | 250 | 550 | 7.8 |
| *mild steel* | 247 | 841 | 7.58 |
| *maraging steel* | 2617 | 2693 | 8 |
| *copper* | 70 | 220 | 7.7 |
| *annealed copper* | 33 | 210 | 7.7 |

*Table 10:Possible materials table*

In comparison from the table above, for copper: $UTS = 220\ [MPa]$, almost ten times lower than that of steel. Thus, even though resistivity of copper is better, the structure could theoretically be built from steel due to its better mechanical properties. A resistivity comparison would be helpful however since copper has a much lower resistivity when compared to any type of steel. Copper=$5.96 \times 10^7 \frac{S}{m}$, Steel=$6.2 \times 10^6 \frac{S}{m}$, almost 10 times higher. Other possible materials include tungsten due to its excellent mechanical as well as thermal and electrical properties, but it is expensive and harder to machine, and beryllium-copper, a high strength copper alloy. A very effective graph to compare materials to each other would be that of electrical resistivity vs ultimate tensile strength. Epigrammatically for the three material types mentioned above:

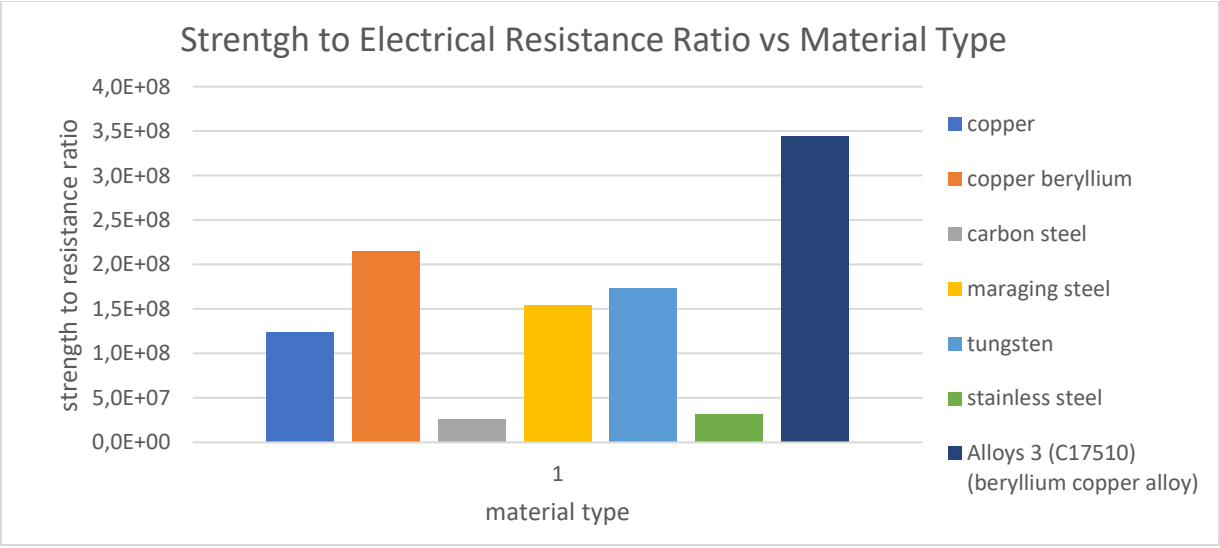


*Figure 114: Comparative diagram of different materials for their structural and electrical properties*

Best material seems to be a copper beryllium alloy, since it has both good electrical conductivity and extremely high ultimate tensile strength. Its thermal conductivity is also high, but its melting point is fairly low ($900\ degC$), lower than for pure copper ($1000\ degC$). Thus, tungsten should be used for the switch contacts since its melting temperature is $3422\ degC$.

# 9 THERMAL ANALYSIS

Since the operation of the motor involves very high currents, it is expected to present high thermal loads as well, due to ohmic losses. Therefore, a thermal analysis was done, to explore the temperature ranges during the operation of the device. As previously stated in the structural analysis chapter, since the operating time of the motor is very small, even though the power dissipate through heat is very high, the total energy still remains in manageable ranges. Nevertheless, the cooling of the device was explored, with the use of a cooling channel surrounding the secondary coil. the coolant was chosen to be deionized water, since it will not conduct electricity. Nevertheless, a parametric study on coolant material selection was also done, to find the best fit for the application at hand [Paragraph 9.1.1].

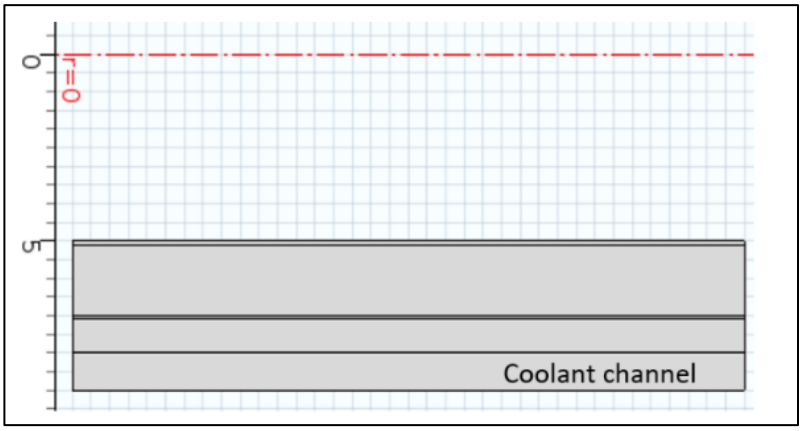


*Figure 115: simulated model in COMSOL Multiphysics to investigate the cooling of the device.*

## Analysis set up

The analysis includes:

1. Heat transfer in solids
2. Heat transfer in fluids
3. Laminar flow

The heat sources present due to primary and secondary currents were modelled as two individual heat sources, only including the domain of the skin effect width. For the simplicity of the analysis the current was kept constant, with its value being that of the maximum current during the whole operational cycle. Also, the domain where the current flows was also kept constant, which is not the case because as previously stated it changes according to the displacement of the projectile [Paragraph 8]. Furthermore, the most unfavorable situation was studied, which is that of zero displacement of the projectile, when all secondary coils are active.

*Heat transfer in solids:*

1. Heat sources to simulate the ohmic effect
2. Material: copper
3. Outer boundaries insulated (they conduct no energy to the environment)

*Heat transfer in fluids:*

1. Material: deionized water
2. Temperature of water at inlet: $0\ degC$
3. The effect of an increased coefficient of thermal conductivity was investigated, and the results are presented below [Paragraph 9.1.2].

*Fluid simulation:*

1. Water simulated under the assumption that its flow is laminar (this is not the case due to its high inlet velocity and the turbulent effects due to its heating, but still offers some insights to the effect that cooling has for the device)
2. Water inlet velocity: $v_{in} = 0{,}1[m/s]$, a parametric study was done to investigate the effect that it has in conducting heat way from the system [Paragraph 9.1.1].
3. Outlet condition: atmospheric pressure

*General:*

1. Simulation time was chosen as: $T_{end} = 1[s]$
2. Exciting current was chosen as: $I = 10000[A]$
3. Resistance of skin layer $R_{skin} = 0.011[\Omega]$
   a. The values above are not representative of the system's operation, but still the thermal behavior of the system as a whole does not change according to the heat source. Therefore, valid conclusions can still be extracted.

## 9.1 Results

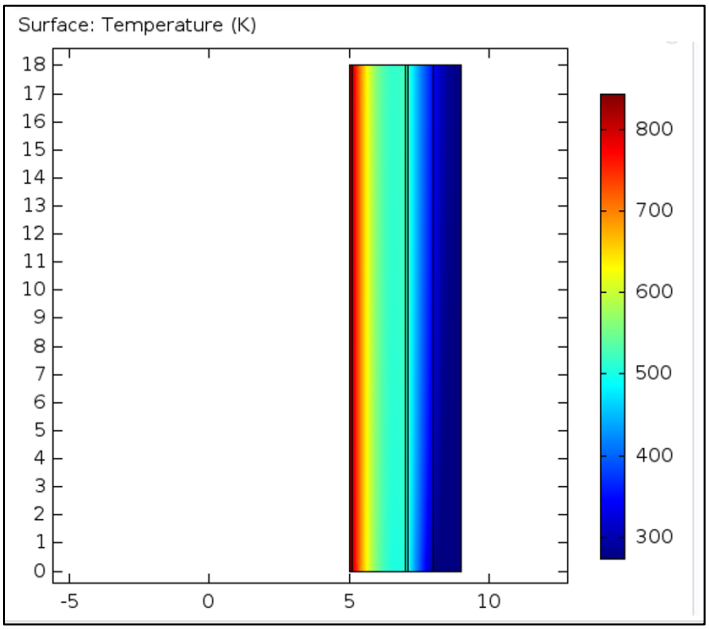


*Figure 116: Temperature profile after 1 [s]*

It can be observed that there is a clear distinction between the domain of the solid where the heating takes place, and the domain of the fluid. This happens because the time constant of the thermal system is very high, and energy is not transferred to the fluid in a sufficiently high manner. Furthermore, the boundary layer formed at the boundary with the secondary coil, acts as a thermal insulator for the rest of the fluid, since the fluid flow is laminar and thus no turbulent effects are investigated. Therefore, for the turbulent scenario heat extracted from the system would be higher.

*Heat extracted from the system*

Coolant instead of flowing in the axial direction, can instead flow in the phi direction (along the periphery of the cylinder). Doing so mass flow is increased, and therefore heat removal increases. if the axisymmetric problem is unwrapped in a plane, then a simpler analysis can take place demonstrating the effects of cooling. Also, this way of cooling is easier to implement since it allows for easier support for the barrel.

Thermal boundary layer theoretical calculation, for laminar flow:

In order to properly investigate the heat removal from the device, the thermal boundary effect needs to be examined. For a laminar flow on a vertical wall, which is similar to the flow at hand here, the following apply:

$$\delta_T = \delta_v Pr^{-\frac{1}{3}} \quad [10] \tag{45}$$

- $\delta_v$: is the thickness of the velocity boundary layer thickness
- $\delta_T$: is the boundary layer thickness

$$\delta_T = 5\sqrt{\frac{\nu z}{u_0}} Pr^{-\frac{1}{3}} \tag{46}$$

- $u_0$: freestream velocity
- $Pr$: Prandtl number
  - $Pr = \frac{c_p \mu}{\kappa}$
    - $c_p$: specific heat
    - $k$: thermal conductivity
    - $\mu$: dynamic viscosity

- $z$: distance downstream from the start of the boundary layer
- $v$: kinematic viscosity

In the table below all parameters affecting the thermal boundary's layer thickness can be seen, separated into categories that either lower or enlarge the aforementioned width.

| ***HIGH*** | ***LOW*** |
|---|---|
| Thermal conductivity: $k$ | Specific heat at constant pressure: $c_p$ |
| Dynamic viscosity: $\mu$ | Density: ρ |
| Kinematic viscosity: $v$ | Dynamic viscosity: $\mu$ |

*Table 11: Parameters affecting thermal boundary layer*

It is clear, that the width of the channel's dimensions where coolant flows should be of the same order of magnitude as the width of thermal the boundary layer, since the rest of the fluid does not contribute to the extraction of heat. However, if the channel is too thin, then viscus losses increase, so a right balance exists, where viscus losses remain low, and channel width is also small, as to not pump useless coolant.

### 9.1.1 Parametric study with coolant velocity

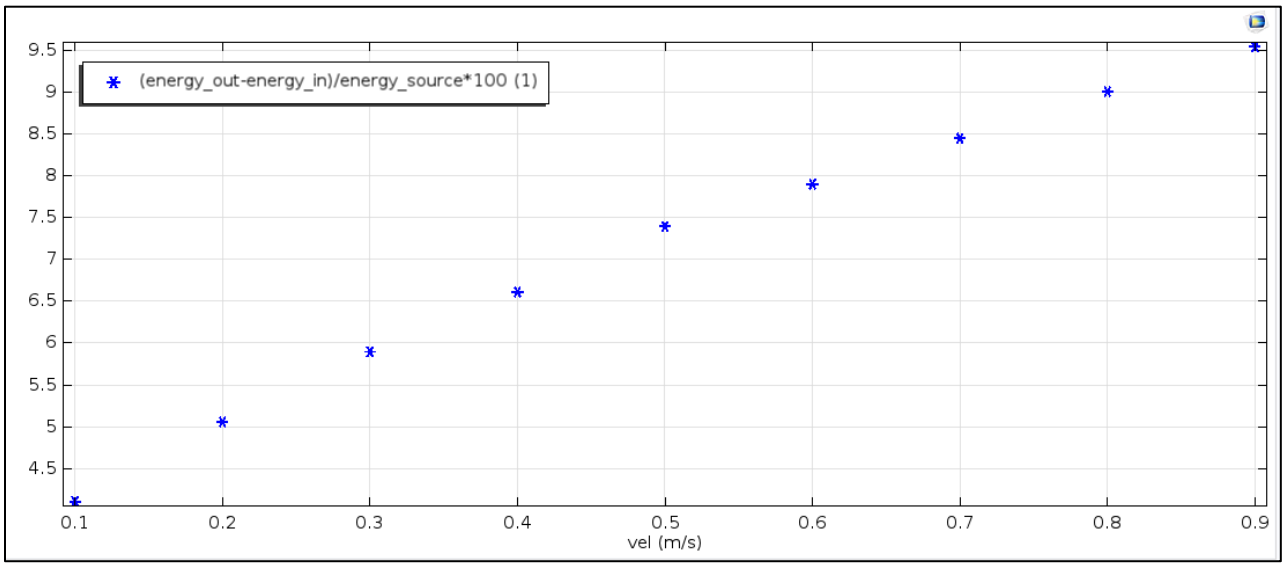


*Figure 117: Percentage of dissipated heat from cooling channel as a function of coolant inlet velocity*

From the graph above the obvious can be observed. As inlet velocity of coolant increases, so does the energy extracted from the system, even though the thermal boundary layer decreases. In fact, this relationship seems to be almost linear, with inlet speed. Nevertheless, very poor behavior of the cooling system (no cooling at all), which in part can be attributed to the thermal boundary layer, which acts as an insulator for the rest fluid flow. Addition of flow diverters inside the cooling channel could mitigate this problem, since better mixing of the hot and cold fluid flows would occur.

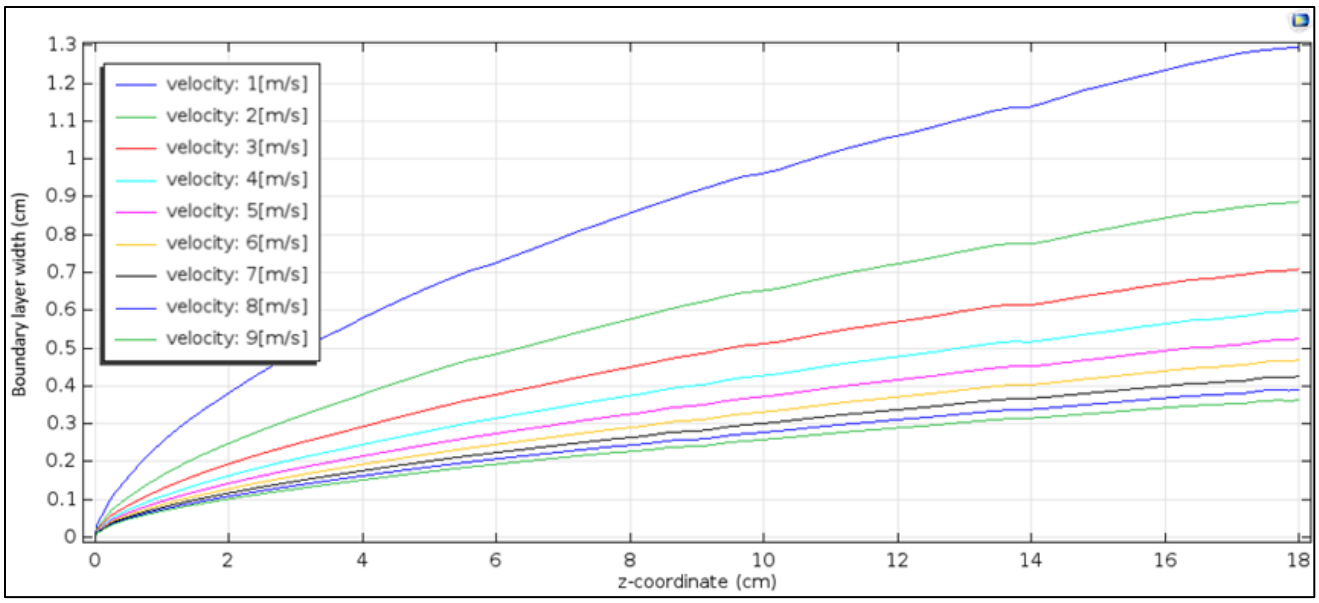


*Figure 118: Analytically calculated thermal boundary layer width, for different inlet velocities*

This is compared with the thermal profile created to ensure that the results are valid.

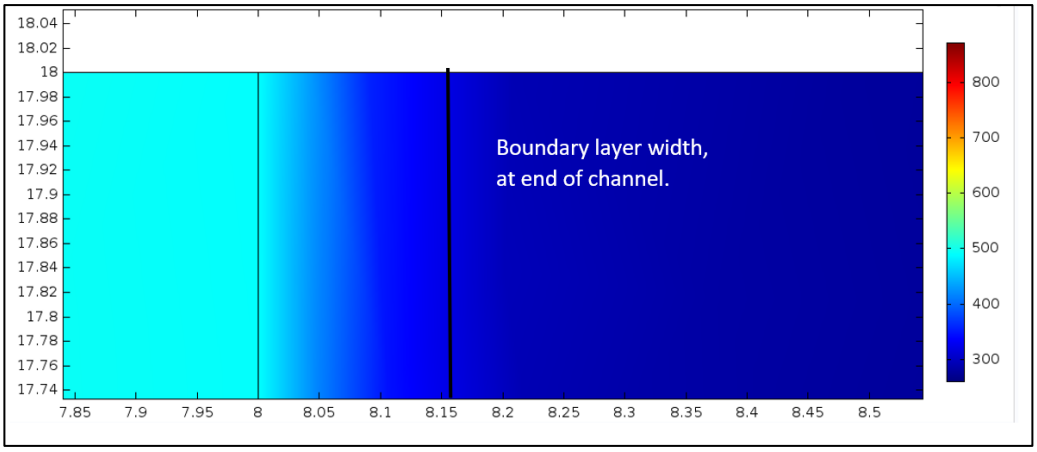


*Figure 119: Zoomed view at the end of the cooling channel, where thermal boundary layer thickness can easily be seen*

The theoretical estimation of the boundary layer closely matches the one calculated from COMSOL, which is bound by the black line in the figure above. In this figure a well, the clear divide between the fluid and solid domain can once again be seen.

### 9.1.2 Parametric study with coolant type

In this section the effect of coolant material will be investigated. A parametric analysis was done for 4 different materials as the graph and table below indicate. It is obvious from the graph that the best type of coolant is deionized water.

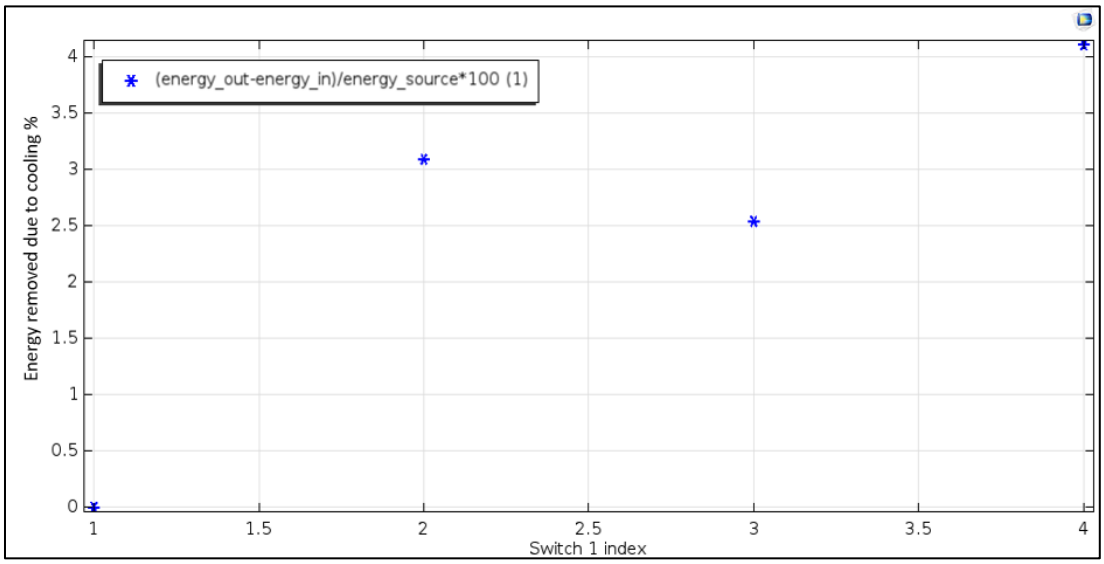


*Figure 120: Percentage of dissipated heat, for different coolant fluids*

| SWITCH INDEX | SELECTED MATERIAL |
|---|---|
| 1 | Air |
| 2 | Engine oil |
| 3 | Transformer oil |
| 4 | water |

*Table 12: Material used as coolant*

## 9.2 Thermal constant of the system

With the analysis presented above, it can be seen, that for the very short operating times of the device, cooling is not really necessary, since in order for the coolant to extract heat from the system, heat needs to travel through the width of both primary and secondary coils, which for structural purposes and robustness is big. Since however the time constant for thermal systems is very low, by the time that one operating cycle is complete, heat will have yet to travel to the cooling channel and thus little to no energy will have been extracted. It also adds complexity to the construction and operation of the device, requiring more complex support, as well as pumps for the cooling circuit, plumbing, and perhaps even a heat exchanger to cool the coolant down. If the coolant could be placed closer to the heat sources, then it would make sense to use it, but since this adds too much unwanted complexity, the device will operate without any coolant. Cooling of course could be used not only to extract heat from the system, but to also protect some sensitive equipment from the heat produced. In this case, a cooling channel like the one seen here could be used, to effectively act as an insulator between the sensitive equipment and the heat sources.

# 10 SWITCH DESIGN

In this section a big part of the device proposed will be discussed, which is the switching process, and more specifically the switch that makes the operation possible. Firstly, requirements that the switch should comply by are posed.

## 10.1 Switch requirements

1. Able to handle high currents, with quick rise time.
2. High Voltage (arcing)
    a. Suppress arc
    b. Conduct heat away
3. Able to be used multiple times, with little wear
4. Quick switching time
5. Easy to implement switching mechanism (requires little force)
6. Stability, once switched off, remains at that state

*Switch operation:*

Effectively what a switch does is to raise the resistance of a branch of a circuit, to such high levels and quick enough as not to allow for current to flow anymore. This resistance change can be accomplished by changing the resistance of the material itself (like in solid state switches for example), through a change in geometry, or through an addition of an extra resistance (classic switch where added resistance is that of the air gap between the contacts of the switch). All the alternatives presented below are based on one of the three mechanisms presented here.

The following, 6 switch types will be discussed in this chapter:

1. Hydraulic switch
2. Liquid metal switch
3. Mechanical switch
4. Electromagnetic switch
5. Solid state switch
6. Plasma switch

## 10.2 Hydraulic switch

As a first alternative for a quick acting switch, capable of conducting high currents without degradation, a hydraulic switch, making use of a liquid metal will be discussed.

*Switch properties/operation:*

1. Use of mercury (or in general liquid metal) to close contacts
2. Operation depends on the displacement of a conductive liquid metal, by another non conducting liquid such as water or transformer oil
    a. Properties of switch depend on the properties of liquid metal, as well as the dielectric strength of the second fluid, displacing the liquid metal.
3. From the maximum voltage produced while the switch opens (due to system's inductance), and the dielectric strength of the displacing material, the minimum mercury displacement can be found, when the switch is turned off, as for no arcing to occur between the switch's leads.
4. By having a rough estimation of the total displacement of the liquid metal, and the switching time during which the displacement occurs (this was set earlier as a switch requirement):
    a. The average velocity of the moving domain can be found
    b. As well as the acceleration of the fluid domain, which correlates to a given pressure difference.
5. Design of hydraulic circuit includes:
    a. Gas accumulator, one for high pressure, and another for the fluid to travel to.
    b. Place to accommodate contacts of the switch
    c. One-way valve, to restrict fluid backflow
    d. Simple valve to trigger the motion of the fluid due to the pressure differential
        i. Its design will be examined separately
        ii. Door valve, where door raises to allow fluid to pass. Initial push and then fluid flow raise the rest due to pressure differential
            1. Fluid structure interaction
    e. Domain for mercury, transformer oil
    f. Place to allow for a heat exchanger to be retrofitted (to conduct heat during switching away)
    g. In this way, a closed hydraulic circuit is formed, with the option of changing the fluids when deemed necessary

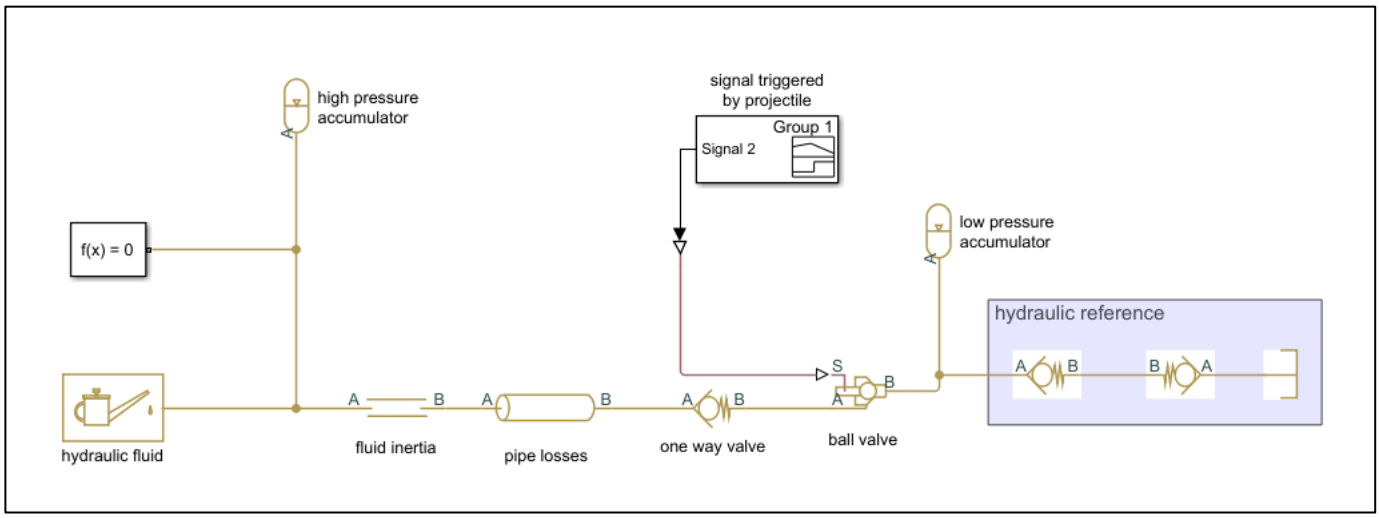


*Figure 121: Simple hydraulic circuit as simulated in the SIMSCAPE environment*

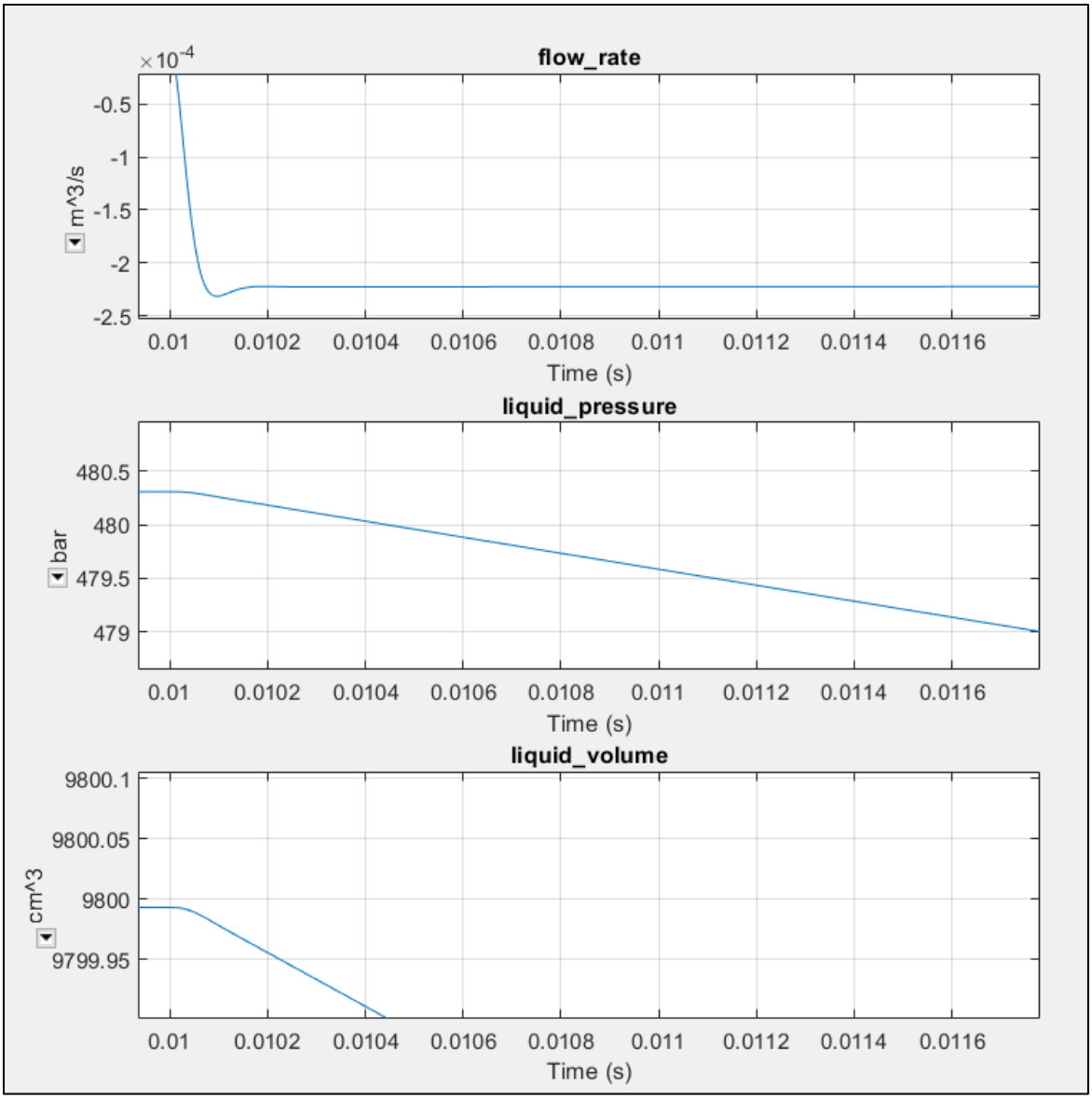


*Figure 122: Results from hydraulic system's simulation*

*Simple hydraulic simulation using SIMSCAPE*

1. Pipe diameter: $d_{pipe} = 2mm$
2. Pipe total length: $L_{pipe} = 5\ cm$
3. Fluid travel to break switch, depends on arc voltage ($V_{arc}$): $L_{travel} = 2\ mm$
4. Total volume difference: $V_{diff} = \frac{L_{travel} d_{pipe}^2}{4} = 0.024 cm^3$
5. Final fluid volume in accumulator: $V_{accumulator_{initial}} - V_{diff} = 9799.976\ cm^3$

From diagrams above, switching time can be found from the volume difference calculated in 5, when fluid volume in accumulator reaches the level calculated above. This time difference is:

$$dt_{switch} = 0.001\ s$$

This switching time is small, but not small enough for the application at hand. In the calculations above the mass of the fluid in the accumulator was not accounted for. Therefore, the time calculated above would be even higher. The switching time could be made smaller with a higher-pressure differential for example, but this would lead to problems in the dynamic behavior of the switch and the design of the hydraulic circuit.

## 10.3 Liquid metal switch, switching done through an electrical signal

The figure below illustrates the operating principle of the switch design. An electrolyte filled fluidic channel is located on top of a copper sheet. The channel intersects a pocket filled with the Gallium based alloy Galinstan, situated above the ground plane (copper sheet). The first figure (to the left) represents the off switch, since the Galinstan bubble does not intersect the electrolyte filled channels. When an electrical actuation signal is applied however, the Galinstan flows into the channel, at a minimum energy position and closes the switch [11].

Galinstan motion is triggered via electrocapillary actuation, where a low voltage creates a gradient in the interfacial tension between the Galinstan and the surrounding electrolyte, which weakens the tension locally allowing the fluid to flow.

The paper analyzing the design of the switch at hand, does not provide any switching times of power rating. It is however fair to assume that switching time will be slow, since the electrochemical action does not produce high forces. As for the current rating, since the contacts are of liquid metal, there does not seem to be any significant current limitation.

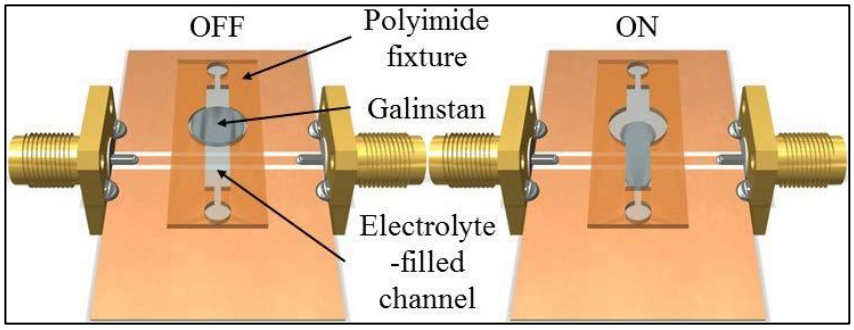


*Figure 123: Figure of the liquid metal switch, demonstrating its operation*

## 10.4 Mechanical switch

In a classic mechanical switch, contacts are brought apart through mechanical means. In the device at hand for example the motion of the projectile, pushes the contacts apart. In general, this is the most common type of switch, but faces some problems due to its operation. Since the contacts need to be brought apart, a certain mass needs to be accelerated, which requires a certain force (like in the simple analysis of the hydraulic switch above, Paragraph 10.2). In this scenario however, this accelerating mass is even higher, and the mechanical force is low. This has as a consequence a high switching time. Furthermore, arcing problems exist, which can fuse the contacts together. A custom mechanical switch however could be made for this device specifically, which satisfies the requirements stated above. The main disadvantage thus of the purely mechanical switch is its switching time, which if triggered by the motion of the projectile directly will be low. This would impede however with the uninterrupted motion of the projectile.

A switch design similar to the mechanical, is the electromagnetic switch, which closes the switch contacts with an electromagnetic force. In that way the forces the switch experiences are of the same order of magnitude as for the projectile, and thus a small switching time can be achieved. This type of switch will be examined next.

## 10.5 Electromagnetic switch

In this design family, the switch contacts are brough apart due to an electromagnetic force. Many possible designs exist, an electromechanical relay for example makes use of a solenoid to part the relay contacts. For this application however a custom switch is needed, due to the extreme nature of the phenomena at hand (high forces, velocities, frequencies, stresses and small switching times)

*Railgun type switch*

This type of switch is very similar to the railgun operation. A conductive bar closes the circuit between two parallel rods. The bar remains stationary, until the projectile triggers a system that effectively releases the bar, which travels the length of the rods (very small length) and when their end is reached, the circuit becomes open-circuited. The switching time of this design, fits the requirements set by the rest of the device, since the forces propelling the bar are of similar magnitude to the ones propelling the projectile. And for a small enough travel displacement manages to open the circuit at the desired instance. Of course, a phase shift can exist, where in essence the projectile triggers the bar in motion, and the circuit opens at a later time, when the projectile is situated at the proper point in space.

This design offers many advantages, mainly in its efficiency, and simplicity. Its two main disadvantages are as follows. Firstly, the triggering mechanism, which releases the bar, poses some problems, since it needs to release the bar fast enough for switching to occur at the desired time. Secondly, welding of the contacts shut, due to high currents. A minor problem is the added inductance of the switch to the rest of the system. This however can be easily resolved, by having two counter rotating coils, with a total inductance a fraction of the initial system.

Although the design presented here has many similarities with the classic railgun, it can be implemented in a much simpler way, since in contrast with the railgun the displacement of the switch's contacts is much smaller. Below a revised design is presented with solutions to the two major problems listed above. In bibliographic sources, such a design was found, making use of a segmented railgun to quickly close the switch powering a high-power railgun [12]. Other than the classic railgun design, another design was thought of as well, which will be presented below, and tries to solve the two main problems an electromagnetic switch has.

### 10.5.1 Improved design, triggering mechanism

The triggering mechanism of the switch is implemented with the use of a hydraulic system. More specifically the stiffness of the system depends on the pressure of the hydraulic fluid in the chamber, as seen in the figure below. High pressure corresponds with high stiffness whereas low pressure with low stiffness. The motion of the projectile triggers the opening of the valve, which immediately equalizes the pressure with that of the atmosphere, thus effectively lowering the stiffness of the switch. As a result, due to the high repulsive forces on the rails, the switch's contacts are pushed apart, thus opening the switch. Here, as well as in the purely hydraulic switch the mass of the moving objects has to be accounted for (mainly that of the hydraulic fluid). However, in contrast with the hydraulic switch the forces acting on the rails here are much larger, thus producing higher forces and accelerations capable of meeting the requirements set forth at the beginning.

*Improved design, Contact welding:*

Use of conductive material like a liquid metal for example such as mercury.

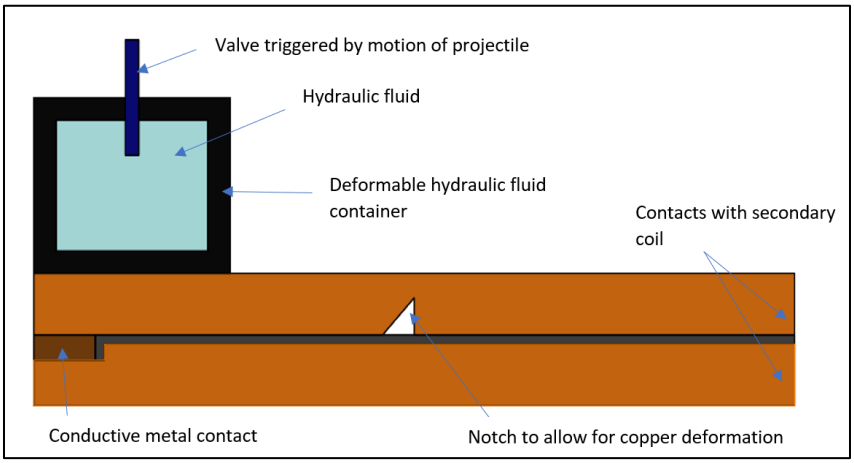


*Figure 124: Simple schematic of the electromagnetic switch proposed above. Simple hydraulic circuit which varies system's stiffness*

### 10.5.2 Electromechanical switch based on the magnetohydrodynamic effect

In this version instead of the contact itself accelerating away from the stationary switch, the conductive fluid connecting them does so. This phenomenon called “magnetohydrodynamic effect” was used as an experimental propulsion system for submarines. The operating principle is the same as before, but the projectile triggers the motion of the fluid, which itself opens the switch. It is obvious that for this design to work, a better and more rigorous analysis needs to be carried out. Due to the limited time during which the thesis at hand was completed, no such analyses were done [13].

Due to the skin effect, depth at which current would flow if conductors where of substantial width would be very small relative to the whole conductor width. Thus, thin contacts are selected. The depth of the liquid metal connecting them is larger than the width at which a spark would occur, if the liquid was removed. Instead of a secondary fluid (like water with high dielectric constant) filling the gap of the conductive one, air does so, because adding another liquid would increase the complexity of the switch. This however depends on an analysis that should take place to investigate the generation of an electric arc.

### 10.5.3 Automatic (passive) electromagnetic switch

In this switch design, the switch’s contacts open automatically when the projectile reaches a certain displacement near each coil subassembly. This is possible since the part of the secondary that disconnects (opens the circuit) is connected with a section of the primary coil. in this way. In this way, the force that the “assembly” experiences, according to the displacement of the projectile is as follows.

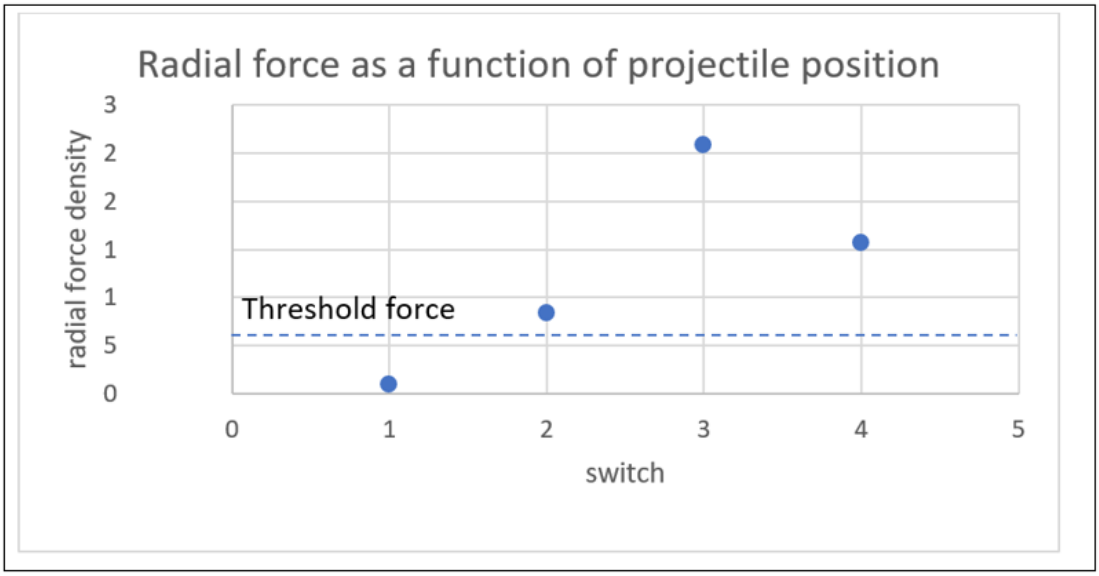


*Figure 125: Radial force as a function of projectile displacement, threshold force is also plotted where:*

1: Refers to the configuration where the inner coil (projectile) has not yet reached the coil assembly
2: Refers to the configuration where the projectile has reached the coil assembly and all three coils are active, here disconnection occurs.
3: Refers to the configuration where the projectile has reached the coil assembly, but stationary secondary is not active
4: Refers to the configuration where the projectile has left the coil assembly and secondary is not active

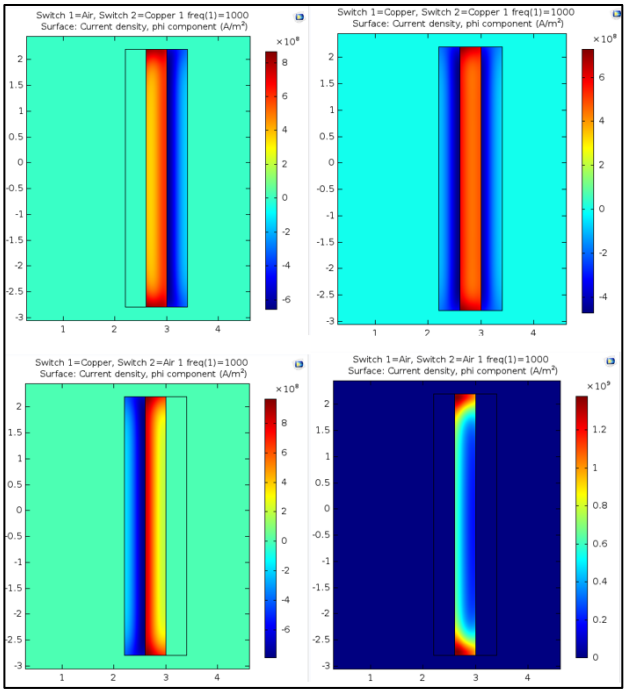


*Figure 126:4 Different states between coils are graphed, which correspond to a particular projectile displacement.*

System tends to disconnect stationary secondary coil as projectile passes through it. To begin with, the system is stable, since force tends to compress the contacts of the secondary, frictional forces and system's stiffness counteract electromagnetic force. When force reaches a certain threshold it automatically disconnects the stationary secondary's contacts. This threshold is reached when the projectile is next to the stationary coil assembly (point 2 in graph above). The magnetic field also suppresses the arc that would be generated between the contacts of the coil (as in a magnetic blowout coil).

As mentioned earlier, the key fact that makes the switch's operation possible is that, part of the secondary that disconnects, is connected with the primary, so that it experiences the force from the primary as well. The switch, can be made in such a way that its stiffness prevents it from opening when force is below the aforementioned threshold. It would be better however, if the threshold could be set in an external way, as to allow for easy calibration. A rough design of the switch proposed above can be seen here.

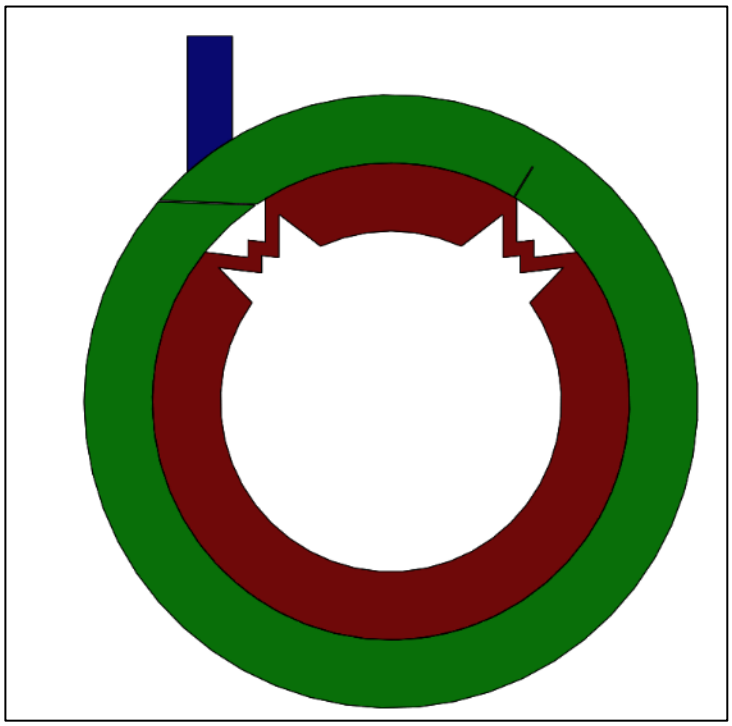

*Figure 127:Passive electromagnetic switch, schematic design 1*

*1.* Notches allow for deflection; their design is exaggerated (the important thing is for deflection to occur. Many mechanisms exist to allow for the desired deflection, here the easiest was implemented, which basically in a local region changes the stiffness of the coil

2. In green coil (secondary) notch allowing for movement can be seen, as well as the place where contact between the switch's leads happens.

3. Blue component is used to locally change the stiffness of the coil assembly, effectively changing the threshold force.

4. Here the coils are depicted as one turn solid coils. They could be made however to have multiple turns. The basic switch design would remain unchanged.

5. The design above could be made in such a way that before the projectile reaches the coil assembly, the force on the contacts is negative (see diagram above, first point). Doing so when the projectile reaches the coil assembly, the force switches sign pushing the contacts apart. A big advantage of this design is that no adjusting mechanism is needed to change the threshold force. This can be seen in the following graph [Fig.129].

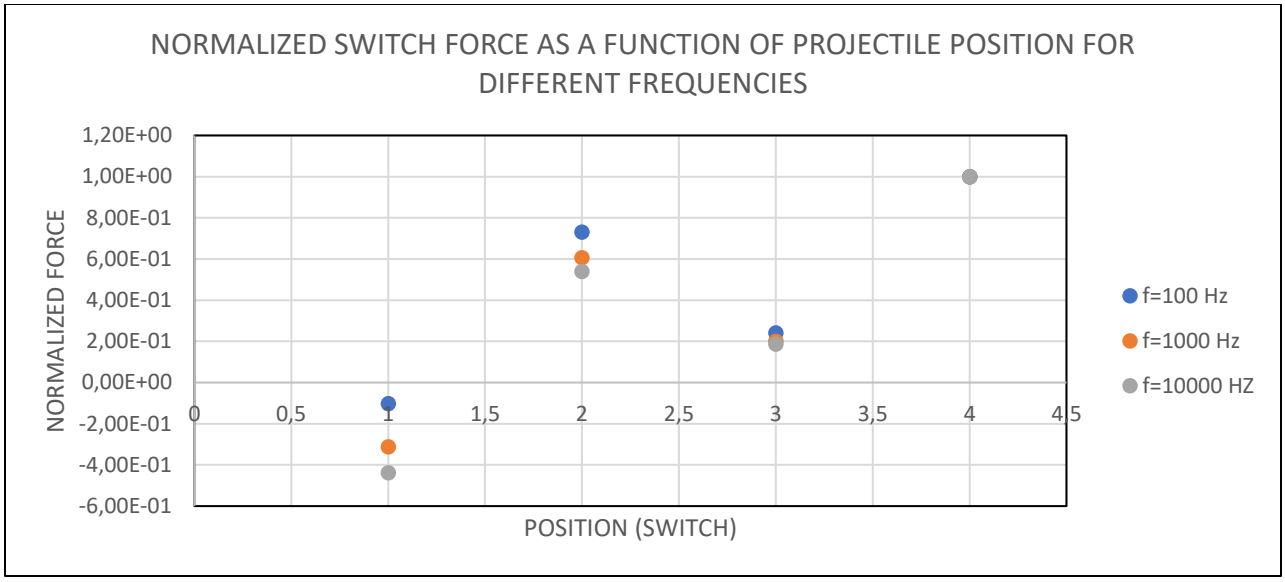


*Figure 128:Normalized radial force as a function of frequency, and projectile displacement, for optimized design.*

*Design 2:*

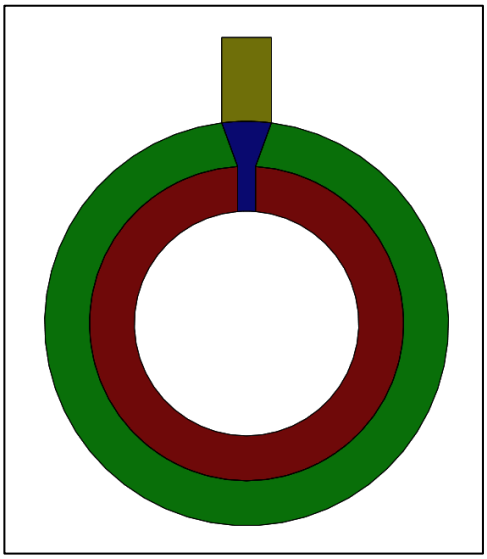

*Figure 129:Passive electromagnetic switch, schematic design 2*

1. $Green$: stationary secondary coil
2. $Red$: primary coil
3. Blue: moving contact
4. $Yellow$: stiffness adjustment (spring for example, with very small travel)

Operation is the same as earlier, blue part moves radially outwards independently from the rest of the coil assembly, open-circuiting the secondary coil, while leaving the primary coil's operation intact (due to the varying contact angle between primary and secondary with the moving contact). Same as earlier, magnetic field from primary coil extinguishes the arc that would have been produced as contacts open. Frictional forces between blue (moving part) and stationary structure help to counteract the effect of the electromagnetic force before the projectile reaches the coil assembly. Between the contacts a resistant to melting material is placed, to reduce the possibility of contact fusing.

*Design 3:*

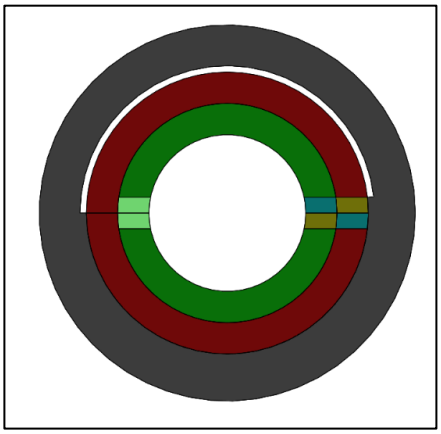

1.$Red$: primary secondary coil
2.$Green$: primary coil
3.$Gray$: support
4.$Blue$: positive terminal
5.$Yellow$: negative terminal
6.$Light\ green$: connection with flexible wire

Same as before, this switch opens automatically once projectile is aligned with the coil assembly. More specifically, upper red and green part of the coils shown to the left, move as one, thus experiencing a net force from both coils. Lower green and red parts of the coils are fixed to the grey support and are immovable.

*Figure 130: Passive electromagnetic switch, schematic design 2*

## 10.6 Solid state switch

Solid states switches are often used in electronics, where required switching times are extremely small. The power the switch handles however is not high enough for the application at hand (since they operate with semi conductive materials, which have physical limitations to the amounts of current and voltage they can conduct). Therefore, one would think their use is prohibitive in this type of application.

Nevertheless, since the ban of ignitrons in the United States, due to Mercury being a hazardous material, several solid-state switch designs were refurbished to allow for the switching of high voltage and current, short duration pulses.

As an example of this technology a design of such a switch will be presented with the following ratings [14]:

1. Voltage: $20\ kVdc$
2. Current rating: $12.6\ kA$ exponential decay waveform
3. Current rise time: $10\frac{kA}{\mu s}$
4. Pulse duration: $10\mu s$
5. Cooling option (transformer oil or deionized water act as coolants)
6. Only turns on, and not off (similar switches exist where both actions can be accomplished.

| Characteristic | Description | Thyristor (1600 V, 350 A) | GTO (1600 V, 350 A) |
|---|---|---|---|
| $V_{T\ ON}$ | On state voltage drop | 1.5 V | 3.4 V |
| $t_{on}$ | Turn on time, gate current | 8 µs,200 mA | 2 µs,2 A |
| $t_{off}$ | Turn off time | 150 µs | 15 µs |

*Table 13:solid state switch characteristics*

To sum up, solid states switches can indeed be used for the application at hand.

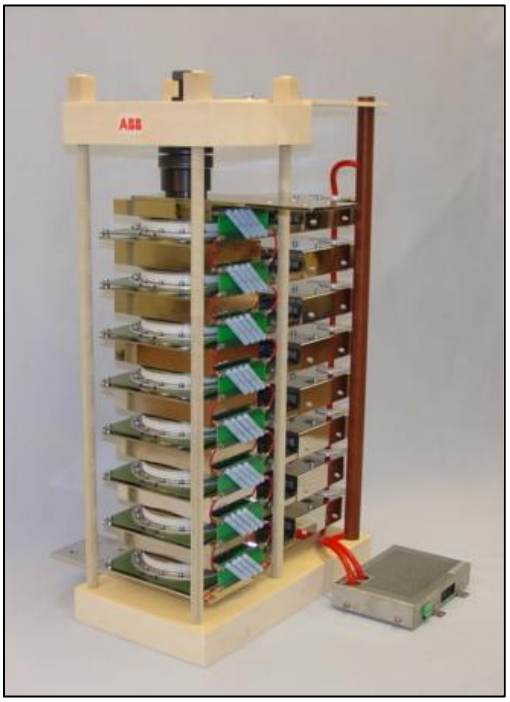


*Figure 131: High-power solid-state switch assembly*

## 10.7 Plasma switch, ignitron

Plasma switches and ignitrons, have very small switching times (small enough for the application here). They present however higher resistance, and more complexity than other switch types. Nonetheless, they could be used to switch the secondary coils off. An analysis of this type of switch however will not be presented here, since it is out of the scope of this project.

### 10.7.1 Plasma switch 1

During normal operation (conducting state) small arc exists between the switch's contacts. To switch off the secondary coil, the arc bridging the contacts gets extinguished. Since the arc's resistance is situated at the secondary of a transformer it is known, that with more turns of the secondary, the resistance that the primary sees would be smaller by a factor of $T^2$ ($T = \frac{N_1}{N_2}$). However, by increasing the transformer ratio the voltage at the secondary increases as well. This has as an added advantage the formation of a larger arc to work with, which will be easier to extinguish. The arc could be extinguished by the release of a high velocity air stream, or with the use of a magnetic blowout coil. Moreover, the projectile itself could extinguish the arc. To be more specific, as the projectile passes through the arc, and more specifically between its terminals, where the arc exists, pushes them slightly apart and leaves on them an oil residue, of high viscosity, thus breaking the arc. To initiate the arc once again for another operational cycle, this oil needs to be removed from the contacts, and for them to be brought closer. The total displacement given to the contacts is small, and essentially the arc does not break due to the terminal's movement, but rather due to the addition of the oil substance, since it has a very high dielectric strength.

*Theory on electric arcs, plasma:*

Arc flows through air that has become plasma. Plasma is a state of matter where atoms lose some of their valence electrons. This is why a plasma is such a good conductor of electricity, and why it can be extinguished with a magnetic field.

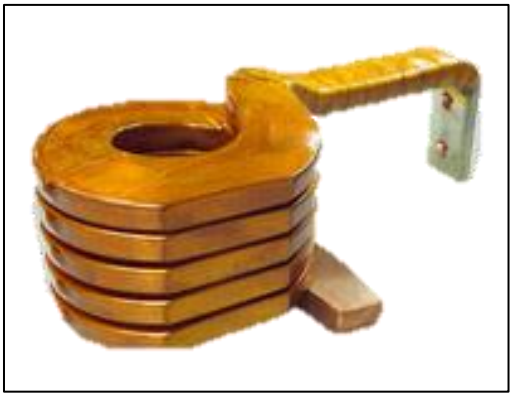

*Figure 132: possible design of secondary coil, with multiple turns.*

As previously stated, the formation of an arc adds an extra resistance in series with that of the secondary coil's, whose effect needs to be investigated, since as resistance gets larger operation of the device becomes worse.

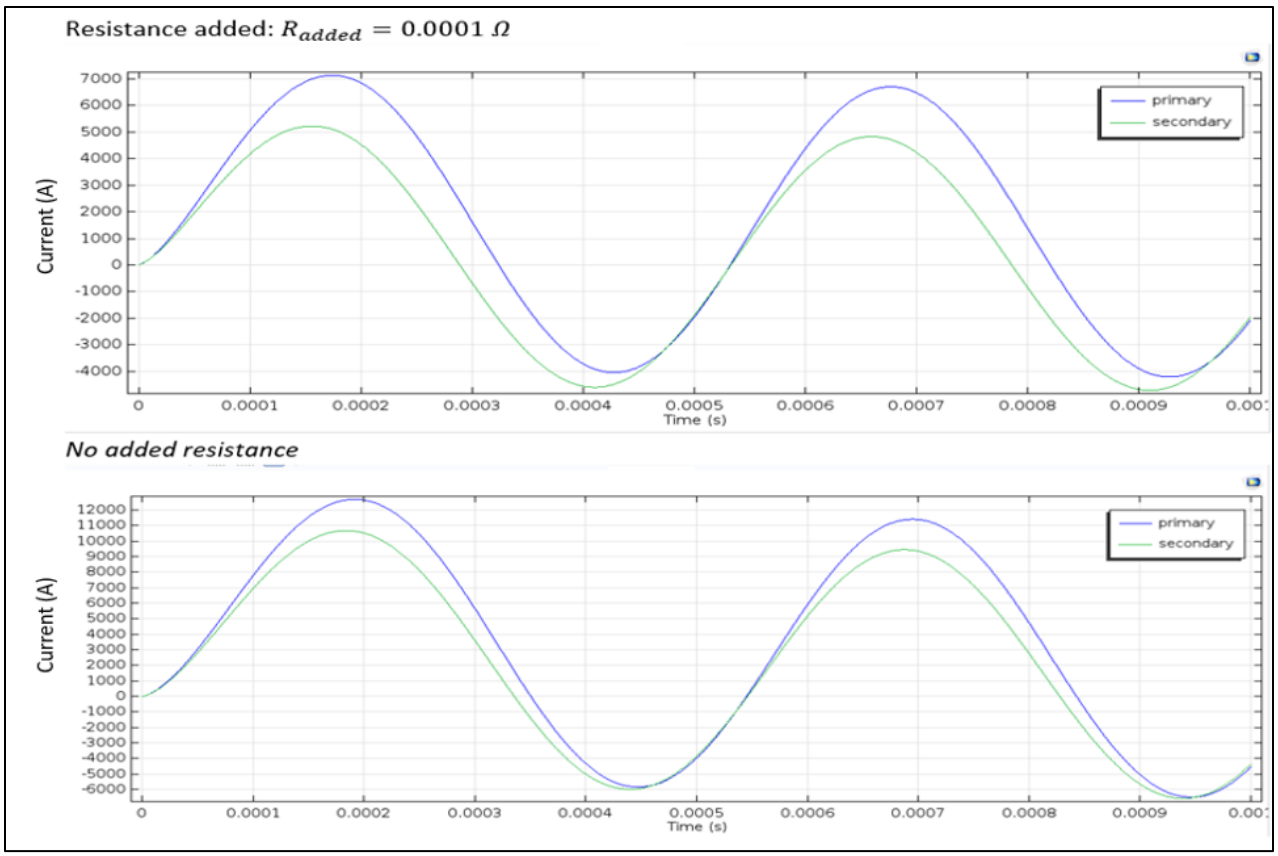


*Figure 133: secondary coil current waveforms, with and without the added resistance due to the arc*

Effectively what is important, is the added resistance due to the arc that the primary coil perceives to be as small as possible. This depends on the number of turns that the primary and secondary coils have ($T = turn\ ratio$). If the secondary has 10 times more turns than the primary, then the added resistance that the primary sees due to the switch in general ( or in this case the arc) is $R_{added} = \frac{R_{arc}}{T^2}$. The resistance of the arc however depends on the current passing through it, like formula (47) shows. Since it does not depend in a linear relation with the current ($I^{0.85}, 0.85 < 1$), whereas due to transformer action it does, it would still make sense to have more turns in the secondary.

Resistance of arc is given by the empirical formula below [15]:

$$R_{arc} = 25\frac{\sqrt{L_{arc\ length\ [Inches]}}}{I^{0.85}\ [A]}\ [\Omega] \tag{47}$$

*Switch design comparison*

| | ***SWITCH TYPE*** | | | | |
|---|---|---|---|---|---|
| ***CRITERIA*** | Hydraulic | Plasma 2 | Mechanical | Electromagnetic | Passive Electromagnetic |
| Small Switching time | NO | YES | NO | YES | YES |
| Added complexity | HIGH | LOW | MEDIUM | MEDIUM | MEDIUM |
| Arcing | NO | YES | YES | YES | YES |
| Extinguish arc (Blowout Coil) | | | HARD | EASY | VERY EASY |
| Stability | YES | NO | NO | NO | YES |
| Multiple use | YES | YES | YES | YES | YES |
| Small added resistance | YES | NO | YES | YES | YES |
| High Power | YES | YES | YES | YES | YES |
| Rapid Reuse | NO | NO | YES | YES | YES |

*Table 14:Switch comparison table*

In the table above the solid-state switch was not included, since most requirements apply to it by default. The main drawbacks it presents are high cost complexity, but other than that fits perfectly for this mass accelerator. From the table above it can be seen that the switch which better satisfies the set criteria is the passive electromagnetic switch, mainly due to its low complexity easy arc suppression, and most importantly of all its very high stability. Thus, this as well is a switch that could be implemented in the device, to switch the stationary coils off.

# 11 DEVICE'S LIMITATIONS

Limitations can arise from all of the simulation aspects the device has been examined in this thesis, which include:

## 11.1 Structural analysis limitations

a. Due to material strength, a certain accelerating force can be produced, before the whole structure fails catastrophically. This limitation will be termed $structural\ limit$, and obviously depends on the geometry of the device as well as the primary current [Paragraph 8].

## 11.2 Thermal analysis limitations

b. Due to extreme thermal loads a certain current limit exists, were primary and stationary coils could partially melt due to the very high currents. This maximum temperature will be termed $temp_{maximum}$, and depends on the driving current, material selection, geometry and cooling options for the device [Paragraph 9].

## 11.3 Circuit analysis limitations

c. A certain limit exists to the maximum efficiency of the device, as discussed in more detail in the $RLC$ circuit, efficiency section. This limitation arises from the materials, as well as from the current distribution due to the skin effect and the devices dimensions [Paragraph 6.3].

## 11.4 Magnetic material limitations

d. Limit to magnetic field inside magnetic material (applies only to configurations where ferromagnetic material for core or sleeve is used). This saturation limit can of course be exceeded, but the configuration loses some of its attractive features, mainly its efficiency. Limitations on other materials apply as well, for example melting point for thermal study etc. this however, is mentioned on limitations above [Paragraph 7].

## 11.5 Switch limitations

e. Two main limiting factors exist. Maximum current the switch can conduct, which essentially limits the force, and thus the final velocity. Another limitation applies for the switching time of the switch, which once again is very closely correlated with the final velocity of the projectile [Paragraph 10].

## 11.6 Current limitation:

One might think that currents associated with the operation of the device are very high, and no conductor is able to handle them without melting. This however is not the case, since the current a conductor can handle is a function not only of its geometric features, but of the time it is expected to carry it. From the table below for example, the largest in dimeter wire, in continuous operation conducts current of $260\ [A]$ max. For a smaller time, frame however, it can handle $182.000[A]$. the device at hand belongs to the second category, high currents, small time frames.

| | | | | **Ampacity, at $20\ °C$** | | | **Fusing current** | | |
|---|---|---|---|---|---|---|---|---|---|
| **WG** | **Diameter** | **Area** | **Resistance/length** | **$60\ °C$** | **$75\ °C$** | **$90\ °C$** | **According to [1]** | **According to [2]** | |
| | **$mm$** | **$mm2$** | **$m\Omega/m$** | **$A$** | | | **$10\ s$** | **$1\ s$** | **$32\ ms$** |
| (4/0) | 11.684 | 107 | 0.1608 | 195 | 230 | 260 | $3.2\ kA$ | $33\ kA$ | $182\ kA$ |
| (3/0) | 10.405 | 85 | 0.2028 | 165 | 200 | 225 | $2.7\ kA$ | $26\ kA$ | $144\ kA$ |
| (2/0) | 9.266 | 67.4 | 0.2557 | 145 | 175 | 195 | $2.3\ kA$ | $21\ kA$ | $115\ kA$ |
| (1/0) | 8.251 | 53.5 | 0.3224 | 125 | 150 | 170 | $1.9\ kA$ | $16\ kA$ | $91\ kA$ |

*Table 15: Coil wire diameter, with rated ampacity and maximum current possible as a function of time; [1] Preece;[2] Onderdonk*

# 12 CONCLUSION

In conclusion, this design and its many different configurations seem to show promise for use in the acceleration of small, as well as big loads. More analyses need to be done, but is stands as a solid alternative to a conventional railgun or induction coil-gun, as it allows for high projectile velocities with a robust design.

A rigorous analysis revealing the physical way force is produced was done, and then implemented for the launcher at hand. The same analysis could be applied to all other kinds of electromagnetic motors (linear or rotary), and provides an intuitive way of how force gets produced, as well as the background to maximize said force. This type of analysis greatly simplifies the FEA that would otherwise need to be done, since it decouples the electromagnetic problem with the dynamic (kinematic), allowing for an electromagnetic analysis to first take place in the frequency domain, and then through the use of a simple circuit for the forces etc. to be calculated.

This workflow can be implemented when analyzing all types of motors, and makes it extremely easy to run parametric studies, like the ones seen here. Thus, the procedure for optimizing the design at hand will not be very time consuming, if the simulating workflow above is applied.

*Next steps:*

1. Fully unified analysis of electromagnetic operation in a single simulation. The moving projectile would also be simulated with its accompanying dynamics.
2. Investigation of iron core and sleeve designs more, since they could act as an easy to be built proof of concept.
3. Optimization of the design for a certain projectile mass as an input. This applies for all possible configurations. More specifically a simulation could be set up where with the projectile's mass as an input the proposed dimensions of each launcher configuration would be calculated, for certain efficiency and structural criteria to hold true.
4. Possible train like design, where stationary and moving parts are inverted, to be used in applications where lower final velocities are required.
5. More rigorous definition of the "inductance change rules", in such a way that all possible ways of producing an inductance gradient are correctly identified and put down in a more mathematical way.
6. One possible way of reducing damping ratio of the system is the use of superconducting materials. On one hand they could be use since they essentially present zero electrical resistance. On the other, due to their property of excluding magnetic lines from passing through them, a funnel for the magnetic field lines could be constructed, where big primary and stationary secondary coils are used and a small projectile, since field lines are concentrated by the superconducting funnel [16].

# 13 REFERENCES


[1] B. S. Go, D. V. Le, M. G. Song, M. Park and I. K. Yu, "DESIGN AND ELECTROMAGNETIC ANALYSIS OF AN INDUCTION-TYPE COILGUN SYSTEM WITH A PULSE POWER MODULE," Changwon National University; Hanwha Defense System, Changwon.

[2] "Electrical 4 U," 11 July 2019. [Online]. Available: https://www.electrical4u.com/synchronous-motor-working-principle/. [Accessed 10 September 2020].

[3] "Electrical 4 U," 21 July 2020. [Online]. Available: https://www.electrical4u.com/induction-motor-types-of-induction-motor/. [Accessed 10 September 2020].

[4] "first light," first light fusion ltd. , 2020. [Online]. Available: https://firstlightfusion.com/. [Accessed 10 March 2020].

[5] R. Hawke, A. Susoeff, J. Assay, J. Balk, C. Hall, C. Konrad, M. McDonald, K. Schulder, G. Wellman, R. Hickman, M. Shahinpor and J. Sauve, "STARFIRE: HYPERVELOCITY RAILGUN DEVELOPMENT FOR HIGH-PRESSURE RESEARCH," *IEEE transactions on magnetics,* vol. 25, no. 1, pp. 223-227, 1989.

[6] G. Turnbull, "Maxwell's Equations," 29 October 2019. [Online]. Available: https://ethw.org/Maxwell's_Equations. [Accessed 1 July 2020].

[7] S. Jahn, "Non-ideal transformer," 29 December 2017. [Online]. Available: http://qucs.sourceforge.net/tech/node50.html. [Accessed 10 April 2020].

[8] Q.-a. Lv, Z.-y. Li, B. Lei, K.-y. Zhao, Q. Zhang, H.-j. Xiang and a. Y.-c. Xing, "On Velocity Skin Effect- Part I:," Shijiazhuang Mechanical Engineering College, Shijiazhuang, 2010.

[9] J. T. Tzeng, "Structural Mechanics for Electromagnetic Rail Guns," U.S. Army Research Laboratory, 2015.

[10] K. P. Burr, T. R. Akylas and C. C. Mei, "TWO-DIMENSIONAL LAMINAR BOUNDARY LAYERS," MIT campus project School-wide Program on Fluid MechanicsModules on High Reynolds Number Flows, Cambridge, Massachusetts.

[11] G. B. Zhang, R. C. Gough, M. R, Moorefield, A. T. Ohta and W. A. Shiroma, "An Electrically Actuated Liquid-Metal Switch With Metastable Switching States," Department of Electrical Engineering, University of Hawai‘i at Mānoa, Honolulu, 2016.

[12] M. Schneider, D. Eckenfels, W. Wenning, F. Hatterer and R. Charon, "THE USE OF A SEGMENTED RAILGUN ASHIGH-CURRENT SWITCH," French-German Research Institute (ISL).

[13] D. W. SWALLOM, I. SADOVNIK, J. S. GIBBS, H. GUROL, L. V. NGUYEN, H. H. and V. D. BERGH, "Magnetohydrodynamic Submarine Propulsion Systems," *Naval Engineers Journal,* 1991.

[14] A. Welleman, R. Leutwyler and J. Waldmeyer, "High Current, High Voltage Solid State Discharge," ABB Switzerland Ltd, Semiconductors, Lenzburg.

[15] LAWRENCE E. FISHER, "Resistance of Low-Voltage AC Arcs," *IEEE TRANSACTIONS ON INDUSTRY AND GENERAL APPLICATIONS,,* Vols. IGA-6, no. NO. 6, pp. 607-616, 1970.

[16] A. Sanchez, C. Navau, J. Prat-Campsand and D.-X. Chen, "Antimagnets: controlling magnetic fields withsuperconductor–metamaterial hybrids," *New Journal of Physics,* vol. 13, p. 11, 2011.

[17] K. Daneshjoo, M. Rahimzadeh, R. Ahmadi and M. Ghassemi, "Dynamic Response and Armature Critical Velocity," *IEEE TRANSACTIONS ON MAGNETICS,* vol. 43, pp. 126-131, 2007.

[18] S. O. Starr, R. C. Youngquist and R. B. Cox, "A low voltage “railgun”," *American Association of Physics Teachers,* vol. 81, pp. 38-43, 2013.